

ASSESSMENT OF THE IMMUNOGENICITY AND FORMULATION OF
RECOMBINANT PROTEINS FROM SARS-CoV-2 AS VACCINE ANTIGENS

A THESIS SUBMITTED TO
THE GRADUATE SCHOOL OF NATURAL AND APPLIED SCIENCES
OF
MIDDLE EAST TECHNICAL UNIVERSITY

BY

Duygu KESER

IN PARTIAL FULFILLMENT OF THE REQUIREMENTS
FOR
THE DEGREE OF MASTER OF SCIENCE
IN
BIOLOGY

SEPTEMBER 2022

Approval of the thesis:

**ASSESSMENT OF THE IMMUNOGENICITY AND FORMULATION OF
RECOMBINANT PROTEINS FROM SARS-CoV-2 AS VACCINE
ANTIGENS**

submitted by **DUYGU KESER** in partial fulfillment of the requirements for the degree of **Master of Science in Biology, Middle East Technical University** by,

Prof. Dr. Halil Kalıpçılar
Dean, Graduate School of **Natural and Applied Sciences**

Prof. Dr. Ayşe Gül Gözen
Head of the Department, **Biological Sciences**

Prof. Dr. Gülay Özcengiz
Supervisor, **Biological Sciences, METU**

Examining Committee Members:

Prof. Dr. Mustafa Akçelik
Biology, Ankara University

Prof. Dr. Gülay Özcengiz
Biological Sciences, METU

Assist. Prof. Ahmet Acar
Biological Sciences, METU

Date: 15.09.2022

I hereby, declare that all information in this document has been obtained and presented in accordance with academic rules and ethical conduct. I also declare that, as required by these rules and conduct, I have fully cited and referenced all material and results that are not original to this work.

Name Last name : Duygu Keser

Signature :

ABSTRACT

ASSESSMENT OF THE IMMUNOGENICITY AND FORMULATION OF RECOMBINANT PROTEINS FROM SARS-COV-2 AS VACCINE ANTIGENS

Keser, Duygu
Master of Science, Biology
Supervisor: Prof. Dr. Gülay Özcengiz

September 2022, 112 pages

COVID-19 is an infectious disease caused by SARS-CoV-2. The virus was first detected in Wuhan, China in late 2019, and the outbreak was declared a pandemic in January 2020 by WHO, and continues to spread worldwide. As of July 2022, more than 575 million confirmed cases have been detected all over the world, and more than 6 million people died from the disease. One of the most important public health measures in combating the spread of infectious diseases is vaccination. Despite the existence of rapidly developed and administered vaccines in the later stages of the COVID-19 pandemic, there is still a need to develop more effective and safe vaccines against this pathogen. As a result, there is an urgent need to examine proteins with high immunogenicity that can be employed in novel vaccines. The genome of SARS-CoV-2 encodes four structural proteins and other accessory or nonstructural proteins. The present study is on the evaluation of the immunogenicity of the S1 and S2 region protein fragments in the Spike protein and the whole nucleocapsid protein for the formulation of a recombinant subunit vaccine against SARS-CoV-2. S1, S2 gene fragments and the N gene were amplified by PCR and cloned into the pGEM®-T Easy vector. The genes were then inserted into the

pET-28a (+) vector and their gene expression was achieved in *Escherichia coli* BL21(DE3) cells. Recombinant proteins were purified by His-tag affinity chromatography. Western blot analyzes were performed with monoclonal antibodies and immunized mice sera. Serum-specific IgG levels were measured by the ELISA method, and the increased level of total antibodies to all three antigens showed that a robust humoral response was developed in the immunized group of mice. Moreover, in the analyzes depend on the ELISA results, a significant increase was observed in the antigen-specific IgG2a titers, which indicate the cellular response, in the immunized group compared to the control group. The increase in IFN-gamma levels observed as a result of the performed cytokine ELISAs indicated a strong cellular response to recombinant antigens and, in addition to the antibody response, indicates that these three antigens are suitable vaccine antigen candidates to combat the COVID-19 pandemic.

Keywords: SARS-CoV-2, COVID-19, Recombinant protein vaccine, Immune response, Spike, Nucleocapsid

ÖZ

SARS-CoV-2'DEN ELDE EDİLEN REKOMBİNANT PROTEİNLERİN AŞI ANTİJENLERİ OLARAK İMMÜNOJENİSİTESİNİN DEĞERLENDİRİLMESİ VE FORMÜLE EDİLMESİ

Keser, Duygu
Yüksek Lisans, Biyoloji
Tez Yöneticisi: Prof. Dr. Gülay Özcengiz

Eylül 2022, 112 sayfa

COVID-19, SARS-CoV-2 nin neden olduğu bulaşıcı bir hastalıktır. Bu virüsün 2019 sonlarında Çin in Wuhan kentinde tespit edilmesinden ve neden olduğu enfeksiyona DSÖ tarafından Ocak 2020 de pandemi statüsü verilmesinden bu yana dünya çapında yayılmaya devam etmektedir. Temmuz 2022 itibariyle tüm dünyada 575 milyondan fazla doğrulanmış vaka tespit edilmiş ve 6 milyondan fazla insan bu hastalık nedeniyle hayatını kaybetmiştir. Aşılama bulaşıcı hastalıkların yayılmasıyla mücadelede en önemli halk sağlığı önlemlerinden biridir. COVID-19 pandemisinin sonraki aşamalarında hızla geliştirilen ve uygulanan aşuların varlığına rağmen, bu patojene ve varyantlarına karşı hala, daha etkili ve güvenli aşuların geliştirilmesine ihtiyaç vardır. Bu nedenle yeni aşılarda kullanılabilecek yüksek immünojenik etkiye sahip proteinlerin incelenmesine ihtiyaç vardır. SARS-CoV-2 genomu, dört yapısal proteini ve diğer yardımcı veya yapısal olmayan proteinleri kodlar. Mevcut çalışma, Spike proteinindeki S1 ve S2 bölgesi protein parçalarının ve tüm nükleokapsid proteininin SARS-CoV-2'ye karşı bir rekombinant alt birim aşı formülasyonu açısından, immünojenisitesinin değerlendirilmesini içermektedir. Özetle, üç antijene

karşı artan toplam antikor seviyesi, sağlam bir hümmoral tepkinin geliştirildiğini göstermiştir. Hedef gen parçaları ve N geni PCR ile çoğaltılmış ve pGEM[®]-T Easy vektörüne klonlanmıştır. Genler daha sonra pET-28a (+) vektörüne yerleştirilmiştir ve *Escherichia coli* BL21(DE3) hücrelerinde gen ifadeleri sağlanmıştır. Rekombinant proteinler His-tag afinite kromatografi yöntemiyle saflaştırılmıştır. Monoklonal antikorlar ve bağışıklanan fare serumları ile Western bot analizleri yapılmıştır. ELISA tekniğı ile seruma özgü IgG seviyeleri ölçülmüştür ve her üç antijene karşı artan toplam antikor seviyesi, bağışıklanan fare grubunda sağlam bir hümmoral tepkinin geliştirildiğini göstermiştir. ELISA kullanılarak kontrol grubuna kıyasla hüccresel yanıtı gösteren antijene özgü IgG2a titrelerinde önemli bir artış gözlenmiştir. Gerçekleştirilen sitokin ELISA testlerinin sonucunda tespit edilen IFN-gama seviyelerindeki artış, antikor yanıtına ek olarak rekombinant antijenlere karşı güçlü bir hüccresel yanıtın da oluştuğunu kanıtlamıştır. Sonuç olarak, çalışmamız adı geçen üç rekombinant antijenin COVID-19 pandemisi ile mücadele için hazırlanacak rekombinant bir çoklu altünite aşı için oldukça uygun aşı antijeni adayları olduğunu ortaya koymaktadır.

Anahtar Kelimeler: SARS-CoV-2, COVID-19, Rekombinant protein aşılar, Bağışıklık tepkileri, Spike proteini, Nükleokapsid proteini

To my beloved family...

ACKNOWLEDGMENTS

I would like to express my gratitude to Prof. Dr. Gülay Özcengiz. She helped me to develop as a scientist, for which I owe her the utmost thanks. She always had faith in me and pushed me forward. I sincerely appreciate all the insights and expertise she shared with me. Also, I would like to express my endless thanks to the esteemed Dr. Erkan Özcengiz, who has guided me by constantly helping me in regard to the subject, source, and methodology of my work.

I am grateful to my labmates Sergen Akaysoy, Gözde Çelik Günçe, Caner Aktaş, Meltem Kutnu, Alan Berk Doğan, Selin Koçak as well as my ex-labmates Naz Kocabay and Nazlı Hilal Türkmen for their support, friendship, and cooperation. I also, would like to thank my dear friends, Tunç Özbek, A. Caner Osmanağaoğlu, Ecem Şimşek and Selin Ernam, who did not spare me their support and friendships.

In particular, none of this would have been possible without my family. To my mother Suna Öner Keser, and my father Birhan Keser, I would like to convey my sincere thanks for their unending support, love, and understanding.

I also want to give special thanks to my sister Berfin. I will always be grateful to her for standing there for me and never giving up her support in my most difficult and stressful moments. I would also like to thank Cookie for all the entertainment and emotional support.

TABLE OF CONTENTS

ABSTRACT.....	v
ÖZ	vii
ACKNOWLEDGMENTS	x
TABLE OF CONTENTS.....	xi
LIST OF FIGURES	xvi
LIST OF ABBREVIATIONS.....	xviii
CHAPTERS	
1 INTRODUCTION	1
1.1 COVID-19.....	1
1.1.1 Emergence of SARS-CoV-2	1
1.1.2 Characteristics of SARS-CoV-2	2
1.1.3 Symptoms, Diagnosis, and Treatment	12
1.1.4 Viral Entry and Replication of Virus	14
1.1.5 General Host Immune Response.....	16
1.2 Vaccine Studies.....	19
1.2.1 Nucleic Acid-Based Vaccines	23
1.2.2 Viral Vector Vaccines	24
1.2.3 Whole Virus Vaccines	24
1.2.4 Subunit Vaccines	25
1.3 Adjuvants	26
1.4 Variants	27
1.5 Present Study.....	29

2	MATERIALS AND METHODS	33
2.1	Bacterial Strains and Plasmids.....	33
2.2	Growth Media	34
2.3	Solutions and Buffers.....	34
2.4	Enzymes and Chemicals	34
2.5	Bacterial Strains' Maintenance and Growth Conditions.....	34
2.6	Design of Specific PCR Primers.....	35
2.7	PCR (Polymerase Chain Reaction).....	36
2.8	Agarose Gel Electrophoresis	37
2.9	Ligation Reactions	38
2.10	Preparation of Competent <i>E. coli</i> cells	39
2.11	Transformation of Bacteria.....	40
2.12	Plasmid DNA Purification.....	40
2.13	Restriction Enzyme Digestion	41
2.14	Recombinant Protein Overexpression and Extraction.....	41
2.15	Recombinant Protein Purification.....	42
2.16	Determination of Protein Concentration.....	42
2.17	Sodium Dodecyl Sulphate Polyacrylamide Gel Electrophoresis and Staining of Gels	43
2.18	Western Blotting.....	44
2.19	Immunization Experiments.....	45
2.20	Spleen Cell Culture and Detection of Antigen-Specific T-cell response (IFN-gamma).....	46
2.21	Measurement of Antibody Titers with Enzyme-linked Immunosorbent Assay (ELISA)	47

2.22	SARS-CoV-2 Neutralization Assay	48
2.22.1	Microneutralization Assay.....	48
2.22.2	RBD-ACE-2 Binding Assay.....	48
2.23	Statistical Analyses	49
3	RESULTS AND DISCUSSION	51
3.1	Selection of the Most Appropriate Immunogens	51
3.2	Cloning of S1 and S2 Gene Fragments from Full Spike (S) Expression Vector pUNO1-SARS2-S, and Nucleocapsid Gene from Nucleocapsid Expression Vector pUNO1-SARS2-N	52
3.2.1	Amplification of S1 and S2 Gene Fragments and Nucleocapsid Gene and Cloning into pGEM-T Easy Vector	52
3.2.2	Subcloning of RBD-containing S1 Gene Fragment, S2 Gene Fragment, and Nucleocapsid Gene into pET-28 a (+) Expression Vector.....	57
3.3	Expression of Recombinant S1, S2 Fragment Proteins and Nucleocapsid Proteins in <i>E. coli</i> BL21 (DE3).....	60
3.4	Purification of Poly-His-Tagged Recombinant S1, S2 Fragment Proteins, and Nucleocapsid Proteins via Affinity Column Chromatography	63
3.5	Western Blot Analyses of Recombinant S1, S2 Fragment Proteins, and Nucleocapsid Proteins.....	66
3.6	Immune Responses Against Recombinant S1, S2 Fragment Proteins, and Nucleocapsid Protein	68
3.7	Determination of IFN- γ Response of Immunized Mice.....	72
4	CONCLUSION.....	77
	REFERENCES	81
	APPENDICES	99
A.	STRUCTURES OF PLASMID VECTORS AND SIZE MARKERS.....	99

B.	COMPOSITION AND PREPARATION OF CULTURE MEDIA.....	103
C.	SOLUTIONS AND BUFFERS.....	104
D.	SUPPLIERS OF CHEMICALS, ENZYMES, AND KITS.....	110

LIST OF TABLES

TABLES

Table 1.1 Summary of convenient vaccine candidates against SARS-CoV-2	22
Table 2.1 <i>E.coli</i> strains that were used, and their genotypes	33
Table 2.2 Cloning and expression vectors.	34
Table 2.3 PCR amplification primers, restriction digestions.....	36
Table 2.4 A addition reaction mixture.	38
Table 2.5 pGEM-T Easy Vector ligation reaction mixture.....	38
Table 2.6 pET-28a (+)Vector ligation reaction mixture.	39
Table 2.7 Polyacrylamide gel recipe for SDS-PAGE	43
Table 3.1 Computer-aided analyses of S1, S2 gene fragments and nucleocapsid genes and the respective proteins	57

LIST OF FIGURES

FIGURES

Figure 1.1 SARS-CoV-2, SARS-CoV, MERS-CoV, and other beta coronaviruses on the phylogenetic tree according to whole genome analyses. (GISAID, 2020)	3
Figure 1.2 The genomic organization of SARS-CoV-2 (Alanagreh <i>et al.</i> , 2020). Western blot.....	5
Figure 1.3. Structure of Spike protein. (CAS,2020).....	7
Figure 1.4 Block presentation of Spike protein of SARS-CoV-2 NTD (Gupta <i>et al.</i> 2021).....	8
Figure 1.5 Viral entry to host and replication cycle of SARS-CoV-2.(Uk <i>et al.</i> 2020).....	16
Figure 1.6 Summary of host response against SARS-2 virus (Strange, 2020).....	18
Figure 1.7 Summary of SARS-CoV-2 vaccine platforms (Jighefee, 2021)	21
Figure 1. 8 Spike protein amino acid changes in SARS-CoV-2 variants of concern (Source: American Society for Microbiology).....	28
Figure 2.1 PCR conditions for S1, S2 gene fragments, and N gene.....	37
Figure 2.2 Protein concentration calibration curve.	43
Figure 2.3 The sandwich setup diagram of Western blot transfer.....	45
Figure 3.1 The S1 gene fragment amplification product.....	52
Figure 3.2 The S2 gene fragment amplification product.....	53
Figure 3.3 N gene amplification product.....	53
Figure 3.4 Validation of S1 gene fragment cloned in pGEM-T Easy vector.	54
Figure 3.5 Validation of cloning of S2 gene fragment into pGEM-T Easy vector..	55
Figure 3.6 Validation of cloning of N gene in pGEM-T Easy vector	55
Figure 3.7 Nucleotide sequence of S1 fragment amplicon.....	56
Figure 3.8 Nucleotide sequence of S2 fragment amplicon.....	56
Figure 3.9 Nucleotide sequence of N gene amplicon.....	56
Figure 3.10 Verification of cloning of S1 gene fragment into pET28a(+).	58
Figure 3.11 Verification of cloning of S2 gene fragment into pET28a(+).	59

Figure 3.12 Verification of cloning of Nucleocapsid gene into pET28a(+)	60
Figure 3.13 SDS-PAGE detection of the expressed recombinant S1 fragment protein.	61
Figure 3.14 SDS-PAGE analysis of recombinant S2 fragment protein expression.	62
Figure 3.15 SDS-PAGE detection of the expressed recombinant S1 fragment Nucleocapsid protein.	63
Figure 3.16 SDS-PAGE detection of purified recombinant S1 fragment protein.	64
Figure 3.17 SDS-PAGE detection of purified recombinant S2 fragment protein.	65
Figure 3.18 SDS-PAGE detection of purified recombinant N protein.	65
Figure 3.19 Western blot analysis	66
Figure 3.20 SARS-CoV-2 Spike S1 fragment protein (pS1: 33 kDa) WB analysis.	67
Figure 3.21 SARS-CoV-2 Nucleocapsid protein (pN: 46 kDa) WB analysis	67
Figure 3.22 Level of total Immunoglobulin G	69
Figure 3.23 Level of Immunoglobulin G2a	70
Figure 3.24 Neutralization antibody levels of immunized mice sera against RBD.	71
Figure 3.25 Production of IFN- γ by spleen cells of immunized mice.	73

LIST OF ABBREVIATIONS

ABBREVIATIONS

S1: Spike S1 fragment gene

S2: Spike S2 fragment gene

N: Nucleocapsid gene

SARS-CoV-2: Severe Acute Respiratory Syndrome Coronavirus 2

MERS-CoV: Middle East Respiratory Syndrome Coronavirus

COVID-19: Coronavirus Disease 19

WHO: World Health Organization

ORF: Open Reading Frame

bp(s): Base pair(s)

E. coli: *Escherichia coli*

ELISA: Enzyme-linked immunosorbent assay

Nsp: Nonstructural Protein

S: Spike glycoprotein

E: Envelope

N: Nucleocapsid

M: Membrane glycoprotein

ACE2: Angiotensin Converting Enzyme 2

TMPRSS2: Transmembrane Protease Serine 2

IFN- γ : Interferon gamma

IPTG: Isopropyl- β -D-thio-galactoside

IgG: Immunoglobulin G

MPLA: Monophosphoryl lipid A

kDa: Kilodalton

OD: Optical Density

SDS-PAGE: Sodium Dodecyl Sulphate-Polyacrylamide Gel Electrophoresis

Th: T helper cell

CHAPTER 1

INTRODUCTION

1.1 COVID-19

1.1.1 Emergence of SARS-CoV-2

In December 2019, people with symptoms of pneumonia and respiratory failure, similar to the SARS epidemic in 2003, were hospitalized in Hubei/Wuhan, China. Some of these patients developed severe respiratory problems, which can cause acute respiratory distress syndrome, ARDS, and similar serious problems. According to the report of the Disease Control and Prevention Center (CDC) in China, in January 2020, in the nasopharyngeal swab samples of the patients, an unknown coronavirus was detected (Malik *et al.* 2020; Zhou *et al.* 2020). The 2019 novel coronavirus was named for the new type of coronavirus, and the abbreviation 2019-nCoV started to be used. The official name of severe acute respiratory syndrome coronavirus 2 or, in short, SARS-CoV-2 was given by the World Health Organization in 2020. On January 20, 2020, the World Health Organization published its first status report about the emerging disease, and when this report was published, 282 cases of 2019-nCoV were confirmed in four countries. These countries were China, which is the

origin of the virus, where most of the disease cases were located, Japan, the Republic of Korea, and Thailand. The COVID-19 outbreak was deemed a Public Health Emergency of International Concern by WHO on January 30, 2020. In the middle of March, WHO classified the COVID-19 epidemic as a pandemic (Dawood *et al.* 2020). According to the status report dated 8 June 2020, almost 12 million cases of severe acute respiratory syndrome coronavirus 2 (SARS-CoV-2) infection were confirmed via biological tests, and more than 530 000 people died because of COVID-19. Johns Hopkins University's Center for Systems Science and Engineering (CSSE) reports approximately 570 million confirmed cases and 6 million confirmed dead as of July 2022.

1.1.2 Characteristics of SARS-CoV-2

SARS-CoV-2 possesses traits that are exclusive to the coronavirus family. The virus belongs to the Beta coronavirus 2B genus. Phylogenetic research showed that SARS-CoV-2 is closely related to two coronaviruses isolated from bats and that are comparable to SARS (88–96%), and that it is more distantly related to human SARS coronavirus (79%). When compared to MERS (Middle East respiratory syndrome coronavirus), the similarity ratio dropped to 50% (Lai *et al.* 2020). The coronaviridae family of lineage-b beta-coronaviruses includes SARS-CoV-2. This family is a member of the orthomavirae kingdom, the pisonivirecetes class, the pisuviricota phylum, the ribovaria realm, and the order nidovirales (Jaimes *et al.* 2020).

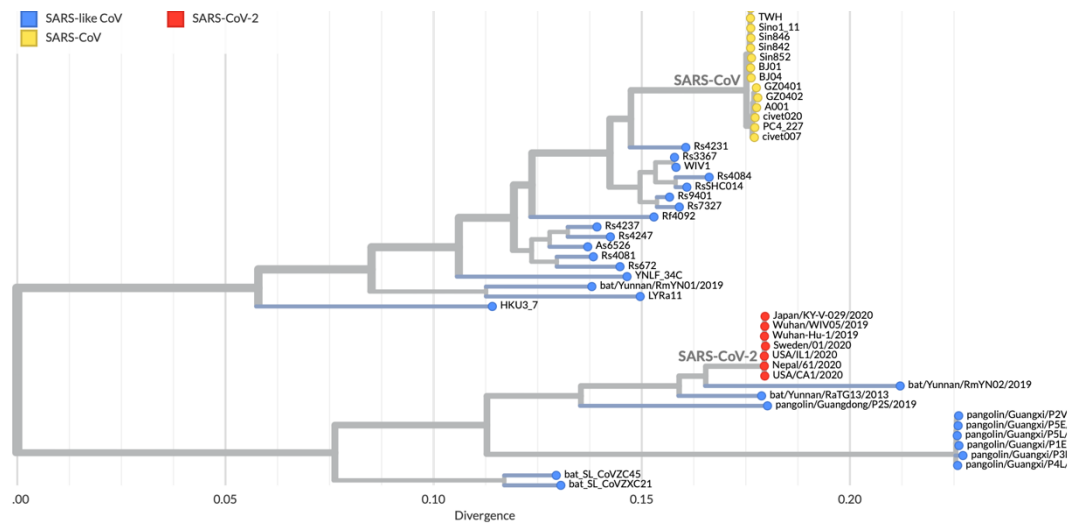


Figure 1.1 SARS-CoV-2, SARS-CoV, MERS-CoV, and other beta coronaviruses on the phylogenetic tree according to whole genome analyses. (GISAID, 2020)

Coronaviruses are generally large in size and are spherical in shape. SARS-CoV-2 has a single-stranded, positive sense RNA genome. Their genetic material, which is RNA, is enclosed in a lipid envelope with spike-like glycoproteins embedded in the surface of the virus. These viruses get their name from the Latin word "corona", which means "crown". This word alludes to the distinctive morphology that can be easily discerned while examining them under an electron microscope (Perlman *et al.* 2020). SARS-CoV-2 is the pathogen that causes the disease COVID-19. The genome size of the virus is ~29.9 kb. The genome of SARS-CoV-2 encodes accessory proteins and several non-structural proteins that are mostly responsible for RNA processing, such as endoribonuclease, RNA replicase, RNA-dependent RNA polymerase, and proteins that mediate host invasions like papain-like and 3C-like (chymotrypsin-like) proteases, besides four main structural proteins that are called Spike, Membrane, Nucleocapsid and Envelope proteins (Khan *et al.*; 2020, Zhu *et al.* 2020; Zhou *et al.* 2020).

The poly(A) tail at the 3' end and the 5' end cap structure allows the Coronavirus genome to act as mRNA in host cells, enabling the translation of proteins involved in replication. Structural and accessory proteins make up one-third (10 kb) of the viral genome, while non-structural proteins (nsps), including the replicase gene, cover most of the coronavirus genome (Fehr *et al.* 2015). 14 open reading frames (ORFs) in SARS-CoV-2 encode 27 distinct proteins (Wu *et al.* 2020). The organization of the open reading frames of SARS-2 coronavirus is as follows: The untranslated region is located at 5' (5' UTR) which is followed by 14 open reading frames. The biggest ORF of the coronavirus genome is ORF1a/b which encodes polyproteins, which are then cleaved into 16 nsps. The chopped proteins function in the replication complex, transcription, invasion, etc. In the continuation of this region, there are accessory protein-encoded 9 ORFs located between the Spike (S)-coding region, the Envelope (E) protein-coded region, the Membrane protein (M) sequence, and the Nucleocapsid (N) sequence, followed by the 3' UTR region and the poly-A tail. (Figure 1.2)

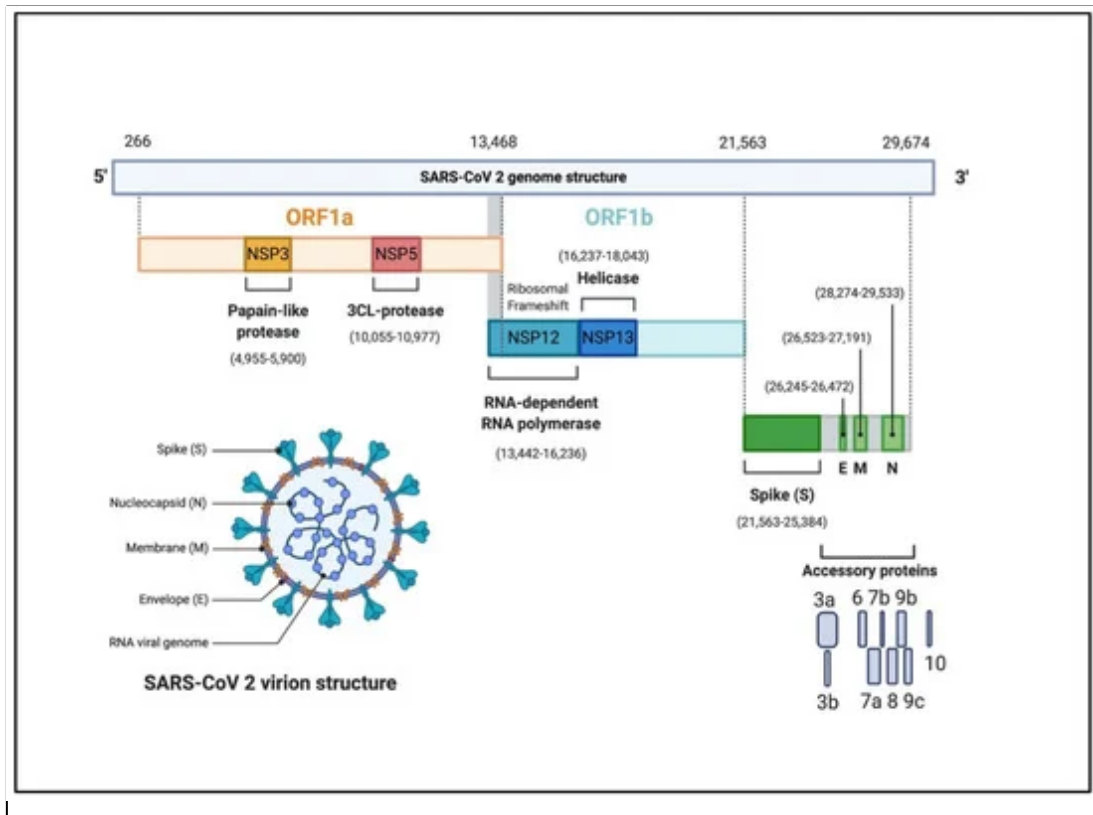


Figure 1.2 The genomic organization of SARS-CoV-2 (Alanagreh *et al.*, 2020).
Western blot

The 3' UTR region encodes accessory proteins like ORF-3a, 6, 7a, 7b, 8, and 10. These proteins are responsible for many different mechanisms related to the virulence of the pathogen. For example, host-virus interaction, cellular death mechanism, evasion of host cells, and regulation of host transcription system are controlled by coronaviruses' accessory proteins. However, these proteins do not have a crucial role in replication and the viral cycle (Redondo *et al.*, 2021). The genetic arrangements of SARS and MERS coronaviruses are considerably similar to the ORFs of SARS-CoV-2 (Lu *et al.*, 2015; Rota *et al.*, 2003).

The shape of SARS-CoV-2 is a sphere with a diameter of 80-120 nm, and it is mostly enveloped by lipids, envelope proteins, membrane proteins, and spike proteins embedded in the envelope (Wang *et al.* 2022). Homotrimeric, glycosylated S proteins present in the form of numerous outward protrusions on the surface of the virus give the virus the configuration of a solar corona, so this type of virus is called CoV. Within the lipid bilayer of the virion are nucleocapsids that are helically wrapped around the +ssRNA and capsid proteins. Basically, SARS-CoV-2 has four crucial structural proteins these are Nucleocapsid; a complex of viral RNA and capsid protein, Spike protein; a glycoprotein found in viral surface responsible for host interaction, Membrane protein; which is involved in the construction of the membrane, and Envelope; which participates in the structure of the envelope, at the 3' end of the genome (Yadav *et al.* 2021).

1.1.2.1 Structural Proteins

Coronaviruses have surface glycoproteins called Spike proteins, that look like sharp spines in their envelope. These glycoproteins are responsible for the virion's ability to recognize and bind host receptors. The spike protein consists of 1273 amino acids and has a molecular weight of approximately 180 kDa. (Kumar *et al.* 2020). The monomeric form of S protein is made up of a C-terminal section which is the intracellular part of the glycoprotein, an external N-terminus (an ectodomain element), and a transmembrane (TM) domain linked to the viral membrane (Huang *et al.* 2020). The monomeric structure consists of two subunits, S1, which hosts the host receptor binding sites, and S2, which allows for membrane fusion. As shown in Figure 1.3, the spike protein has a trimeric form with the S1 subunits placed in the outer body while S2 act as stems (Chen *et al.*, 2020).

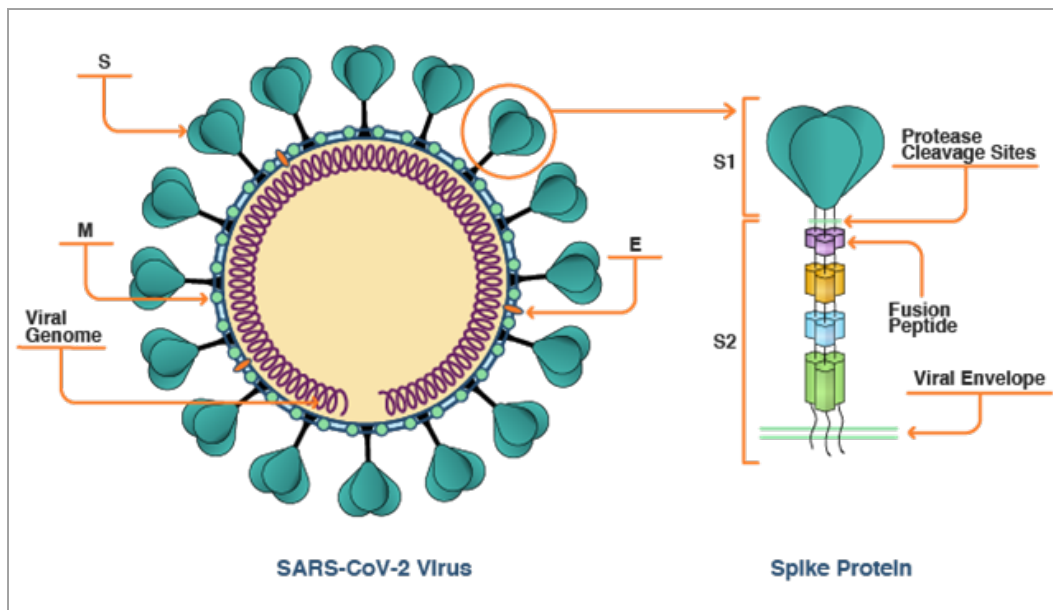


Figure 1.3. Structure of Spike protein. (CAS,2020)

As shown in Figure 1.4, the S1 subunit of the Spike protein starts with a signal peptide consisting of 13 amino acids. This peptide is followed by an extracellular N-terminus, which contains epitopes important for binding host receptors. After NTD, there is a receptor binding domain (RBD), which is the key sequence for binding to the host receptor. The most important part of the RBD in terms of virus-host connection is the receptor binding motif. The S2 unit, on the other hand, allows the virus to transmit its genetic material to the host after the virus-host connection is established. For this reason, the S2 subunit consists of a fusion peptide (FP), hydrophobic heptad repeats (HR1 and HR2), a transmembrane region, and at the end, a cytoplasmic region (Xia *et al.* 2020).

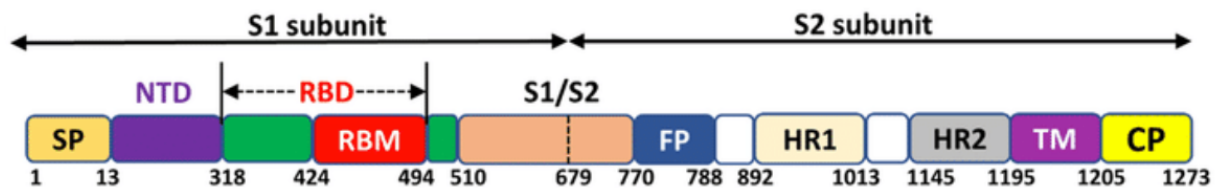


Figure 1.4 Block presentation of Spike protein of SARS-CoV-2 NTD (Gupta *et al.* 2021)

Previous studies show that virus-host cell fusion begin with the attachment of the spike protein to the mammalian ACE-2 receptor. To interact with and enter a host cell, the spike protein's S1 and S2 domains must undergo morphological modifications by the serine protease TMPRSS2. The receptor binding domain (RBD) is a highly immunogenic short segment of the Spike that binds to the receptor sequence to facilitate viral attachment and penetration. RBD of the novel coronavirus is located between residues 331 and 524. RBD-specific polyclonal antibodies are effective in preventing SARS-CoV-2 entrance into ACE-expressing cells. This is assumed to be because of the RBD's critical neutralizing domain (CND), which generates a powerful neutralizing antibody response. Furthermore, suppressing SARS-CoV-2 pseudo viruses via RBD-specific polyclonal antibodies suggest that the RBD region can be utilized as a possible target against CoV in vaccination research (Min and Sun, 2021). Since the S protein is the primary target for monoclonal, polyclonal, and neutralizing antibodies, pharmaceuticals, vaccines, as well as other inhibitors, developing anti-spike techniques is vital in combatting the outbreak.

Normally, the Spike protein has a metastable structure, in its pre-fusion conformation. When the virion encounters host cell receptors, the conformation of the Spike protein is rearranged so that the virus can enter the host cell. The spike

protein is covered with polysaccharide molecules that camouflage the virus and allow it to evade the host's immune response (Watanabe *et al.*).

Envelope membrane (E) proteins, another structural protein, are responsible for the assembly and release of virions. (Fehr *et al.* 2015). Protein E consists of only 75 aa. However, its importance in viral assembly and morphogenesis is quite high. E proteins and M protein both have roles in membrane curvature. When the expression of E is inhibited, replication does not abolish completely. However, the virions had been considerably attenuated, with much lower titers (Kuo and Masters, 2003; DeDiego *et al.*, 2007). Protein E is only present in small amounts and most likely forms ion channels. It was also revealed to be capable of inducing the production of proinflammatory cytokines by activating p38 kinase and NLRP3 inflammasome (Guerdeno *et al.* 2014, Nieto-Torres *et al.* 2015). E proteins are not necessarily required for viral replication but are required for infectivity and pathogenesis. Therefore, coronaviruses with knockout E gene are strong candidates for vaccine studies (Schoeman and Fielding, 2019).

Membrane or, in other words, Matrix proteins are responsible for viral assembly, RNA packaging, and the release of virions and work together with the other three structural proteins, especially E proteins. M proteins consist of 222 amino acids. The most prevalent structural protein in the coronavirus is the M protein. M proteins form the different shapes of the virus by giving membrane curvature to the viral envelope, especially through their interaction with E proteins (Tang *et al.*, 2020). It blocks the entrance of IFN-beta-stimulating transcription factors into the nucleus by blocking the RIG-I pathway together with the Nucleocapsid protein (Mu *et al.*, 2020).

In the process of packaging viral RNA into ribonucleocapsids, nucleocapsid proteins (N) are crucial. The amino acid sequence of SARS-CoV-N is 90% consistent with former coronaviruses. This demonstrates how vital the nucleocapsid is for coronaviruses (Bai *et al.*, 2021). The N-terminal domain (NTD) holds the RNA genome. In contrast, the C-terminal domain anchors the ribonucleoprotein complex

to the viral membrane via its association with the M protein (Khan *et al.*, 2021). The viral ribonucleoprotein cocoon is formed by folding RNA wrapped around the proteins during the RNA-N protein interaction. The key role of SARS-CoV-2 N protein is to wrap the viral genome, but it also contributes to the host's immune system escape mechanisms by exhibiting VSR (viral suppressors of RNAi) activity in mammalian cells (Cui *et al.*, 2015). It was also revealed that the N protein has several effects on IFN activity. N protein decreases IFN- β expression and enhances SARS-CoV-2 replication by suppressing the STAT1/STAT2 pathway and nuclear translocation (Mu *et al.*, 2020). High Anti-SARS-CoV-2 N IgG and IgM antibody titers have been reported in the sera of COVID-19 patients, so it can be said that N is the main immunogen of SARS-CoV-2 (Liu *et al.* 2020). It was discovered that prior CoV N proteins had a substantial immunogenic impact and that the N protein was upregulated throughout the disease (Okada *et al.* 2005). As a result, SARS-CoV-2 N is critical in terms of both therapeutic and diagnostic approaches. Previous research has shown that N protein is critical for both specific T cell proliferation and cytotoxic T cell response. The acquisition of long-term T-cell memory is crucial for vaccine efficacy. The identification of long-lasting memory T cells reactive to the N protein of SARS-CoV-2 in a patient who had been infected in 2003, 17 years earlier by SARS, highlights the importance of vaccine formulations including N protein (Lin *et al.* 2014, Le Bert *et al.* 2020).

The partnership of the Nucleocapsid protein with the M protein regulates RNA synthesis and replication (Naqvi *et al.*, 2020). Also, N protein is essential for viral nucleation, assembly, envelope development, and budding. Furthermore, it plays a crucial role in CoV pathogenesis, and as a consequence of these features, it is the most potent protein among CoV immunogens for vaccine and therapeutic investigations (McBride *et al.* 2014).

1.1.2.2 Nonstructural and Accessory Proteins

The structural protein genes that are resident in the 5' region of the viral RNA genome in the open reading frame 1 a and 1 b encode several non-structural proteins, including NSP1 to NSP11 in ORF1a and NSP12 to NSP16 in ORF1b. Nsp1 is an essential virulence factor that suppresses the host cell's protein production pathways and allows the virus to evade the immune system by mainly inhibiting type-1 IFN. The mutant nsp1 protein is a promising option for live attenuated viral vaccines (Yan *et al.*, 2021). Another nonstructural protein that encoded in the SARS-CoV-2 genome is nsp2. Nsp2 influences host mitochondrial cell biogenesis by binding to prohibitin 1 and 2 proteins (Cornillez-Ty *et al.* 2009). It is also involved in endosome trafficking. Because of these features, nsp2 is also thought to be a potential therapeutic target for attenuated vaccines (Yan *et al.*, 2021). The Nsp3 protein is the largest protein found in Coronaviruses. The Nsp3 encoded papain-like protease domain oversees polyprotein processing, which involves chopping polyproteins into replication complex subunits. Nsp3 also prevents ubiquitination and diminishes the host immune response by suppressing host transcription factors (Shin *et al.*, 2020). Nsp4 interacts with the host cell's ER and is involved in DMV formation. Nsp5 is a 3C-like protease and the core protease of SARS-CoV-2. This protein is responsible for converting polyprotein1ab to nsp5. Nsp7 and 8 serve as primase to nsp12, an RNA-dependent RNA polymerase in charge of replication. Nsp14 is a 3' to 5' exoribonuclease triggered by nsp10 responsible for proofreading (Gupta *et al.*, 2020). Coronavirus accessory proteins contribute to escape from the host immune system by altering cytokine production; they are critical proteins in this regard. Furthermore, these proteins influence mitochondrial activity and mediate apoptosis and inflammasome activation (Redondo *et al.*, 2021).

1.1.3 Symptoms, Diagnosis, and Treatment

After the virus settles in the body, there is an average incubation period of 2-14 days. Dry cough and low-grade fever are the typical symptoms of COVID-19 infection. Following the cough and fever symptoms, anosmia and ageusia develop. While most COVID patients can recover at home within 5-10 days without the need for serious medical attention, 10% of patients' symptoms persist into the 2nd week. The likelihood of developing a severe illness, needing hospitalization, and requiring emergency care increase as infection symptoms persist. The most apparent signs of COVID-19 infection occur in the respiratory system. Sputum, cough, shortness of breath, difficulty breathing, and fever are the most common symptoms. In addition, symptoms such as joint pain, headaches, fatigue, vomiting, and diarrhea can also be seen (Gupta *et al.* 2020).

Clinical checks, radiographic scanning, and laboratory tests are used to diagnose cases. Because radiological scan results and emerging symptoms of SARS-CoV-2 infection vary between patients, laboratory tests are the standard test method for definitive diagnosis. Laboratory tests can be divided into molecular and serological tests (antibody-dependent and antigen-dependent tests.) Among these tests, the gold standard, the fastest, and most accurate tests are molecular tests; these are real-time RT-qPCR (Reverse transcriptase quantitative PCR) and sequencing. Upper or lower respiratory tract samples such as a nasopharyngeal swab, lavage, sputum, or aspirate sample are used for RT-PCR. However, blood, stool, and urine samples can be used for diagnosis when necessary. The World Health Organization recommends targeting Envelope (E) and RNA-dependent RNA polymerase (RdRp) coding gene sequences in PCR-based diagnostic tests (WHO, 2020). Other than E and RdRp sequences, primers targeting N and ORF1a/b can also be utilized to identify infections (Chu *et al.* 2020). Detection of SARS CoV-2 via next generation sequencing (NGS) is another molecular diagnosis method. Viral sequencing provides accurate results and offers the opportunity to watch for mutations and emerging variants. Besides molecular tests, serological tests can be used to diagnose

coronaviral infection. However, such tests are not precise at the beginning of the disease because serological tests are primarily dependent on the detection of antigen-specific IgG or IgM, and antibodies are produced days after the initiation of infection (John *et al.*, 2021). Although new diagnosis methods have been found since the pandemic's beginning, RT-qPCR, and CT visualization of lungs, which are both effective and precise, are still the most widely used methods.

Throughout the pandemic, several therapeutic procedures have been tested for COVID-19 patients. Given the structural and genetic characteristics of SARS-CoV-2, these approaches include protease inhibitors, RNA polymerase inhibitors, nucleoside analogues, neutralizing monoclonal antibodies, immune modulators, interferon α and β , endonuclease inhibitors, fusion inhibitors, convalescent plasma therapy, and immunosuppressive drugs. Various treatments have been tested, however, in subsequent experiments most of them proved to be ineffective.

One of these therapeutics is the anti-parasitic Ivermectin. The mode of action of ivermectin, an antimalarial drug, is based on blocking the hosts' nuclear transport proteins known as the importin α/β -1, thus, reducing the host's antiviral response and generating a pro-inflammatory impact (Vora *et al.* 2020). However, ivermectin, has not received FDA approval against viral infections.

Another therapeutic used in COVID-19 patients is Remdesivir, an analog of adenosine that binds to viral RdRp, interfering with its activity and suppressing viral replication. Remdesivir has been administered previously during SARS and MERS outbreaks and has received emergency approval by the FDA for use in COVID-19 patients (FDA, 2020).

Chloroquine and hydroxychloroquine, which are used in treating malaria, are among the therapeutics tested for their effectiveness against COVID-19. Chloroquine inhibits the cellular ACE2 receptor from becoming glycosylated and might prevent the virus from attaching to the host. In vitro studies have shown that these two molecules potentially prevent the movement of SARS-CoV-2 into endolysosomes from early endosomes, possibly inhibiting viral genome release (Wang *et al.*, 2020).

However further studies have showed that these molecules do not have a beneficial effect on COVID-19 patients (Self *et al.*, 2020).

The RNA polymerase inhibitor Favipiravir, previously tested against Ebola and Influenza, was tested for use against COVID-19 but was found to be ineffective in clinical studies (Hassanipour *et al.*, 2021). At the beginning of the epidemic, patient plasma therapy was applied to seriously ill patients. Tocilizumab, a monoclonal antibody against another therapeutic (IL-6R), has also been used against SARS-CoV2. The immunosuppressant property of Tocilizumab inhibits the inflammatory response. In addition to the treatments mentioned here, there are many more successful and unsuccessful treatment studies.

1.1.4 Viral Entry and Replication of Virus

The mechanism of attachment and fusion of the virus to the host cell is carried out by the spike glycoprotein, a structural protein that is a fundamental component of the viral entry process. When the first interaction between host surface receptor and virus glycoproteins is established by the S1 (extracellular) part of Spike protein, the transmembrane portion of Spike, the S2 subunit, mediates the fusion. Virus glycoproteins interact with the host cell by recognizing the ACE2 receptor on the surface. Alveolar epithelial cells are the cells that express Angiotensin-converting enzyme 2 (ACE2) the most in the body. Therefore, the regions where ACE2 is most concentrated are the lungs, intestines, heart, and kidneys (Zhou, 2020). The RBM region located inside the receptor binding domain (RBD) of the spike protein binds the ACE-2 receptor, and extracellular proteases in the host cleave the S protein. The transmembrane protease serine 2 (TMPRSS2) on the host cell is the main enzyme that cleaves the Spike into its S1 and S2 subunits. Because there is a furin cut-off point between the S1/S2 regions, it was initially thought that the furin enzyme also contributed to this separation; however, unlike other coronaviruses, the furin-mediated cleavage was not observed in SARS-CoV-2 (Tang *et al.* 2020). While S1

remains bound to the Ace-2 receptor, S2 is activated by cleavage, the host-virus fusion takes place via endocytosis, and the viral genetic material is liberated to the host cytoplasm (Hoffman *et al.*, 2020).

After the virus has entered the host, the hosts translation mechanism is used to translate viral proteases and polyproteins pp1a/ab via ORF 1a and ORF 1b (Liu *et al.*2020). Polyproteins 1a and 1ab are chopped by 3C-like protease and Papain-like protease into 16 effector proteins to form a replication complex that creates a full-length negative strand template(Figure 1.5). It becomes a complex with RNA polymerase so that both viral structural and accessory proteins are translated. The newly synthesized proteins and RNA come together to generate new virions, and these virion buds are transported to the Golgi via the ER, where they accumulate in the vesicles and are released out of the cell by exocytosis (Guo *et al.*, 2020).

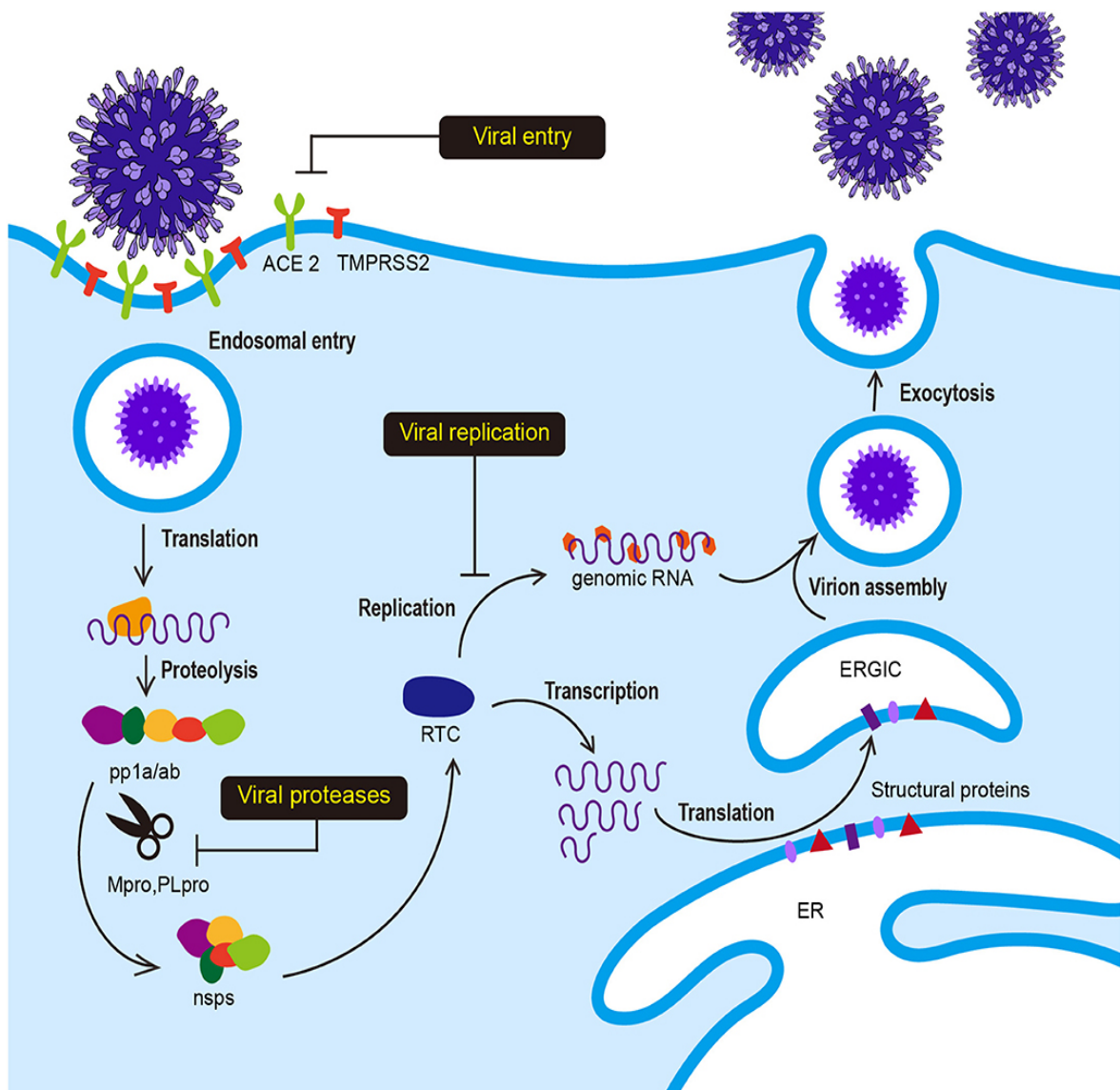


Figure 1.5 Viral entry to host and replication cycle of SARS-CoV-2.(Uk *et al.* 2020)

1.1.5 General Host Immune Response

Studies show that the innate immune response has a vital role in the fight against COVID-19. Innate immune sensing, one of the most crucial components of the

body's defense against viruses, acts as the first line of protection against viruses. When the cell is infected with SARS-CoV-2, which has a single-stranded RNA genome and is recognized by innate immune system members, TLR-expressing Dendritic cells are the initial cells that recognize the virus. TLR7 and TLR8, are receptors of the immune system that recognize ssRNAs, that detect coronaviral RNA in endosomes. CoV can also be detected by the dsRNA detector TLR3, as viral RNA acts as dsRNA during RNA replication in endosomes while RIG-1 detects it in the cytosol (Vabret *et al.* 2020).

Signals sensed by TLR receptors activate transcriptional factors IRF3/7 and NF- κ B, which facilitate the production of cytokines. The NF- κ B pathway induces pro-inflammatory cytokine production, predominantly IL-6 and TNF- α , while the IRF pathway triggers anti-viral response via IFN production (Felsenstein *et al.*, 2020).

The transcription of genes that produces pro-inflammatory cytokines like TNF-, TGF-, IL-1, IL-6, IL-8, IL-12, IL-18 are induced by NF- κ B activation. Moreover, chemokines are secreted, including CCL2, CCL3, CCL5, CXCL8, CXCL9 and CXCL10. These molecules also induce macrophage activation, resulting in the release of more pro-inflammatory cytokines. As a result, people with COVID-19 create a barrage of cytokines that can harm organs in a direct, indirect, or synergistic manner or cause acute respiratory distress syndrome (ARDS) (Li *et al.*, 2022).

The pathogenicity of COVID-19 also causes activation of the NLRP3 inflammasome and subsequently, the release of IL-1 β results in pyroptosis (Azkur *et al.*, 2020). Envelope protein and nsp3a proteins synthesized from ORF1a play a vital role in the activation of the NLRP3 inflammasome and cell death (Chen *et al.*, 2019; Torres *et al.*, 2015). Innate immune response against Coronavirus infections is summarized in Figure 1.6.

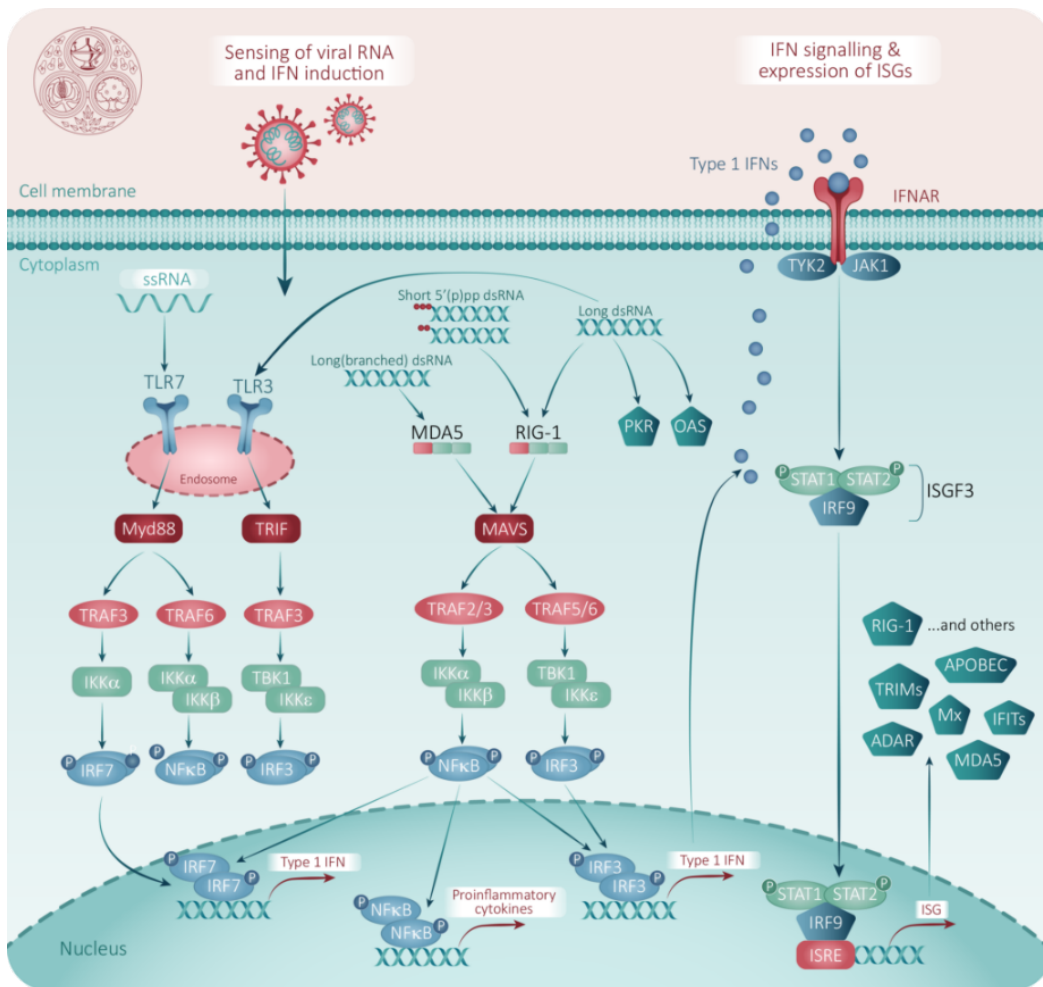


Figure 1.6 Summary of host response against SARS-2 virus (Strange, 2020)

Besides the innate immune response, T and B cells play critical roles in the immune response to viral infections. The adaptive response is divided into cell-mediated immune response driven by T cells and humoral immune response based on B cells and antibodies. CD8⁺ T cells are critical for limiting viral transmission through their cytotoxic role. CD4⁺ T cells are required for the proliferation of CD8⁺ T cells and the formation of CD8⁺ memory T cells (Hosseini *et al.*, 2020). Th1-type cytokines are responsible for killing the pathogens by creating proinflammatory responses. Interferon-gamma is the main Th1 cytokine and is also related to IgG2a, while Th2-

type cytokines include ILs, which have more of an anti-inflammatory response (Berger, 2000; Elgert, 2009).

It has been discovered that the antibody-related response to CoV-2 produces identifiable IgG and IgM antibodies, similar to previous CoV infections. B cells respond quickly to the N protein at the initiation of the infection, but antibodies specific to the S protein can be detected one week after the first symptoms manifest (Huang *et al.*, 2020; Wu *et al.*, 2004). Despite being smaller than the S protein, the N protein has high immunogenicity and lacks any glycosylation sites, which causes the generation of N-specific neutralizing antibodies to occur early in acute infection (Meyer *et al.*, 2014).

1.2 Vaccine Studies

In response to the COVID-19 pandemic's high transmissibility and rapidly rising death toll, epidemic control strategies such as shutting down public transportation, shifting to remote work, and a full curfew were seen as effective measures to combat the disease's spread. However, such measures have a significant effect on the global economy and could not be implemented for long. This has highlighted the critical need for an effective vaccination to preserve public health and mitigate the pandemic's economic and social consequences (Kudlay, 2022).

In 1796, when Edward Jenner performed the emblematic experimental inoculation of an adolescent with pus obtained from a milkmaid infected with vaccinia virus which resulted in his immunization against smallpox. Later, Louis Pasteur advanced the concept of vaccine technology using microbiology studies, and vaccination has proven to be a cornerstone for human health (Kyridiakis, 2021). The vaccination strategy that succeeded 200 years ago against the smallpox virus is the number one strategy to prevent infectious diseases like the COVID-19 pandemic. Since the discovery of vaccines, vector-based vaccines, whole virus-based vaccines, protein- or VLP-based subunit vaccines, and RNA- or DNA-based genomic vaccines have

been developed, and some of them are approved for human use. Even though normal vaccine development is often a lengthy process that requires extensive effort and lasts years to complete all clinical phases, there are presently more than 350 vaccine candidates against COVID in pre-clinical testing and clinical phases based on various vaccine platforms. (WHO)

The primary purpose of vaccines is to provide protection against a specific pathogen by inducing antibody and cellular responses. Historically, the majority of authorized vaccines focused on inducing protective and effective neutralizing antibodies against the target pathogen, conferring neutralizing immunity in vaccinated people. The immunological condition in which viral infection is entirely inhibited is known as neutralizing immunity; neutralizing antibodies can prevent an infectious agent from infecting a cell. They do this by blocking the receptors on the virus or the cell, for example, or by neutralizing the agent's biological impact. While T cell-mediated immunity ensures the destruction of the virus after the infection starts, neutralizing immunity prevents the host cell from being infected. Balancing immunity is not very common; this type of immunity is rare in viruses that infect the lower respiratory tract, such as influenza virus and coronaviruses (Kyriakidis *et al.*, 2021). In addition, the antibody response may diminish shortly after vaccination against the coronavirus. The immune response to human coronaviruses may not be long-lasting, and recurrent infections may occur with the same virus after some time, as demonstrated in human challenge tests (Callow *et al.* 1990). Although B cell-mediated immunity is an important part of the immune system, a rising body of evidence shows that T-cell-dependent immunity is crucial and lasts longer (Gallais, 2021; Sekine, 2020). As a result, vaccination techniques that elicit high cellular responses in addition to humoral protection provide a considerable advantage in the current epidemic.

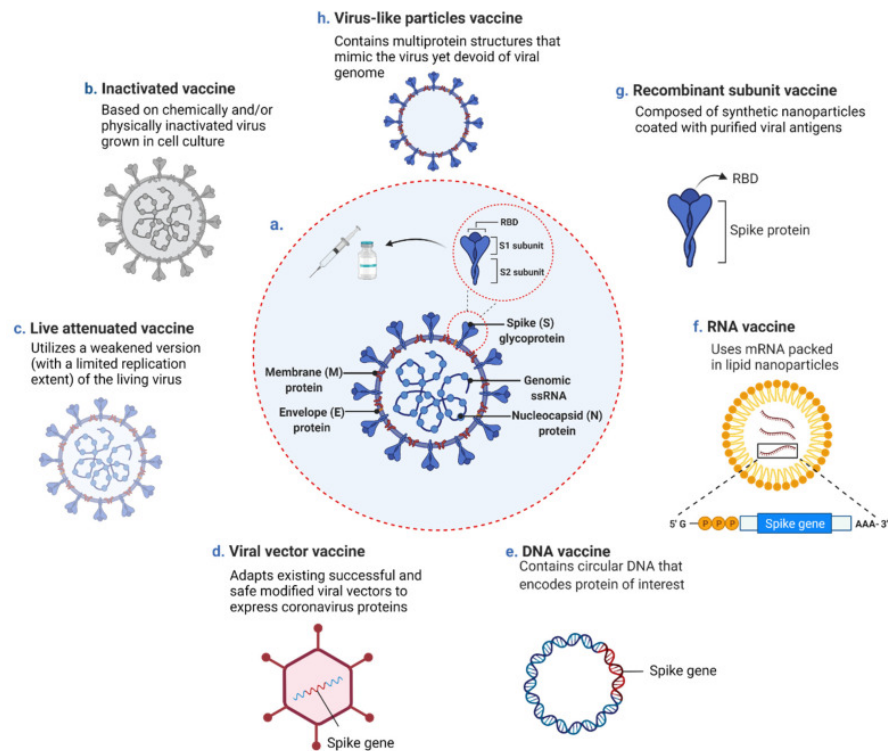


Figure 1.7 Summary of SARS-CoV-2 vaccine platforms (Jighefee, 2021)

As shown in Figure 1.7, different platforms are used for COVID-19 vaccine development studies. These include traditional approaches such as protein subunit vaccines, inactivated virus vaccines, live attenuated viruses, and newer platforms such as adenovector-based vaccines and DNA or RNA-based genetic vaccines. Since the emergence of the virus, vaccines have been developed on various platforms and are still being developed. Some of the vaccines from different platforms designed against Covid-19 are listed in Table 1.1.

	Sputnik-V	ChAdOx1-S	VAT00008	NVX-CoV2373	CoronaVac	BNT-162b2	mRNA-1273
Platform	Viral vector	Viral vector	Protein subunit	Protein subunit	Inactivated whole virus	mRNA	mRNA
Description	Ad26 and Ad5 non-replicating adenoviral vectors	Replication defective adenoviral vector	Adjuvanted recombinant spike protein-based, produced via baculovirus expression system	Spike recombinant protein expressed via baculovirus vector, adjuvanted with M Matrix adjuvant	Chemically inactivated whole virion	Spike mRNA encapsulated with lipid nanoparticles	Spike mRNA encapsulated with lipid nanoparticles
Manufacturer	Gamelaya Research Institute	Oxford/Astra-Zeneca	Sanofi-GSK	Novavax	Sinovac	Pfizer	Moderna
Doses	2	2	2	2	2	2	2
Efficacy	91.4%	67.1%	75.1%	90%	83%	95%	94.5%
Reference	Jackson, 2022	Jackson, 2022	GSK, 2022	Pulendran, 2021	Jackson, 2022	Pollack, 2020; Jackson, 2022	Pollack, 2020; Jackson, 2022

Table 1.1 Summary of convenient vaccine candidates against SARS-CoV-2

1.2.1 Nucleic Acid-Based Vaccines

The mechanism of genetic vaccines is the introduction of a DNA or mRNA sequence encoding a particular antigen for the host to synthesize, thus activating the host's immune system. The antigen is generated by the expression system of the host cells using the genetic material provided to the host. A high host immunity against the antigen protein can be developed to prevent and treat illnesses. Production of this type of vaccine requires stages such as antigen sequence design, optimization, in vitro transcription, genetic material separation, and integration into a carrier and protective molecules. Especially in RNA-based vaccines, which are encapsulated with lipid nanoparticles that protect the RNA strands and enable their fusion into cells. FDA-approved vaccines from Pfizer BioNTech (BNT162b2) and Moderna (mRNA-1273) companies against COVID-19 are vaccines containing the full-length Spike mRNA. ZyCoV-D is the only approved vaccine against Covid that provides immunization using a needle-free method. Moreover, it is the first plasma DNA vaccine that contains Spike genetic code developed against COVID-19 (Blakney and Bekker, 2022). Although its use as a vaccine is new, studies have shown that it provides a strong immune response. Nucleic acid-based vaccines offer several benefits over traditional vaccinations, including simplicity of design, rapid manufacturing, and low production costs. In addition, gene vaccines can stimulate both cellular and humoral immunity. The main drawback of these vaccinations is that they must be kept at extremely low temperatures to preserve the genetic material.

Nucleic acid vaccines are promising because they are non-infectious, induce both T and B cell responses, and are suitable for large-scale production. However, issues involving the stability and immunogenicity of these vaccines have still not been fully resolved (Cuiling *et al.*, 2019).

1.2.2 Viral Vector Vaccines

This type of vaccine is based on combining the genetic material obtained from the target pathogen with a vector obtained from another virus that is incapable of replication in the host cell because essential genes do not exist and injecting this viral vector into the host. As they enable antigens to be expressed in the host cell, non-infectious or not-replicating recombinant viral vectors employed in vector-based vaccines induce a cytotoxic T cell response. Neither the viral vector, nor the antigen containing genetic material in these vaccines are not capable of causing infection. Also, there is no risk of the virus' genetic material being integrated into the host's DNA (CDC, Ura et al.2014). This kind of vaccination does not require the addition of an adjuvant since the CD8+-mediated response triggers the secretion of IFN and other cytokines. Adenovirus (AdV) vectors, modified vaccinia Ankara (MVA) vectors, influenza virus vectors, and adeno-associated viruses are the most used vectors in this type of vaccine. CanSino (Ad5-nCoV), Johnson & Johnson (JNJ-78436735/Ad26.COV), and Oxford University/AstraZeneca vaccine (AZD1222) are vaccines candidates that have been developed with adenoviruses of different serotypes. These vaccines are generated by combining the genetic information of the COVID -19 virus's immune-forming antigenic structure (full-length Spike protein) with adenovirus, whose potency has been decreased (Kyriakidis et al. 2021).

1.2.3 Whole Virus Vaccines

Delivery of the pathogen's attenuated or inactivated form is the foundation of whole virus vaccines designed to elicit a strong immune response. While inactivated vaccines contain pathogens inactivated by gamma radiation, chemical treatment, or heat, live attenuated ones contain weakened, non-replicating forms. In the late 1800s, Louis Pasteur, who laid the foundations of the vaccine concept, first used attenuated pathogens in his studies. Pasteur investigated how to create vaccines from weakened organisms and developed 'first generation' vaccinations against chicken

cholera, anthrax, and rabies (Plotkin et al. 2011). Those types of vaccines include the entire virus. Therefore, it is possible to develop protection from other viral structures in addition to the S protein that is the most widely used antigen in COVID vaccinations, resulting in immunity similar to patients who were infected by COVID-19. The main benefit of whole viral vaccines is that they induce robust both cellular and humoral immune responses. The response is long-lasting because they contain all of the virus' antigens. However, there is also a rare risk of infection due to problems with inactivation or attenuation processes. Therefore, such vaccines may not be appropriate for immune-compromised people (Kyriakidis *et al.*, 2021). Inactivated vaccine technology has been shown to function in humans. However, these vaccines require specialized laboratory equipment to successfully cultivate the pathogen, have relatively long manufacturing periods, and will almost certainly necessitate booster doses (WHO, 2021). Weakened or inactivated viral vaccines like CoronaVac (Sinovac), Covaxin, and BBIBP-CorV (Sinopharm) have been approved against COVID-19. The virus is chemically inactivated with beta-propiolactone in CoronaVac. The Vero cell line was used for inactivation in the Covaxin vaccine, and both were supplemented with Alum adjuvant to bolster the immune response. Besides these examples, there are other inactivated vaccines approved by various authorities, and many vaccine candidate phase studies are ongoing and under development (WHO, 2022).

1.2.4 Subunit Vaccines

Subunit vaccinations only include the parts, or antigens, that best excite the immune system rather than the whole virus. Therefore, these vaccines are also called acellular vaccines. Hepatitis B and acellular pertussis vaccines are the two most well-known subunit vaccines of numerous examples (GAVI). Protein, polysaccharide, and virus-like particle vaccines are the three sub-categories of protein subunit vaccines. Since these types of vaccines contains only certain antigenic parts instead of whole

pathogens, they do not carry any risk of infection and are very safe. Therefore, they can be administered to immune-suppressed patients (Clem, 2011).

Recombinantly synthesized antigen molecules (expressed in mammals, insects, yeasts, or prokaryotic systems) are purified and formulated into vaccines. VLP and protein subunit vaccines are unlikely to cause adverse effects and are biologically safe. However, subunit vaccines are not effective enough in inducing a solid CD8+ immunological response, which is crucial for intracellular pathogens because they contain few unique antigens. Therefore, an adjuvant must be included in the formulation of such vaccines (Hari *et al.*, 2021).

The Spike protein and its RBD region, which generate both neutralizing antibody and T cell responses, are the most used antigens in vaccine candidates developed against SARS-CoV-2 (Grifoni, 2020). The Nuvaxoid vaccine from Novavax is the first authorized subunit vaccine against COVID-19. SARS-CoV-2 Spike antigens were inserted into baculoviruses which infect insect cells. These recombinant viruses infect cells and make them express recombinant Spike protein in moth cells (SF9). The recombinant protein was formulated with Saponin-derived adjuvant Matrix-M, and a robust immune response against the SARS-2 virus was shown in phase studies (GAVI, 2022; Pulendran *et al.*, 2021).

1.3 Adjuvants

Ramon used the term adjuvant, firstly in 1924, to describe chemical or biological substances that, when combined with a particular antigen, produce a more significant immunological reaction against that specific antigen. Adjuvants are fundamental components of vaccines that boost their efficiency, as well as the potency and longevity of the immune response (Pulendran *et al.*, 2021). Purified subunit or synthetic vaccines created with recombinant technology or other contemporary methods are usually not very immunogenic, and these vaccine types require a potent adjuvant to elicit a strong and long-lasting immune response (Rabinovich *et al.*,

1994; Perraut et al., 1993). In 1926, Glenny, in his studies with diphtheria toxoid, discovered that a more robust immune response was obtained when he mixed alum salt with diphtheria toxoid. This study is one of the cornerstones of vaccine and adjuvant technology. Adjuvants trigger humoral and cell-mediated immune response in various ways. They can target Antigen-presenting cells (APC) and activate them or stimulate cytokine production. Also, they can slow the release of antigens, creating long-lasting immunity (Alving et al. 1992).

Since its discovery, the most used adjuvant is alum, which stimulates CD4+ helper T cells and antibody responses. Alum's adjuvant effects were primarily mediated by a "depot effect" process involving the gradual release of antigens from the vaccination site (Glenny et al. 1925). By generating tissue injury that results from activation of inflammatory DCs, alum can also trigger adaptive immunity (Kool, 2008). Alum mainly triggers the Th2 response; however, for clearance of intracellular pathogens, especially viral pathogens, Th1 mediated response is essential. For this reason, using a combination of different types of adjuvants together is the best option for the safety and efficacy of vaccines. As a TLR4 agonist, MPLA causes the synthesis of chemokines and cytokines that promote inflammation, which in turn causes the activation and recruitment of immune cells. It also triggers the synthesis of IL-2 and IFN- γ , resulting in a strong Th1 response that is important for the removal of pathogens (Mascart *et al.*, 2003; Ross *et al.*, 2013).

1.4 Variants

Small replication errors, known as mutations, naturally occur in the genomes of viruses when they replicate their genomes. Although most mutations hardly affect the virus's characteristics at all, some of these can alter the characteristics of the virus, such as its capacity to spread and the severity of the disease. Viruses with varying characteristics are called variants. Since the onset of the COVID-19 pandemic, the SARS-CoV-2 genetic variants shown in Figure 1.8 have emerged and spread worldwide.

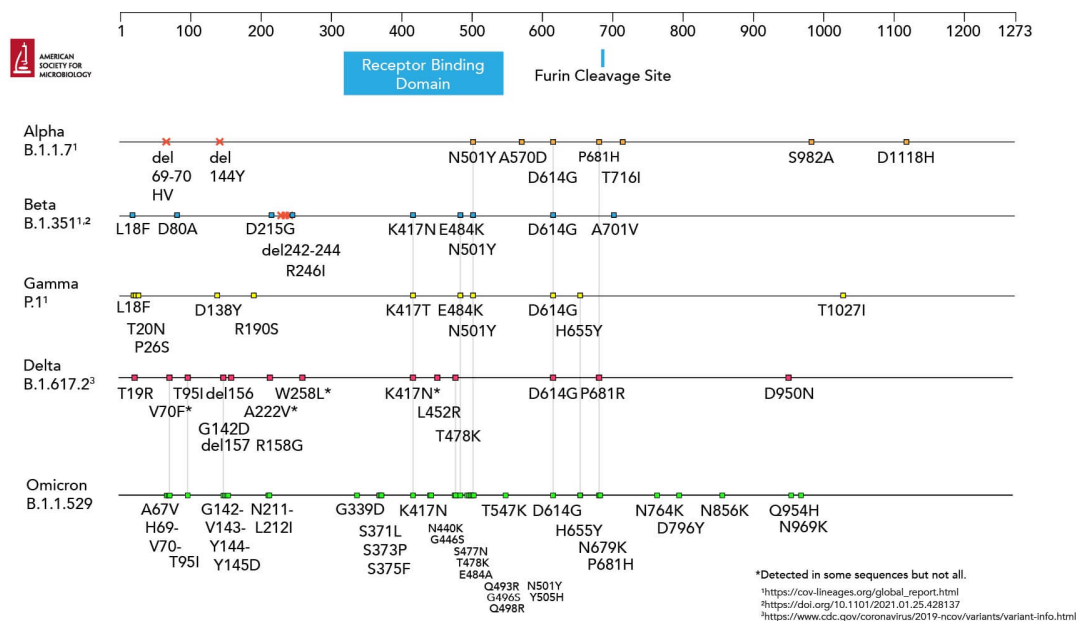


Figure 1. 8 Spike protein amino acid changes in SARS-CoV-2 variants of concern (Source: American Society for Microbiology)

The first coronavirus variant was discovered in the United Kingdom. B1.1.7, also known as the alpha variant, presented itself with eight key mutations in the Spike protein. The substitution of the 501st amino acid from these mutations is thought to boost the virus's affinity for ACE-2 and, consequently, its contagiousness (Nelson *et al.*, 2021). Furthermore, it has been discovered that 69-70 deletions in the NTD region of the virus improve infectiveness and make the virus more difficult to recognize with certain antibodies (Kemp *et al.*, 2021). After the Alpha variant, the Beta-B.1.351 variant with more severe symptoms was detected in South Africa. This variant was shown to be more resistant to monoclonal antibodies and convalescent serum neutralization than the Alpha variant. It is thought that the most crucial reason underlying its resistance to neutralization is the substitution mutation in residue 484 in the RBD (Wang *et al.*, 2021). In April 2021, a new variant surfaced in India, which spread significantly faster and exhibited probable antibody evasion (Singh *et al.*

2021). This variant, called the Delta variant, has substitutions at amino acid positions 452 and 478, unlike previous variants, while points 484 and 501 are the same as the original Wuhan strain. The L452R mutation suppresses host IFN production and facilitates escape from HLA-24-mediated cellular immunity and promotes viral replication by boosting the spikes stability and binding affinity to ACE2 (Motozono, 2021). According to Yadav's (2022) findings, the antibody titer neutralizing Delta variant was found to be two times lower than Alpha.

The B.1.1.529 variant known as Omicron was identified in December 2021, which contains many more mutations (over 30 on Spike alone) than previous variants (Guo et al. 2020). The virus's infectivity is higher, and its affinity for existing neutralizing antibodies is lower due to the N501Y and Q498R mutations, which are thought to increase affinity for ACE2 receptor, and the H655Y, N679K, and P681H mutations, which are thought to increase spike cleavage and facilitate virus transmission. As a result, the variant spreads more quickly (Yin *et al.*, 2022). Due to the large number of mutations in the Omicron genome, a severe decrease in immune serum neutralization ability appears to result in a decrease in vaccine efficacy. Still, T-cell-dependent immunity persists (Dejnirattisai *et al.*, 2022). There is a decrease in the effectiveness of vaccines containing only S antigen against the omicron variant and using the same vaccines as a booster will not provide sufficient protection (Bowen et al., 2022). As a result, approaches such as developing omicron-specific vaccines or vaccines comprising several antigens, as well as enhancing T-cell-dependent immunity, should be implemented.

1.5 Present Study

Even though many vaccines have been developed and are still being developed against SARS-CoV-2, the causative agent of the COVID-19 pandemic, and have had successful results from efficacy tests under development, new vaccine studies continue. The need for new vaccines against this disease continues for many reasons, such as safety issues, boosters, production costs, the sensitivity of mRNA vaccines,

and their need for cold chain transport. The existence of different subpopulations around the world and the different health systems of countries results in the need for different types of vaccines to be produced. Because of these differences, vaccines need to be evaluated not only in terms of efficacy but also in terms of safety, cost, accessibility, stability, duration of action, storage requirements, and modification versus variants (Nohynek *et al.*, 2022). This study is about the assessment of immunogenicity of vaccine antigens against the novel coronavirus produced using recombinant DNA technology. In protein-based vaccines, there is no risk of infection, as no whole virus is given to the body. In addition, there is no risk of developing myocarditis or pericarditis, which have been reported as the side effects of mRNA vaccines. For these reasons, protein-based vaccines are safer, especially for elderly individuals. In addition to being safer, protein-based vaccines are more convenient in terms of transport and storage conditions. Unlike nucleic acid or vector-based vaccines, the ability to be stored and transported in refrigerators for a long time without freezing is one of the most important advantages of protein-based vaccines. Moreover, using a prokaryotic expression system as a production method provides excellent convenience in the production phase.

This study was aimed to immunologically evaluate antigens that can be used for vaccine development studies, which are safe and less reactive, providing a high immunogenic response against SARS-CoV-2.

Regions with high concentrations of B and T cell epitopes were selected based on bioinformatic analysis (Grifoni *et al.*, 2020). Among the antigenically potent regions, the S1 fragment containing RBD was selected for a neutralizing antibody response. In contrast, the S2 fragment was predicted to be rich in T cell epitopes and was selected to induce cell-mediated response. Additionally, the N protein was chosen because it produced the most robust antibody response among SARS-CoV-2 antigens (Jiang *et al.*, 2020). These proteins were obtained by using recombinant DNA technology and the *E. coli* expression system and then formulated with AIOH3

and AlOH₃ + MPLA adjuvants. The cellular and humoral responses of immunized mice were next evaluated.

CHAPTER 2

MATERIALS AND METHODS

2.1 Bacterial Strains and Plasmids

In cloning studies, *Escherichia coli* DH5- α cells were employed as the bacterial host for the pGEM®-T Easy vector system, while *E. coli* BL21 (DE3) strain was used for expression studies with the pET-28a(+) expression vector to express recombinant antigens. pUNO1-SARS-2-S and pUNO1-SARS-2-N vectors were used in cloning studies as sources of target antigen gene sequences. In Table 2.1, the bacterial strains used in this study, their characteristics, and sources are listed, and plasmids are listed with markers and suppliers in Table 2.2. In Appendix A, the structures of the cloning and expression vectors are presented.

Table 2.1 *E. coli* strains that were used and their genotypes

Strain	Genotype	Obtained from
<i>Escherichia coli</i> DH5 α	F- <i>relA1 endA1, supE44(glnV44)</i> <i>thi-1 recA, gyrA96(NaIR) nupG</i> Φ 80dlacZ Δ M15, Δ (<i>lacZYA-</i> <i>argF</i>)U169 <i>hsdR17(rK- mK+)</i> <i>deoR481 purB20</i> λ -	ATCC
<i>Escherichia coli</i> BL21 (DE3 subtype)	F ⁻ <i>ompT dcm lon gal hsdS_B(r_B⁻</i> <i>m_B⁻)</i> λ (DE3 [<i>lacI lacUV5-</i> <i>T7p07 ind1 sam7 nin5</i>]) [<i>malB⁺</i>] _{K-} ₁₂ (λ^S)	Novagen,Merck (Germany)

Table 2.2 Cloning and expression vectors

Name	Length	Marker	Manufacturer
pGEM®-T Easy	3.0 kb	Amp ^r , lacZ	Promega Inc.
pET-28a(+)	5.3 kb	Kan ^r	Novagen, Merck
pUNO1- SARS-CoV-2 Spike	7.2 kb	Bsr ^r	Invivogen
pUNO1 SARS-CoV-2 Nucleocapsid	4.4 kb	Bsr ^r	Invivogen

2.2 Growth Media

Appendix B is a list of the composition of growth media and their preparation.

2.3 Solutions and Buffers

The descriptions of the buffer and the solutions are given in Appendix C.

2.4 Enzymes and Chemicals

Appendix D lists enzymes and chemicals utilized in this study as well as their suppliers.

2.5 Bacterial Strains' Maintenance and Growth Conditions

Two separate strains of *E. coli* were used for cloning and protein expression, DH5 α and BL21, and they were cultured in Luria agar (LA, Merck, Germany) plates and Luria Broth (LB, Merck, Germany) medium. The cultures were kept at 4°C on LA plates and passed to new plates on a monthly basis. The bacteria were cultivated in

liquid media until the mid-log phase, then combined with 30% glycerol in centrifuge tubes and divided into PCR tubes and freeze at -80°C for long-term storage. When antibiotics were required, suitable antibiotics were supplemented to LA and LB media. According to the resistance gene in the plasmid used, ampicillin or kanamycin antibiotics were supplemented into media, with final concentrations of 100 g/mL and 30 g/mL, respectively.

2.6 Design of Specific PCR Primers

Sequences of the primers for S1 and S2 gene fragments, as well as the nucleocapsid gene, were designed based on the sequence at the NCBI GenBank (accession number NC 045512.2).

Suitable restriction cut sites were added to both forward and reverse primers. Additionally, stop codons were added to reverse primers during primer design. NheI (5'-GCTAGC-3') restriction enzyme sites were introduced to forward primers of all three genes. SacI cut sites (5'-GAGCTC-3') were added to the reverse primers of the genes expressing S2 fragment antigen, and BamHI (5'-GGATCC-3') cut sites were added to the reverse primers of the S1 gene fragment and nucleocapsid gene (Table 2.3).

Table 2.3 PCR amplification primers. Restriction cut sites are underlined.

Primer name	Target ORF	Sequence	Size of PCR product
<i>S1-FP</i>	Spike/ S1	5'-cctctctcagaag <u>ctagct</u> gtacgttgaa-3'	819 bp
<i>S1-RP</i>		5'-acggac <u>ggatcct</u> taagtagtgcagca-3'	
<i>S2- FP</i>	Spike/ S2	5'-ttagcgggtacaatc <u>gctagc</u> ggttgacctttgg-3'	489 bp
<i>S2- RP</i>		5'-actgaggaaggag <u>agctct</u> taatagccctttcc-3'	
<i>N- FP</i>	Nucleocapsid	5'-ctgagatcacc <u>ggctagc</u> atgtctgataatgg-3'	1257 bp
<i>N- RP</i>		5'-atgtctggccag <u>ggatcct</u> taggcctgagtt -3'	

2.7 PCR (Polymerase Chain Reaction)

Oligomer Co. (Ankara, Turkey) provided the oligonucleotide primers listed in Table 2.3. The open reading frames of the S1 and S2 gene fragments were amplified via PCR with specialized primers designed with NheI and BamHI restriction cut sites for the S1-fragment gene and NheI and SacI (underlined) restriction cut sites for the S2-fragment gene from Full Spike (S) Expression Vector-Cat. Code: pUNO1-SARS2-S, Invivogen, and the N gene was amplified from Nucleocapsid Expression Vector-Cat. Code: pUNO1-SARS2-N– Invivogen using PCR. PCR was carried out using Phire Green Hot Start II PCR Master Mix (Thermo Scientific, USA).

The PCR mixture contained 25 µL of 2x Hot start Phire Green master mix, 0.5 µg of pUNO1 vector DNA as a template, 2.5 µL of each of the stock forward primer (10µM) and 2.5 µL stock reverse primer (10 µM), and nuclease-free dH2O to complete the total volume to 50 µL. Table 2.4 shows the amplification conditions for

three genes. Amplified products were loaded into 1% agarose gel to check the size of the amplified fragments.

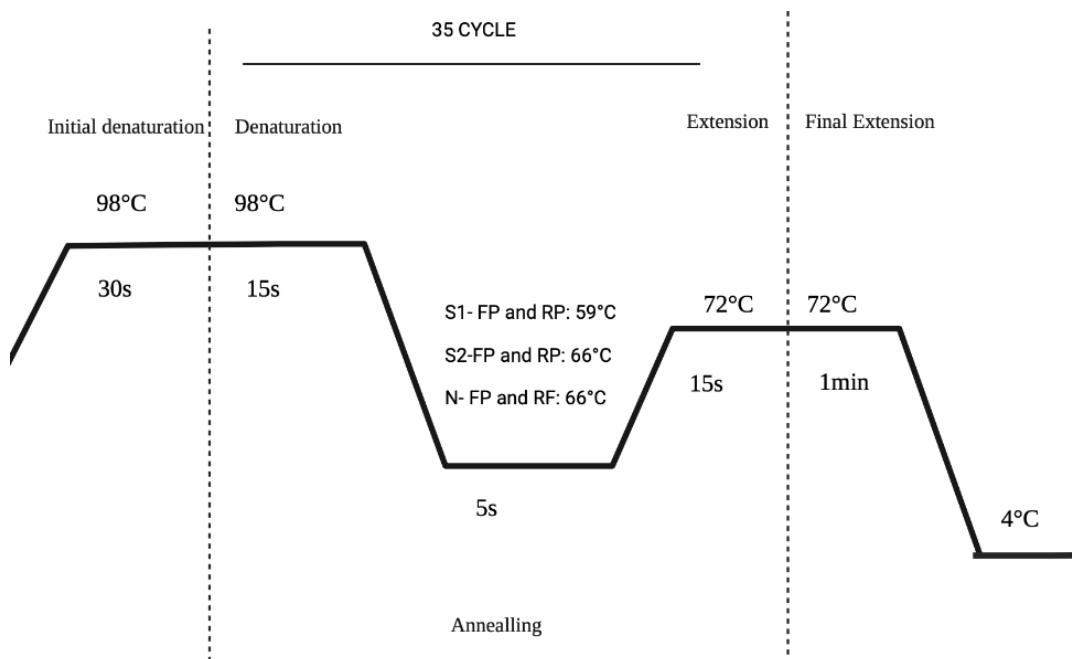


Figure 2.1 PCR conditions for S1, S2 gene fragments, and N gene.

2.8 Agarose Gel Electrophoresis

The agarose gel described in Appendix C was prepared with 1x TAE buffer. EtBr (Ethidium bromide) was added with a final concentration of 0.5 g/mL to stain the DNA, and TAE buffer was utilized as a running buffer in the electrophoresis tank. The concentrations of agarose gels were organized according to the size of the DNA run on the gel and gels of 1% concentration were used in this study. Samples were run at 90 volts for 45-50 minutes. Sample DNA was mixed with 6X loading dye before loading to help track them on the agarose gel. GeneRuler 1 kb Plus DNA ladder (Thermo Scientific, USA) was also loaded to the same gel as a reference to assess the size of the DNA of interest. The DNA bands of interest were seen using

the Vilber Lourmat Gel Imaging System (Vilber Lourmat, Marne-la-Vallee, France). The ThermoScientific-GeneJet Gel Extraction Kit was used to extract the desired gene fragments from the agarose gel after electrophoresis.

2.9 Ligation Reactions

After gel extraction, A addition was performed at 72°C for 30 minutes for A-T ligation. The reaction mixture is shown in Table 2.4. Then, as described in the user manual provided by the supplier, the PCR products were then inserted into the pGEM®-T Easy (Promega) cloning vector via TA-cloning and transformed to E. coli DH5α (Table 2.6). Table 2.7 shows the reaction mixture components for ligation into the pET-28a (+) vector. Both reaction mixtures were incubated at 4°C overnight for ligation to occur.

Table 2.4 A addition reaction mixture

Ingredient	Amount
10X Ligase Buffer	2 µL
dATP	0.4 µL
MgCl ₂	1.2 µL
Taq DNA Polymerase	1 µL
Insert DNA	15 µL
H ₂ O	Complete to a total volume of 20 µL

Table 2.5 pGEM-T Easy Vector ligation reaction mixture

Ingredient	Amount
2X Ligation Buffer	5 µL
50 ng pGEM-T Easy Vector	1 µL
DNA Ligase(T4)	1 µL
Insert DNA	50 ng

dH2O	Complete to a total volume of 10 μ L
------	--

Table 2.6 pET-28a (+) Vector ligation reaction mixture.

Ingredient	Amount
10X Ligation Buffer	1 μ L
pET-28a (+)Vector	100 ng
T4 DNA Ligase	1 μ L
Insert DNA	500 ng
dH2O	Complete to a total volume of 10 μ L

2.10 Preparation of Competent *E. coli* cells

With minor modifications, the competent cells of both *E. coli* DH5 α and BL21 (DE3) strains were prepared using the method described by Hanahan (1985). 50 to 100 mL of LB broth was inoculated with a single colony taken from an LB agar plate and incubated at 37°C at 200 rpm overnight. This was then used as a seed culture for the next step. A new flask containing 250 mL of LB broth was inoculated with a 3 mL seed culture such that the initial OD₆₀₀ was between 0.03-0.05. The culture was incubated at 37°C at 200 rpm until the cells enter the log phase, which was determined by OD measurement. When the OD₆₀₀ reached the range between 0.4-0.6, the culture was cooled by putting the flask on ice, and the cells were centrifuged at 3500 rpm for 5-10 minutes at 4°C. The cell pellet was then resuspended in 25 mL of cold-sterile CaCl₂-Buffer 1 (Appendix C) and chilled on ice for 10 minutes. The cells were then centrifuged at 3,500 rpm for 5-10 minutes at 4°C and the cell pellet was gently dissolved in 5 mL cold-sterile CaCl₂-Buffer 2. (Appendix C). Finally, the cells were divided into 350 μ L aliquots and stored at -80°C.

2.11 Transformation of Bacteria

Competent *E. coli* cells were taken from -80°C and put on ice for 5-10 minutes until they thawed before being used for transformation. In a separate microcentrifuge tube, 10 µL of ligation products were combined with 70 µL of DH5α competent cells. For transformation of BL21 strain, 75 µL of BL21 competent cells and 3 µL of ligation products were combined in a microcentrifuge tube and gently mixed. For 20 minutes, the mixture was chilled on ice. The cells were exposed to heat shock for 50 seconds at precisely 42°C using a water bath, then placed on ice immediately after the heat shock treatment. 920 µL of LB was then added to the cells, which were then incubated at 37 °C at 100rpm for 80 minutes. The cells were then centrifuged at 1000g for 10 minutes, 900 µL of the supernatant was removed, and the cells were resuspended in 100 µL culture medium. Finally, 100 µL of transformed cells were inoculated onto LA plates containing the appropriate antibiotic. Blue-white colony selection was used to select the recombinant colonies LA plates for blue-white colony selection were prepared using 80 mg/mL X-gal and 0.5 mM IPTG in addition to 100 mg/mL ampicillin.

2.12 Plasmid DNA Purification

Recombinant pGEM-T Easy and pET-28a (+) plasmids were isolated from 4 mL of the cultures grown overnight using the GeneJET Plasmid Miniprep Kit (Thermo Scientific, USA) as directed by the manufacturers' recommendations, and the concentrations of the purified plasmids were measured using a NanoDrop device. The isolated plasmids were loaded onto an agarose gel along with a DNA ladder to confirm their size, and isolated plasmids were frozen at -20°C for storage.

2.13 Restriction Enzyme Digestion

The genes encoding the S1 gene fragment and nucleocapsid were cut using NEB restriction enzymes; BamHI and NheI with a suitable buffer (17 μ L plasmid DNA + 2 μ L cut smart buffer + 0.5 μ L BamHI and 0.5 μ L NheI). The S2 gene fragment was cut with SacI and NheI with a suitable buffer (17 μ L plasmid DNA + 2 μ L cut smart buffer + 0.5 μ L SacI and 0.5 μ L NheI). These mixtures were incubated at 37°C for 45 min. After the restriction digestion, the plasmids were loaded onto agarose gel by adding NEB Gel Loading Dye, Purple (6X). After running for 1 hour at 60 V, the separated bands were extracted from the gel with Gel Extraction Miniprep Kit-GeneJET (Thermo Scientific, USA) according to the manufacturer's directions.

2.14 Recombinant Protein Overexpression and Extraction

Cells of recombinant *E. coli* BL21 (DE3) bearing S1, S2 gene fragments, and N gene under the control of the T7 promoter in pET28a(+) vector from a single colony were inoculated into 50 mL of LB (Merck, Germany) containing 30 μ g/mL kanamycin. These cells were grown at 37°C at 200-rpm for 16-18 hours. At the ratio of one in a hundred (2.5 mL), a seed culture was added into 250 mL of LB supplemented with kanamycin and cultured at 37°C at 200 rpm until the O.D.₆₀₀ reached 0.5-0.6, after which overexpression was initiated by supplementing the culture with IPTG at a final concentration of 1mM. An identical flask was cultured without IPTG to serve as a negative control. The culture was incubated at 200 rpm at 37°C for 5 hours to overexpress the recombinant protein. In order to obtain cell lysate for recombinant protein purification, 250 mL culture was divided into 50 mL Falcon tubes and the cells were harvested by centrifugation at 6000 g for 15 minutes at 4 °C and the removal of the supernatant. 5 mL Equilibration buffer (Appendix C) was added to the pellets and used to resuspend the cells. Following three cycles of freezing and thawing, the cells were resuspended and mechanically lysed on ice using a CP70T Ultrasonic Processor (Cole-Parmer, Vernon Hills, IL) 6 times for 10 seconds at 60%

amplitude. After the sonication process, the extract was centrifuged at 4 °C at 15.000 g for 20 min to discard cellular debris. The optical densities of the supernatants were measured at 280nm. To check for overexpression, the cell lysates containing recombinant proteins were run on SDS gels.

2.15 Recombinant Protein Purification

His60 Ni Gravity Columns (Takara, USA) with immobilized nickel ions were used to purify His-tagged recombinant proteins. The column was equilibrated using 5 mL equilibration buffer, then the filtered cell lysate was added onto the column and incubated by slowly inverting the column for 1 hour to allow the target proteins' polyhistidine tail to bind the nickel ions in the column. Then the column was washed using 20 mL wash buffer to allow untagged proteins flow through. Then, the his-tagged recombinant proteins were eluted from the column by adding an elution solution containing imidazole (Appendix C). The eluted proteins' optical densities were measured at 280nm. SDS-PAGE gel electrophoresis was performed to determine the protein purity, and the purified proteins were stored at -20°C for future analysis and vaccine formulations.

2.16 Determination of Protein Concentration

The optimized Bradford assay and OD280 measurements were used to determine the concentrations of the isolated recombinant protein samples. Bradford's approach relies on variations in absorbance generated by a dye that binds to protein. The cell lysate was combined with Bradford reagent, which included 250 mg of Coomassie Brilliant Blue G-250, 125 mL of 96 percent ethanol, and 250 mL of 85 percent ortho-phosphoric acid, which was diluted 1:5 with dH₂O. A calibration curve was constructed for calculating the protein concentrations using OD595 measurements of prepared BSA standards (Figure 2.2).

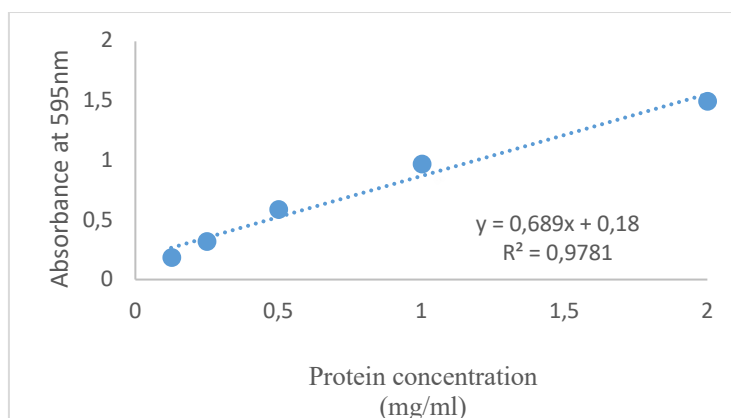


Figure 2.2 Protein concentration calibration curve.

2.17 Sodium Dodecyl Sulphate Polyacrylamide Gel Electrophoresis and Staining of Gels

All SDS-PAGE protocols were performed via a Bio-Rad Cell system (Bio-Rad, USA) with a 4.5% stacking gel and a 15% separation gel. The recipe for the gel is presented in Table 2.8. 6x sample loading buffer was added to track the samples on the gel (Appendix C). The samples were run under a 15mA current for 2 hours using a Mini-Protean electrophoresis device to separate the proteins. Following SDS-PAGE, the gel was stained with Coomassie Blue R-250 for 30 minutes. To remove the background staining, the stained gel was treated in a destaining solution (Appendix C).

Table 2.7 Polyacrylamide gel recipe for SDS-PAGE

	Stacking Gel (4.5%)	Separating Gel (15%)
Acrylamide/bis 30%	2.68 mL	10 mL
dH ₂ O	12.0 mL	4.6mL
Tris-HCl (1.5M)-pH 8.8	-	5 mL
Tris-HCl (0.5M)-pH 6.8	5 mL	-
SDS 10%	200 µL	200 µL
APS 10%	200 µL	200 µL
TEMED	20 µL	20 µL
Total volume	20 mL	20 mL

2.18 Western Blotting

Western blot analyses are based on Towbin's optimized method described in 1979. After performing SDS-PAGE, nitrocellulose membranes and 12 pieces of 3MM Whatman paper were cut into the same size with the polyacrylamide gel and soaked into transfer buffer (Appendix C). Whatman papers, membrane, polyacrylamide gel, and more Whatman papers were placed onto the Trans-Blot Turbo blotting system (Bio-Rad) in an order given in Figure 2.3. The proteins were then transferred from the gel to the membrane using a 1.5mA/cm² current for 8 minutes. Following the transfer, the membrane was incubated in a blocking buffer (TBS buffer supplemented with 10% skim milk), at 4°C overnight. Then, the membrane was washed with 1x TBS supplemented with a mild detergent (Tween-20) for 10 min and shaken gently at 25°C. The membrane was then incubated with 5% skim milk in 1x TBS buffer containing the 1/300 diluted immunized mice serum and shaken at room temperature for 2 hours. The membrane was then washed for 10 minutes before being incubated for 1 hour at 25°C with alkaline phosphatase-conjugated anti-mouse IgG antibody diluted in 5% skim milk added to TBS. The membrane was washed once more and the substrate was prepared according to Bio-Rad's instructions before usage (AP Conjugate Substrate Kit, Bio-Rad, USA). The membrane was incubated in the substrate until color development could be observed.

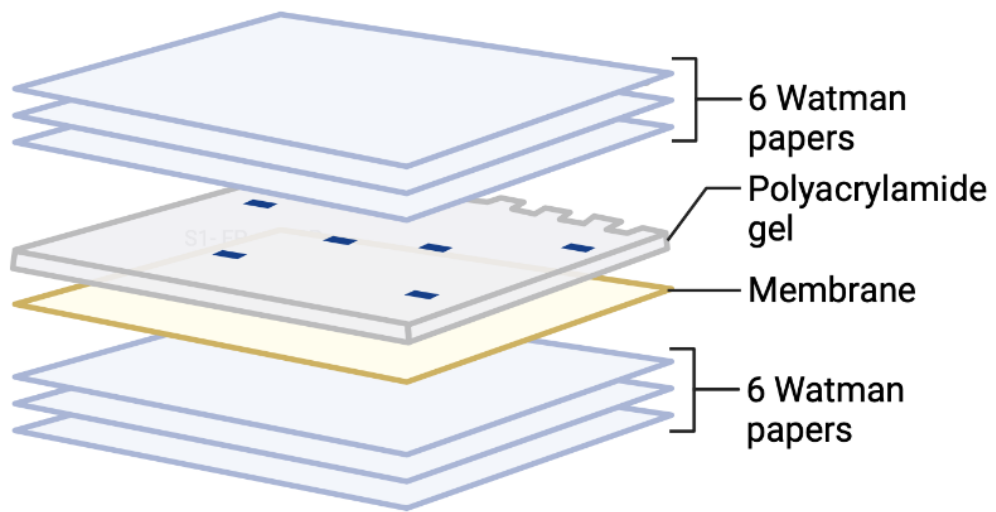


Figure 2.3 The sandwich setup diagram of Western blot transfer

2.19 Immunization Experiments

The Ethical Committee on Animal Experiments at KOBAY Experimental Animals Laboratory Co., Ankara approved the use of animals in our study (2020). Mice experiments were accordingly performed at their facilities with 18-20 g female BALB/c mice. Mice were injected with recombinant proteins adjuvanted with AIOH₃ or AIOH₃ + MPLAPHAD® formulation. Each injection was administered at 15 days intervals. To acquire sera, blood samples were drawn from the mice 14 days after the second injection. The blood samples were centrifuged at 5000 rpm for 20 minutes after being incubated at room temperature for 1 hour, and sera was collected from the upper portion of the tube and stored at -20°C.

2.20 Spleen Cell Culture and Detection of Antigen-Specific T-cell response (IFN-gamma)

The spleens of mice from the control and immunized groups were extracted aseptically and suspended in 5 mL of RPMI 1640 media supplemented with 10% FBS, 3% NEA, and 1% penicillin/ streptomycin (Biochrom, Cambourne, UK). The spleens were homogenized using a cell strainer, and the cells were counted using a hemocytometer. 1×10^6 cells were placed in each well in a 96-well plate, and RPMI was used to fill the remaining 250 μ L of the medium. The plate was incubated for 1 hour at 37°C in a CO₂ (5%) incubator before adding 30 μ g/mL of recombinant proteins S1, S2 or N, and concanavalin A (1mg/mL; Sigma). The latter was used as a control to stimulate cytokine production. To measure IFN-secretion, the culture supernatant was withdrawn after 72 hours.

Thermo Scientific's (Rockford, USA) Mouse IFN- Minikit was used to measure IFN secretion levels according to the manufacturer's recommendations. A Corning™ Costar™ 9018 ELISA 96 well plate was coated using Coating Buffer and 100 μ L/well of capture antibody per well (diluted 1:1000). The plate was incubated overnight at 4°C overnight with the lid on. Afterward, the wells were aspirated and washed three times using 250 μ L wash buffer. 200 μ L/well ELISA/ELISPOT Diluent was used to block wells. It was incubated at room temperature for one hour. The wells were rinsed and 100 μ L/well of samples were added that were prepared in dilutions of 1:4, 1:8, 1:16, and 1:32. They were then incubated overnight at 4°C. The plate was then aspirated and washed three times, and 100 μ L/well-diluted Detection Antibody (1:1000 dilution) was added to all wells. Then the plate was incubated for 1 hour at 37°C. The plate was then washed three times. 100 μ L diluted Streptavidin-HRP (1:1000 diluted in blocking buffer) was added to all wells and the plate incubated for 30 minutes at 37°C. The plate was then aspirated and washed three times. Then, 100 μ L 1X colorimetric substrate tetramethylbenzidine TMB Solution was added to each well and the plate was incubated for 15 minutes at 37°C. After

100 μ L of Stop Solution 1N acid solution was added to each well, and absorbance at 450 nm was measured.

2.21 Measurement of Antibody Titers with Enzyme-linked Immunosorbent Assay (ELISA)

Using sera from the immunized and control groups, IgG and IgG2a responses were quantitated by ELISA. Wells were coated using 2 μ g purified recombinant S1, S2 fragment, and N proteins dissolved in 100 μ L carbonate buffer and then incubated at 4°C overnight. Afterward, a 96-well ELISA plate was aspirated and washed three times. 100 μ L of the blocking solution described in Appendix C was added to each well and the plate was placed in an incubator for 1 hour at 37°C. Murine sera diluted with blocking solution in ratios of 1:100, 1:200, and 1:400 were used as primary antibodies, and after the addition of murine sera, the plate was incubated at 37°C for 1 hour. The plate was then aspirated and washed three times. The secondary antibody used was rat anti-mouse IgG2a alkaline phosphatase-conjugated (Southern Biotech, UK) and rabbit anti-mouse IgG alkaline phosphatase-conjugated (whole molecule) (Sigma-Aldrich) and was diluted in blocking solution at a ratio of 1:3000. The volume recommended by the manufacturer of the secondary antibody was added to each well. The plate was incubated at 37°C for 1 hour. The plate was then aspirated and washed three times. PNPP tablets (Thermo Scientific, USA) were used as an alkaline phosphatase substrate for the colorimetric detection of antibodies. Substrate tablets were dissolved in a suitable diluted buffer as described in the user manual, and the substrate solution was added to each well before they were incubated at 37°C in the dark for 15 minutes. Then, using Thermo Scientific Multiskan TM FC Microplate Photometer, OD_{405 nm} was measured.

2.22 SARS-CoV-2 Neutralization Assay

2.22.1 Microneutralization Assay

Detection of SARS-CoV-2 neutralizing activity was carried out in a BSL3 facility at Ankara University Faculty of Veterinary Medicine using live virus-based microneutralization (MN), using the method described by Hanifehnezhad (2020). Murine serum samples were diluted at 1:5 in High Glucose DMEM medium (Gibco GmBH, Germany). Then, an equal volume of SARS-CoV-2 (100TCID₅₀=105.2/mL) was mixed with serum samples and incubated at 37°C for 1 hour for neutralization. Then, Vero E6 cells were cultured in 24-well plates, and solutions containing SARS-CoV-2 and serum were injected into the wells. The negative control contained only DMEM culture media. The ability of each serum dilution to neutralize SARS-CoV-2 CPE (NT100) 100% of the time was tested four days after infection.

2.22.2 RBD-ACE-2 Binding Assay

A 96-well ELISA plate was coated with 4 µg of RBD-containing protein dissolved in PBS. The plate was kept at 4°C overnight. After the plate was thoroughly washed and dried, 2% BSA solution was added, and the plate was incubated at room temperature for 2 hours and shaken gently. Afterwards, sera diluted between 100-fold and 1600-fold using PBS were added and the plate was incubated for 1 hour while being shaken gently. 25 ng of biotinylated ACE-2 (BPS Biosciences, USA) was added to each well and the plate was incubated for another 30 minutes. After the plate was washed thoroughly, HRP-conjugated streptavidin (BPS Biosciences, USA) solution was added to each well, the plate was incubated for 1 hour and the plate was rewashed. Finally, TMB substrate was added for colorimetric detection, and was left in the dark for 10 minutes. Afterward, 1 N HCL was added to each well and the plate was scanned at 450nm.

2.23 Statistical Analyses

GraphPad Prism (GraphPad Software, USA) version 9.3 for MacOS was used to analyze the ELISA results for antibody titers using one-way ANOVA followed by Dunnett's multiple comparison test. Significance levels (p-value) were considered 0.05 for all studies.

CHAPTER 3

RESULTS AND DISCUSSION

3.1 Selection of the Most Appropriate Immunogens

Neutralizing antibodies protect the host by blocking the attachment mechanism of pathogens to the host cell. These antibodies can inhibit viruses before they bind their target surface receptors. Coronaviruses connect to human alveolar cells through the Spike glycoprotein on their viral surface (Park *et al.*, 2021). The Spike protein has been the main target in developing vaccines against SARS-CoV-2. In our study, the selected regions of the spike protein used to construct S fragment proteins were based on previous bioinformatic epitope analyses (Grifoni *et al.*, 2020; Crooke *et al.*, 2020), and accordingly, the regions comprising both T and B cell epitopes were chosen for molecular cloning. While the RBD in the S1 fragment is critical for neutralizing antibody responses, the S2 fragment with T-cell epitopes was selected to produce both a prolonged T-cell and a cytotoxic viral clearance response.

It was discovered that the antibody response elicited by the nucleocapsid protein may be more potent than that evoked by the Spike protein (Jiang *et al.*, 2020). Furthermore, N protein has been shown to boost IFN-gamma production (Lee *et al.*, 2021). Additionally, because the nucleocapsid protein is the most conserved one among coronaviruses, it was expected to have a low mutation rate as compared to the other structural proteins in newly developed variants. All these characteristics suggested that the nucleocapsid protein can constitute an excellent vaccine antigen.

3.2 Cloning of S1 and S2 Gene Fragments from Full Spike (S) Expression Vector pUNO1-SARS2-S, and Nucleocapsid Gene from Nucleocapsid Expression Vector pUNO1-SARS2-N

3.2.1 Amplification of S1 and S2 Gene Fragments and Nucleocapsid Gene and Cloning into pGEM-T Easy Vector

S1 and S2 gene fragments were amplified by PCR by adding start-stop codons and restriction enzyme cut sites, NheI and BamHI restriction sites for the 819bp long S1, and NheI and SacI restriction sites for the 489bp long S2 fragment from the pUNO1-SARS2-S purchased from InvivoGen (USA). The regions of the S1 and S2 fragments were determined by selecting the regions of the Spike gene that contain B-cell and T-cell epitopes respectively. The N gene was amplified using the Nucleocapsid Expression Vector pUNO1-SARS2-N also purchased from InvivoGen via PCR with N-FP and N-RP primers that contain NheI and BamHI restriction sites and the stop codon. N gene is 1257bp long and consists of 419 amino acids. (Figures 3.1, 3.2, and 3.3)

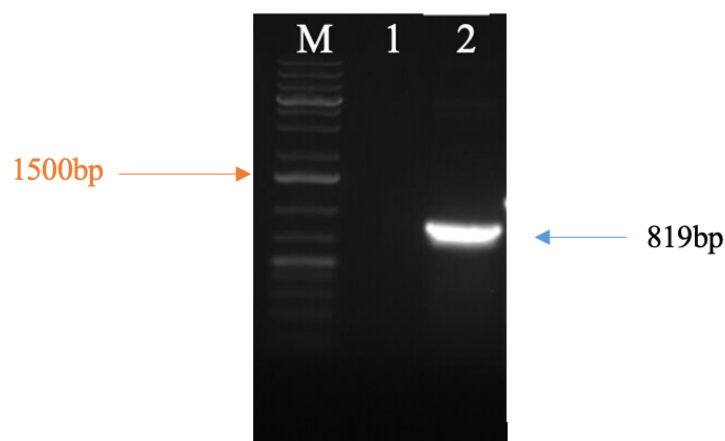


Figure 3.1 The S1 gene fragment amplification product. Lane 1: No template control, Lane 2: 819 bp long S1 gene fragment, M: GeneRuler™ DNA marker.

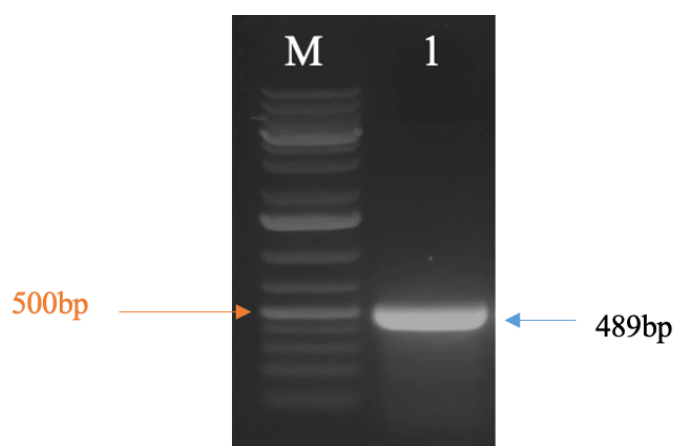


Figure 3.2 The S2 gene fragment amplification product. Lane 1: Amplification of 489 bp long S2 gene fragment, M: GeneRuler™ DNA marker.

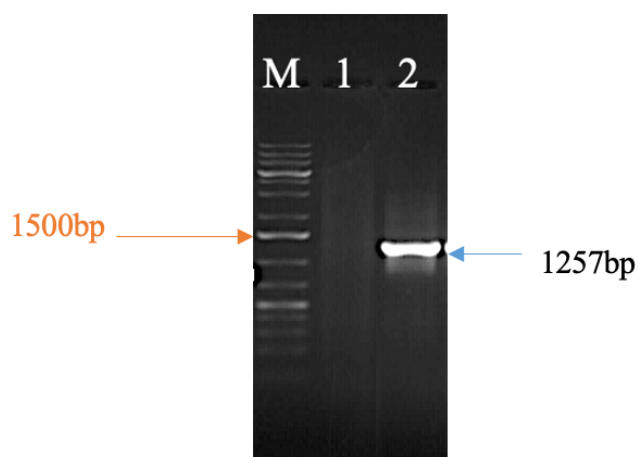


Figure 3.3 N gene amplification product. Lane 1: No template control, Lane 2: Amplification of 1257 bp long N gene, M: GeneRuler™ DNA marker.

Following the PCR amplification, the PCR clean-up protocol was performed using the GeneJet PCR Clean-up kit. The human codon-optimized S1 and S2 gene fragments and nucleocapsid expressing gene were subcloned into the pGEM-T Easy vector.

Chemically competent *E. coli* DH5 cells were transformed with recombinant plasmids and were inoculated onto LA plates supplemented with ampicillin, IPTG, and X-gal to identify recombinant colonies. White colonies were selected, and plasmids were isolated from transformant colonies. Restriction enzyme digestion was performed to confirm that the insert was present. BamHI and NheI restriction enzymes were used to digest plasmids containing the S1 and N genes, while NheI and SacI enzymes were used for the S2 gene (Figures 3.4, 3.5, and 3.6).

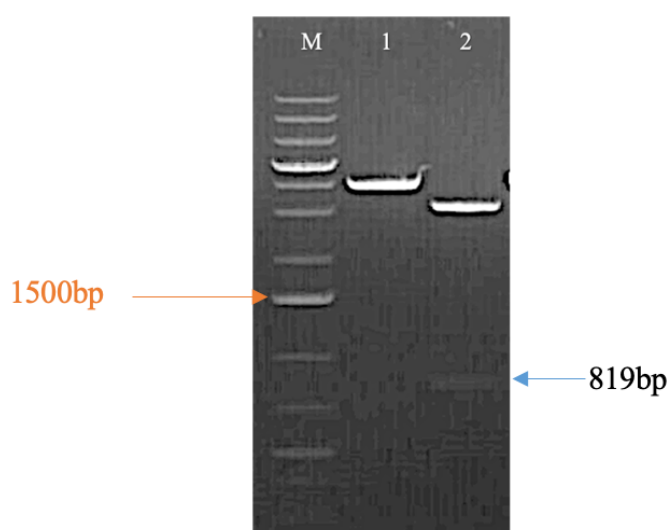


Figure 3.4 Validation of S1 gene fragment cloned in pGEM-T Easy vector. Lane 1: BamHI digested pGEM-T-S1, Lane 2: BamHI-NheI double digested pGEM-T-S1. M: GeneRuler™ DNA marker.

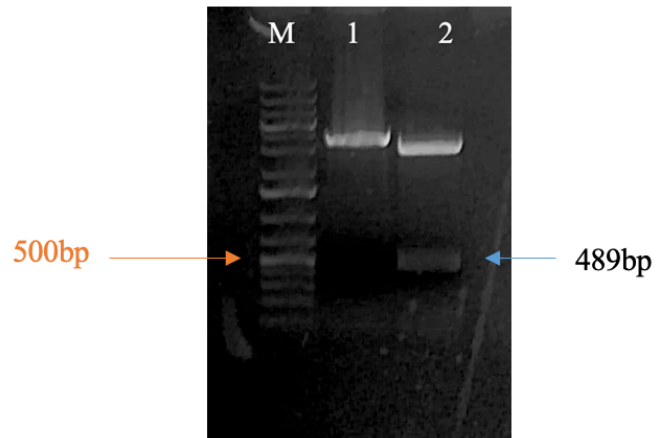


Figure 3.5 Validation of cloning of S2 gene fragment into pGEM-T Easy vector. Lane 1: BamHI digested pGEM-T-S2, Lane 2: BamHI-SacI double digested pGEM-T-S2. M: GeneRuler™ DNA marker.

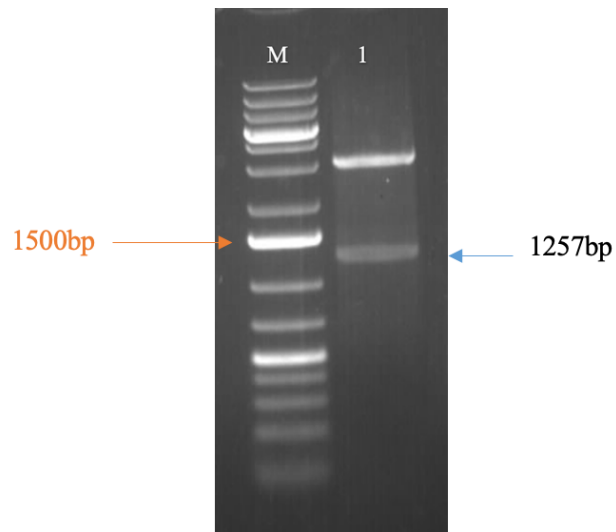


Figure 3.6 Validation of cloning of N gene in pGEM-T Easy vector. Lane 1: BamHI-NheI double digested pGEM-T-N. M: GeneRuler™ DNA marker.

The nucleotide sequences for the three genes are shown in Figures 3.7, 3.8, and 3.9 in the appropriate FASTA format. pUNO-S and pUNO-N vectors reference sequences NC_045512.2 and NC_045512.2 ,respectively, are based on the Wuhan-Hu-1 isolate.

```
TGCACCTCAAGAGCTTACCGTTGAGAAGGGGATTACCAAACAGTAATTTCCGGGTCCAACCCACCGAAAGCATTGTGCGGTTCCCAATATACCAATCTG
TGTCCTTTGGCGAAGTGTCAATAGTACAAGGTTTGTCTTGTGTACGCATGGAATAGGAAACGCATCTCCAATTGTGTCGCTGATTACTCCGTGCTGTACAATT
CCGCCTTTTCTCAACCTTCAAGTGTATGGCGTTTACCTACCAAACCTTAACGACCTGTGCTTCACTAATGTGTATGCCGACTCTTTTGTGATACGAGGGCGATGA
AGTGAGACAGATTGCACCAGGGCAGACCAGCAAAATGCGGACTACAACACTACAGCTTCCAGATGACTTTACCGGATGTGTTATTGCTAGAACTCAAAACAATC
TGGATTCGAAGTGGTGGCACTATAACTACCTGTATAGACTGTTACAGAAATCCAACCTGAAACCTTCGAGCGAGATATAAGCACAGAAATCTACCGGCT
GGAAGTACCGCTGCAACGGCGTGAAGGGTCAACTGTACTTCCATTGCAGAGTTACGGATTCCAGCTACAACGGGGTGGTTACCAACCTATCGTGTG
GTAGTCTGAGTTTGTAGCTCTCCATGCCCGCAGCAGTCTGTGGCCCAAGAAAAGCACCATACTGGTGAAGAACAAATGCGTGAACCTTAACTTAAACGGA
CTCAGGAACCGGCTATTGACGGAGAGTAACAAGATTCTGCCATCCAGCAGTTCCGTCGCGATATTGCCGACTACC
```

Figure 3.7 Nucleotide sequence of S1 fragment amplicon.

```
GGGTGGACATTCGGAGCTGGCGCTGCCTTCAGATTCTTTTGTATGCAGATGGCCTACCGTTTAAACGGCATCGGTGTGACACAAAACGTTCTGTATGAAAAC
AGAACTCATCGCAACCAAGTTCAACAGTGTATCGGTAAGATACAGGATAGCCTGTATCCACTGCCAGCGCATTGGGAAAAGTTGCAGGATGTAGTGAACCCAG
AATGCCAGGCATTAACACCCCTGGTGAACAGCTCTCTTCAAAATTTGGTGGCATTCTAGCGTGTGAATGACATAGTACGGCGTTGGACAAGGTGGAGGCT
GAAGTGCAGATTGATAGCTGATAACTGGCGCCTTCAGTCTTTCAGACTATGTGACCCAGCAGCTATCCGCGCTGTGAATTCGCGCATCCGCTAACCTG
GCAGCAACAAAATGTCGAGTGTGTGTTGGTTCAGTCTAAGAGAGTGACTTTTGGCGGAAGGGTAT
```

Figure 3.8 Nucleotide sequence of S2 fragment amplicon.

```
ATGCTGATAATGACCCCAAAATCAGCGAAATGCACCCGCATTACGTTTGGTGGACCCCTCAGATTCAACTGGCAGTAACAGAAATGGAGAACCGAGTGGGGC
GCGATCAAAACAACGTCGGCCCAAGGTTTACCAATAATACTGCGTCTTGGTTACCGCTCTCACTCAACATGGCAAGGAAGACCTTAAATCCCTCGAGGACA
AGGCGTTCCAATTAACACCAATAGCAGTCCAGATGACCAAATGGCTACTACCGAAGAGCTACCAGACGAATTCGTGGTGTGACGGTAAAATGAAAGATCTCA
GTCCAAGATGGTATTTCTACTACCTAGGAACCTGGGCGAGAAGCTGGACTTCCCTATGGTGTCAACAAAGACGGCATCATATGGGTTGCAACTGAGGGAGCCTTGA
ATACACCAAAAGATCACATTGGCACCCGCAATCTCTGCTAACAAATGCTGCAATCGTGTCACACTTCTCAAGGAACAACATTGCCAAAAGGCTTCTACGCAGAAG
GGAGCAGAGGGCGGCAGTCAAGCCTCTTCTGTTCTCTATCAGTGTGCAACAGTTCAAGAAATCAACTCCAGGCAGCAGTAGGGGAACTTCTCTGTAGAA
TGGTGGCAATGGCGGTGATGCTGCTTGTCTGCTGCTGTGACAGATTGAACAGCTTGAAGAGCAAAATGTCTGGTAAAGGCCAACAACAAGGCCAAA
CTGTACTAAGAAATCTGTGCTGAGGCTTCTAAGAGCCTCGCAAAAACCTACTGCCACTAAAGCATACAATGTAACACAAGCTTTGGCAGACGTTGGTCCAG
AACAAACCAAGGAAATTTGGGGACCAGGAATAATCAGACAAGGAAGTATTACAAAATTTGGCCGCAAAATGACACAATTTGCCCCAGCGCTTACGCGTTCT
TCGGAATGTCGCGCATTGGCATGGAAGTACACCTTCGGGAACGTGGTTGACCTACACAGGTGCCATCAAATGGATGACAAAAGATCCAAATTTCAAAGATCAAG
TCATTTGCTGAATAAGCATATTGACGCATACAAAACATTTCCCAACAACAGAGCCTAAAAAGGACAAAAGAAAGGAGGCTGATGAAACTCAAGCCTTACCGCAG
AGACAGAAGAAACAGCAAACTGTACTTCTTCTGCTGCAGATTTGGATGATTTCTCCAACAATTGCAACAATCCATGAGCAGTGTGACTCAACTCAGGCC
```

Figure 3.9 Nucleotide sequence of N gene amplicon.

Computer-based analysis was used to determine the molecular weights and pI values of proteins (Table 3.1). Protein purification heavily depends on pI values. Because proteins become neutral and tend clustering at or near to their own pI point, identical pI and pH values should be avoided in buffers used for purification.

Table 3.1 Computer-aided analyses of S1, S2 gene fragments and nucleocapsid genes and the respective proteins

Gene	Nucleotide (bp)	pI	Amino acids	Molecular weight (kDa)	Net charge at pH 7.0	G-C content (%)
S1	819	8.59	273	33 kDa	7.4	35.5
S2	489	7.58	163	17.6 kDa	3.9	37.6
N	1257	10.58	419	46 kDa	24.4	47.3

3.2.2 Subcloning of RBD-containing S1 Gene Fragment, S2 Gene Fragment, and Nucleocapsid Gene into pET-28 a (+) Expression Vector

Human codon-optimized S1 and S2 gene fragments and Nucleocapsid (N) expressing genes were subcloned from the pGEM-T Easy vector to pET28a(+) expression vector at the BamHI and NheI restriction sites for S1 gene fragment and nucleocapsid gene, and at the SacI and NheI restriction sites for S2 gene fragment. The T7 promoter directs gene expression in the pET-28a(+) expression vector, which has His-tag sequences at both the C and N termini. S fragments and N gene were cut from the pGEM-T vector using appropriate enzymes, and the genes were isolated from agarose gel separate from the vector. At the same time, the expression vector pET-28a was cut with the same enzymes. S fragments and N gene were then ligated to pET-28a(+). *E. coli* Dh5 α cells were transformed using pET-28a(+) carrying the insert. Cells were inoculated on LB agar plates containing kanamycin, and thus recombinant vectors containing the genes of interest were obtained. Plasmids from recombinant colonies were isolated to transform *E. coli* BL21 cells, and the plasmids were isolated and digested using appropriate restriction enzymes again to confirm cloning. BamHI and NheI enzymes were utilized for restriction enzyme digestion to

verify the S1 and N genes, and NheI and SacI enzymes were used for the S2 gene (Figures 3.9, 3.10, and 3.11).

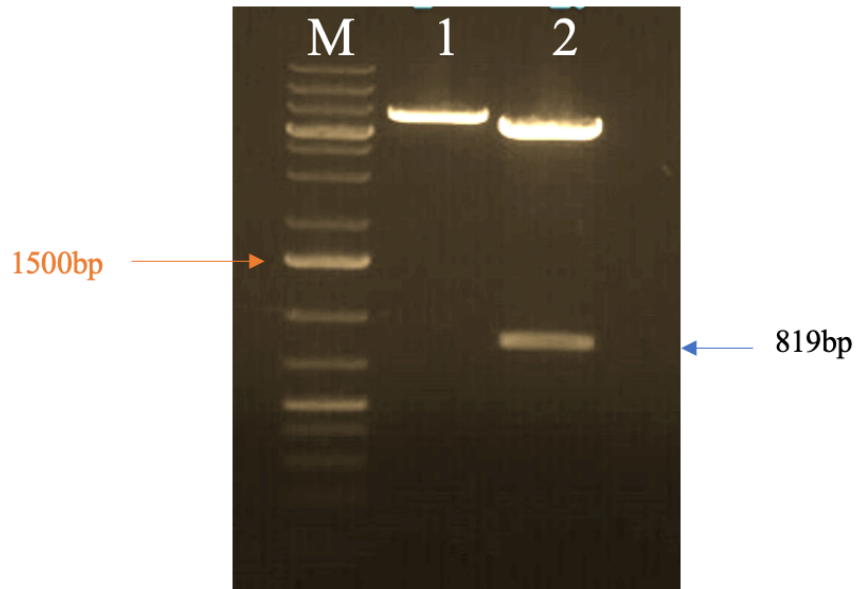


Figure 3.10 Verification of cloning of S1 gene fragment into pET28a(+). Lane 1: BamHI digested pET28a(+)-S1, Lane 2: BamHI-NheI double digested pET28a(+)-S1. M: GeneRuler™ DNA marker.

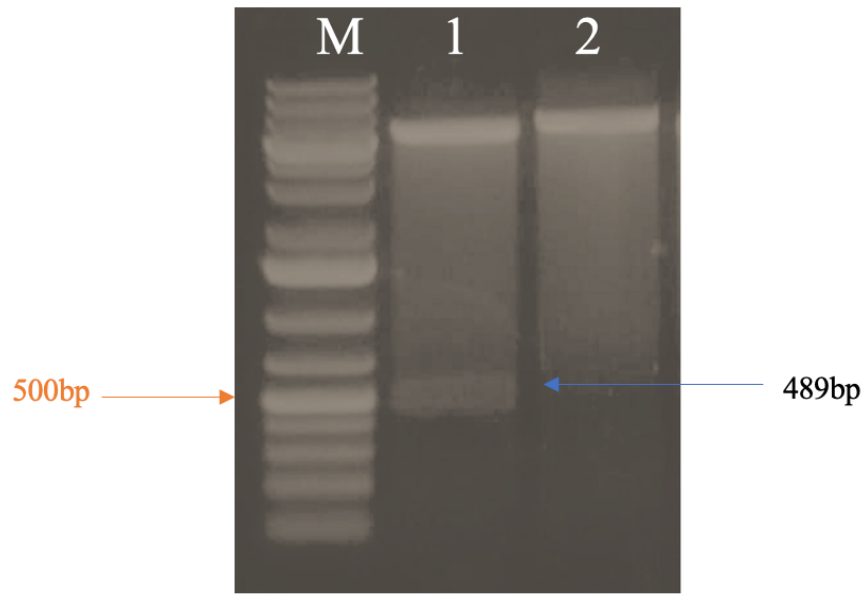


Figure 3.11 Verification of cloning of S2 gene fragment into pET28a(+). Lane 1: SacI-NheI double digested pET28a(+)-S2. Lane 2: SacI digested pET28a(+)-S2. M: GeneRuler™ DNA marker.

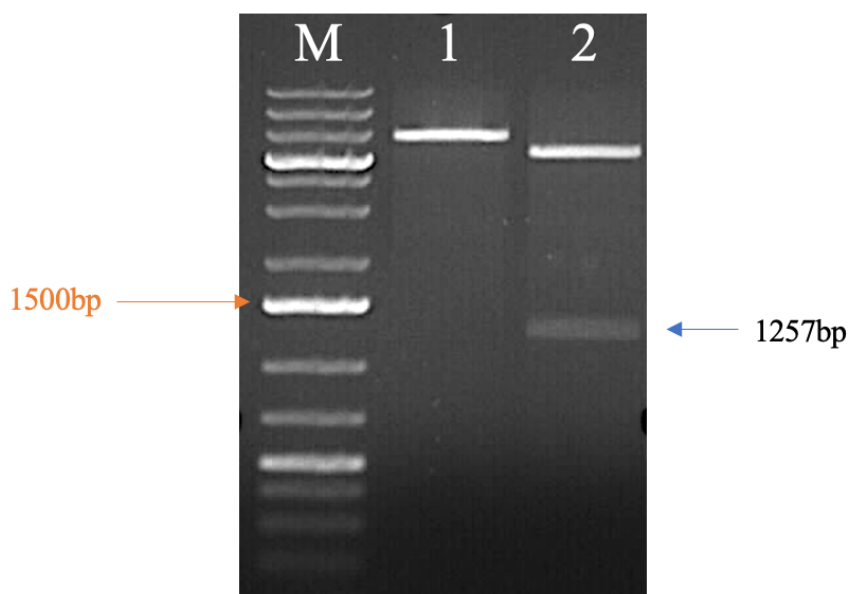


Figure 3.12 Verification of cloning of Nucleocapsid gene into pET28a(+). Lane 1: BamHI digested pET28a(+)-N, Lane 2: BamHI-NheI double digested pET28a(+)-N. M: GeneRuler™ DNA marker.

3.3 Expression of Recombinant S1, S2 Fragment Proteins and Nucleocapsid Proteins in *E. coli* BL21 (DE3)

Prokaryotic expression systems, particularly *E. coli*, among expression hosts like mammal, yeast, insect, or plant, was chosen because it is suitable for mass production and is available with a variety of molecular manipulation techniques; also it provides fast breeding, low-cost, high expression, easy purification of product and a broad variety of applications(Sun et al., 2021). However, *E. coli* has a limited capacity for post-translational changes because of its straightforward cellular anatomy. Complex protein products could have poor biological activity. In addition, improper protein folding can result in insoluble aggregates that are difficult to purify, from forming in the cytoplasm(Perdew et al. 2008, Lodish et al., 2008).

The lacUV5 promoter of the pET28a vector, which directs transcription of T7 RNA polymerase expressed in *E. coli* BL21 cells, can be induced using IPTG. Overexpression of cloned genes and gene fragments is dependent on IPTG induction. Therefore, pET28a recombinant vector carrying target genes was purified and transformed into *E. coli* BL21 cells that were next induced for overexpression.

For each sample, two LB media were inoculated with *E. coli* BL21 (DE3) cells containing recombinant pET-28a(+) plasmids. One culture was treated with IPTG to induce the production of recombinant His-tagged S1 fragment protein (33 kDa), S2 fragment protein (17.6 kDa), and Nucleocapsid protein (46 kDa), while the other served as an uninduced control (Figures 3.13, 3.14 and 3.15).

To assess whether the genes were overexpressed, SDS-PAGE was carried out on the cell lysates and compared to the control lysate. In the polyacrylamide gels, the overexpressed protein appeared as a thick band after staining with Coomassie blue.

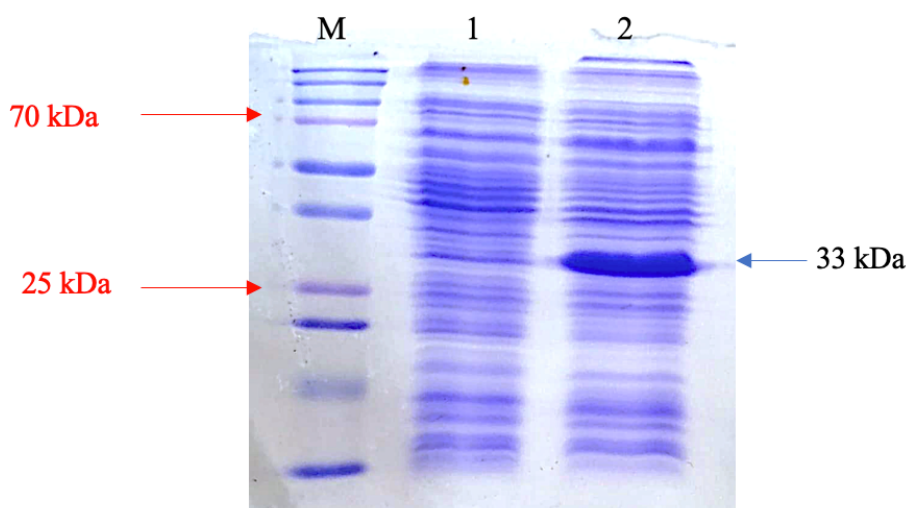


Figure 3.13 SDS-PAGE detection of the expressed recombinant S1 fragment protein. M: Marker (Pageruler[™] marker, #26619), Lane 1: Control, Lane 2: overexpressed S1 fragment protein

The Coronavirus spike protein is rich in aromatic amino acids. Therefore, its solubility in water is relatively poor. Overexpressed proteins may cluster into protein aggregates known as "inclusion bodies" in prokaryotic systems. A denaturing substance should be used to help dissolve these protein aggregates. Urea is an excellent denaturant and disrupts secondary structures inside and between proteins by interfering with hydrogen and disulfide bonds. In this study, 8M urea was used to extract S1 and S2 fragments, while 2M urea was utilized for extraction of N as it did not form inclusion bodies that extensively.

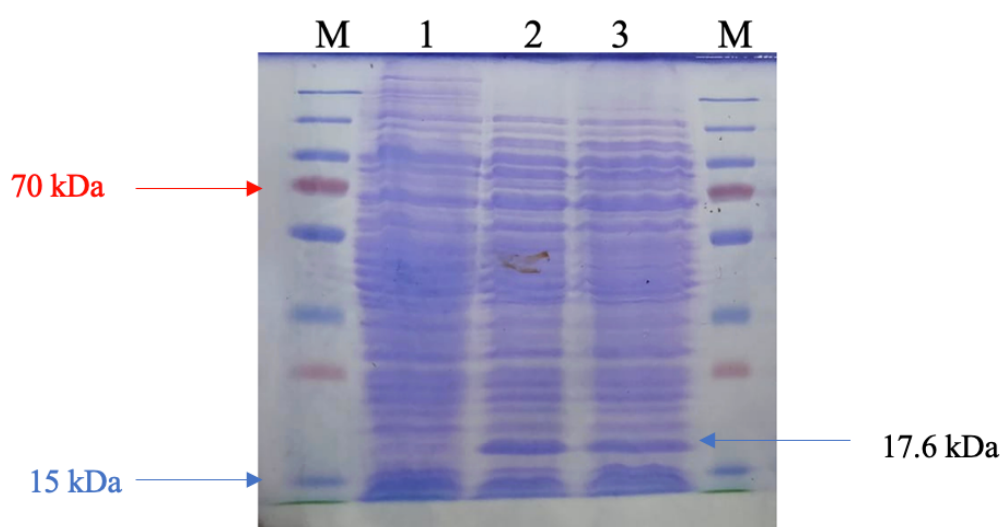


Figure 3.14 SDS-PAGE analysis of recombinant S2 fragment protein expression. M: Marker (PAGERULER™ marker, #26619), Lane 1: Control, Lane 2,3: Expressed S2 fragment protein (IPTG- induced sample).

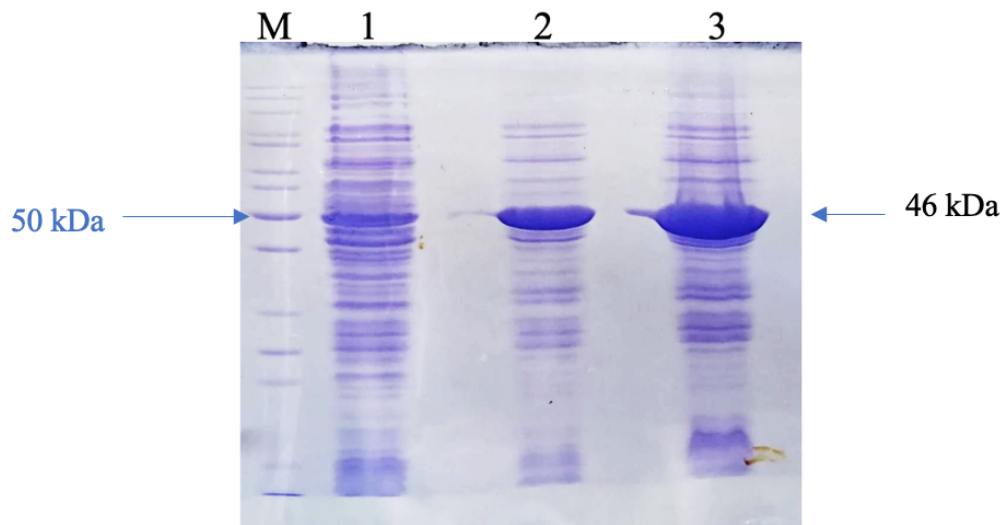


Figure 3.15 SDS-PAGE detection of the expressed recombinant S1 fragment Nucleocapsid protein. M: Marker (Pageruler[™] marker, #26614), Lane 1: Control, Lane 2,3: Expressed Nucleocapsid protein (IPTG- induced sample).

The size of the overexpressed proteins appeared a bit higher than expected on the SDS-PAGE gels due to the addition of His-tag which adds an extra molecular weight of approximately 2.5 kDa.

3.4 Purification of Poly-His-Tagged Recombinant S1, S2 Fragment Proteins, and Nucleocapsid Proteins via Affinity Column Chromatography

His-tagged overexpressed proteins were next isolated using Takara Ni60 columns (USA) that contain Ni-IDA resin, utilizing the binding of the columns' immobilized nickel ions to histidine tags for purification of His-tagged proteins. The SDS-PAGE images of the purified proteins are given in Figure 3.16, 3.17 and 3.18. Because of its small size, hydrophilic nature, insignificant effect on protein folding and

biological activity, and minimal immunogenicity, the PolyHis tag is very suitable for the purification of recombinant antigens (Costa *et al.* 2018). Because of these features, it does not interfere with the immune response caused by the protein of interest. Therefore, this tag was not separated from purified proteins, and if an effect on immunogenicity was seen, it could have been cut off from the TEV cleavage site. After purification, the proteins were filter-sterilized, and those with low concentrations were concentrated using concentrators and stored at -20°C.

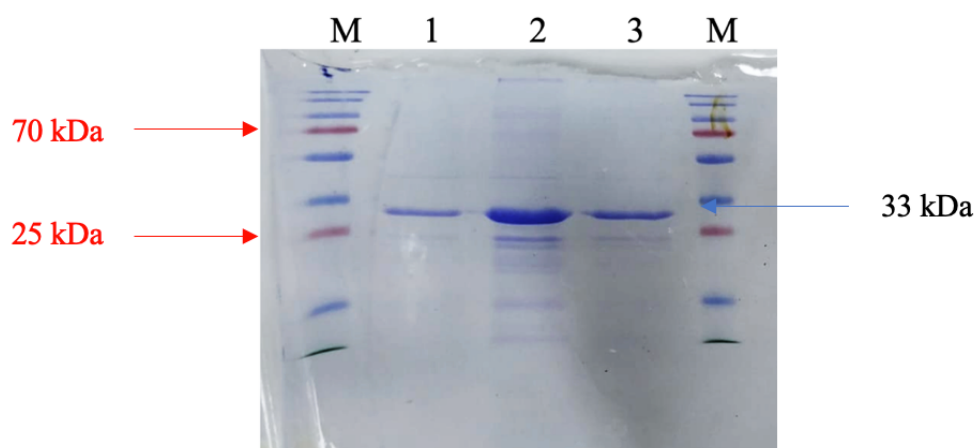


Figure 3.16 SDS-PAGE detection of purified recombinant S1 fragment protein. M: Marker (Pageruler[™] marker, #26630), Lane 1: Purified S1 fragment protein first eluate, Lane 2: Purified S1 fragment protein second eluate, Lane 3: Purified S1 fragment protein third eluate.

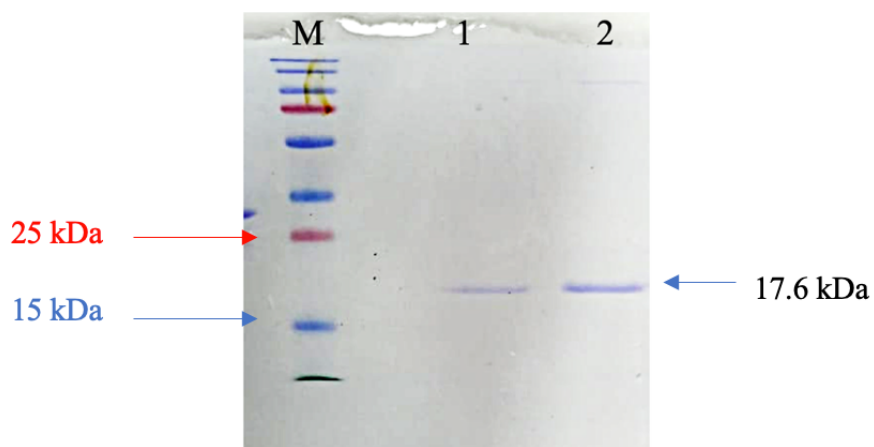


Figure 3.17 SDS-PAGE detection of purified recombinant S2 fragment protein. M: Marker (Pageruler[™] marker, #26630), Lane 1: Purified S2 fragment protein first eluate, Lane 2: Purified S2 fragment protein second eluate.

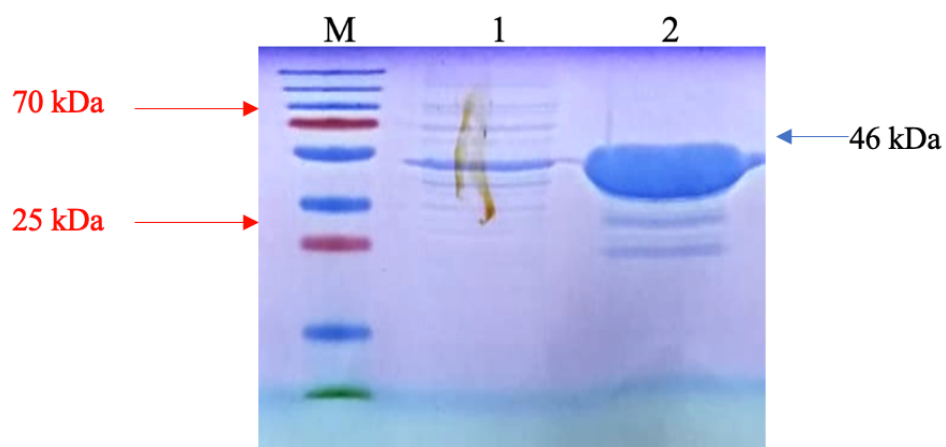


Figure 3. 18 SDS-PAGE detection of purified recombinant N protein. M: Marker (Pageruler[™] marker, #26630), Lane 1: Purified N protein first eluate, Lane 2: Purified N second eluate.

3.5 Western Blot Analyses of Recombinant S1, S2 Fragment Proteins, and Nucleocapsid Proteins

Western blot experiments were performed as previously described using sera collected from mice.

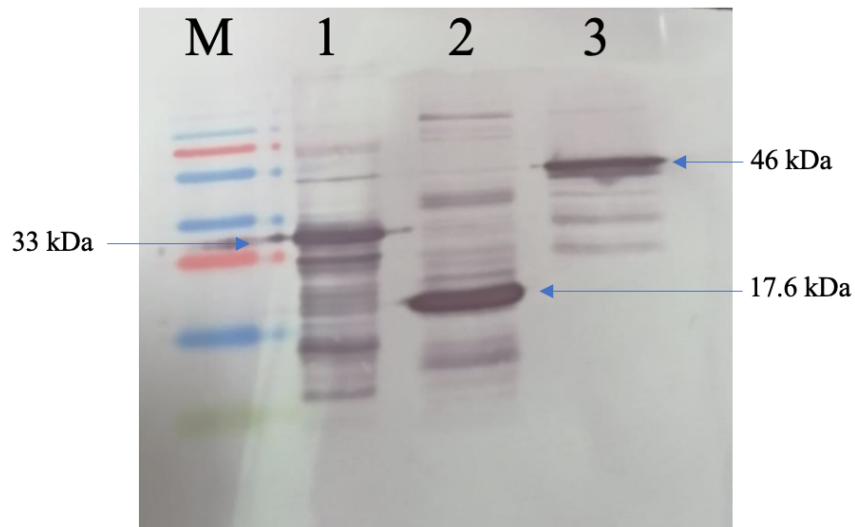


Figure 3.19 Western blot analysis using the serum against Spike protein fragments and Nucleocapsid protein. Lane 1: S1 fragment protein elute, Lane 2: S2 fragment protein elute, Lane 3: Nucleocapsid protein eluate. M: Marker (Pageruler[™] marker, #26630),

The antibodies produced in the immunized mice, as shown in Fig 3.19, interacted strongly with S1 fragment protein (33 kDa), S2 fragment protein (17,6 kDa), and Nucleocapsid protein (46 kDa), as predicted.

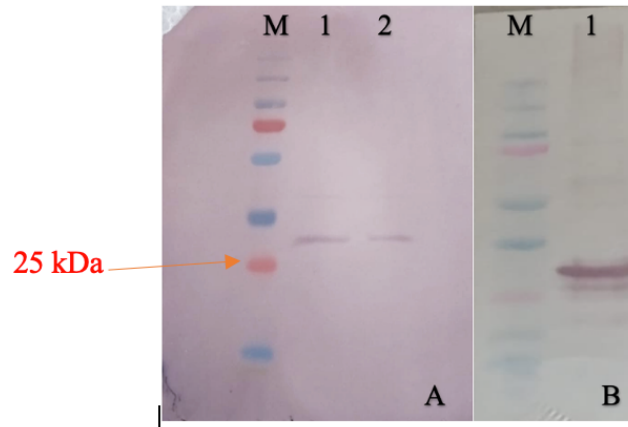


Figure 3.20 SARS-CoV-2 Spike S1 fragment protein (pS1: 33 kDa) WB analysis with A, M: Marker (Pageruler™ marker, #26630), Lane1-2:SARS-Cov-2 Coronavirus Spike Monoclonal Antibody (Invivogen, Anti-Spike-RBD-mIgG2a-CR2022) and B, M: Marker (Pageruler™ marker, #26630), Lane1: Immunized mice serum.

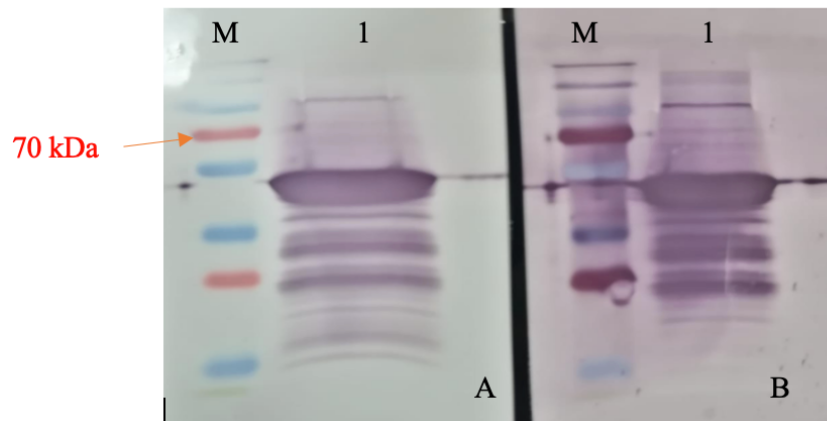


Figure 3.21 SARS-CoV-2 Nucleocapsid protein (pN: 46 kDa) WB analysis with A, M: Marker (Pageruler™ marker, #26630), Lane1: SARS-Cov-2 Coronavirus Nucleocapsid Monoclonal Antibody (Invitrogen-ThermoFisherScientific-MA5-29981) and B, M: Marker (Pageruler™ marker, #26630), Lane1: Immunized mice serum.

Western blot analyses were performed in parallel by using monoclonal antibodies (mIgG2a- CR2022 for S1 and mIgG1- MA5-29981 for N) and immunized mouse sera to demonstrate that the antibody response of mice immunized for the S1 protein fragment and nucleocapsid protein was specific. The results of these analyses shown in Figures 3.20 and 3.21 were nearly the same, as expected for both monoclonal and serum antibodies.

3.6 Immune Responses Against Recombinant S1, S2 Fragment Proteins, and Nucleocapsid Protein

In this study, ELISA tests were performed to measure specific serum antibody levels (total IgG) produced against recombinant antigens. In addition, ELISA tests measuring the level of IgG2a developed against SARS-CoV-2 antigens were performed to evaluate Th1 and Th2 responses. Because serum IgG2a levels indicate Th1 response and correlate with IFN levels, total IgG and IgG2a levels were also measured to determine the response type that occurred. Mouse serum samples immunized with recombinant S1, S2 fragment proteins, and Nucleocapsid protein were compared with a control group immunized with only adjuvant alone to measure the antibody levels. Serum levels of total IgG and IgG2a are shown in Figures 3.22 and 3.23. As expected, immunized mice showed an increase in total IgG levels compared to the control group against all three antigens. In contrast, the rise in IgG2a levels, related to the Th1 immune response, was significantly higher in the formulation containing MPLA adjuvant, which is a TLR4 antagonist, than in the formulation containing only Alum (Figure 3.23).

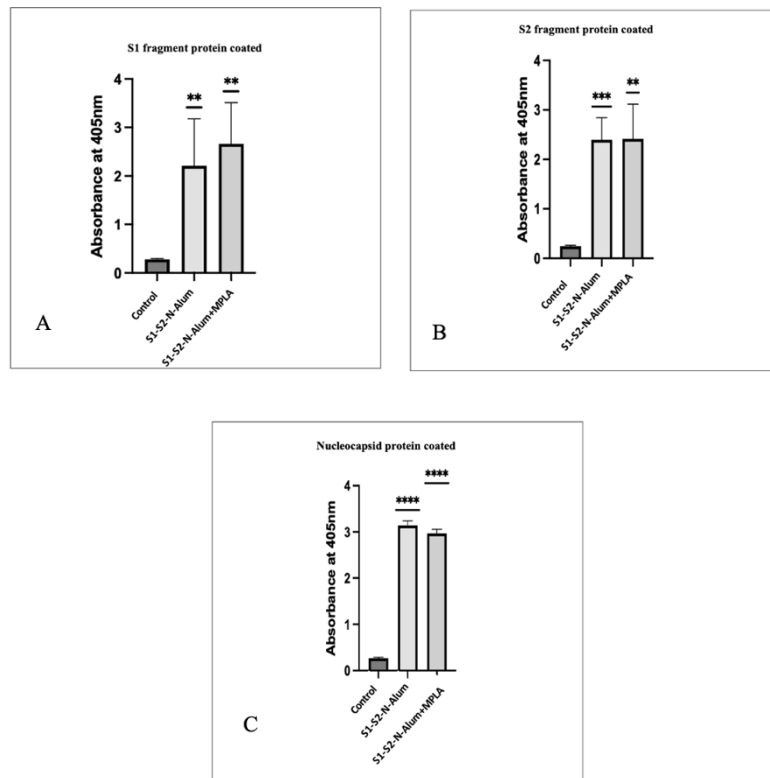


Figure 3.22 Level of total Immunoglobulin G in 1:100 diluted immunized mice sera that were immunized against recombinant S1 fragment protein (A), S2 fragment protein (B), and Nucleocapsid protein (C). A statistically significant ($p < 0.001$) increase compared to control is shown with three asterisks.

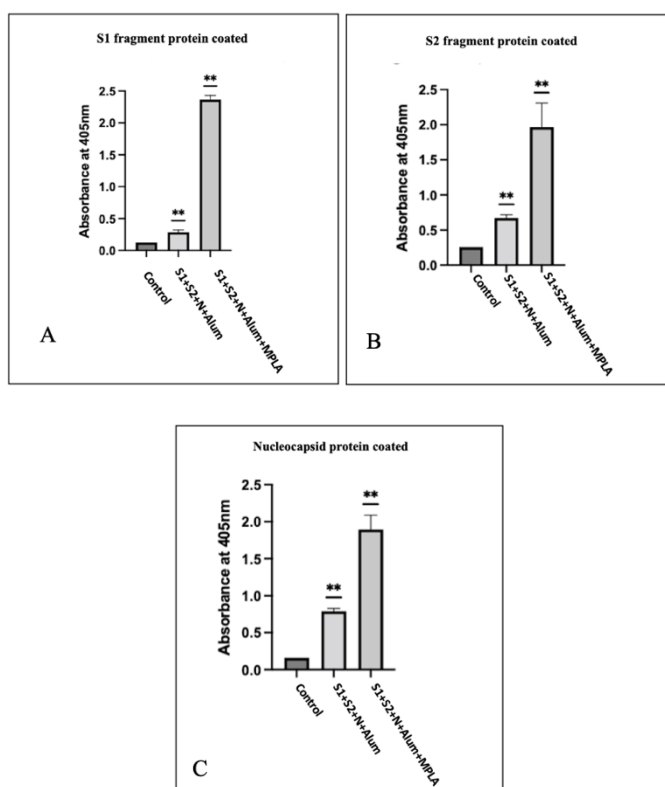


Figure 3.23 Level of Immunoglobulin G2a in 1:100 diluted immunized mice sera that were immunized against recombinant S1 fragment protein (A), S2 fragment protein (B), and Nucleocapsid protein (C). A statistically significant ($p < 0.001$) increase compared to control is shown with three asterisks.

Significantly higher antibody levels of the immunized mice compared to the control groups supported the immunoreactivity of the tested antigens.

Despite the significant innovations in vaccine and drug studies since the beginning of the COVID-19 pandemic, the need to find safer and more effective vaccines and treatments continue. The fact that vaccines approved for immediate use by the FDA during the pandemic cause serious side effects and that the virus constantly mutates and evades immunity provided by vaccines reveals the need for newer, safer, and

more adaptable vaccines (Albert, 2021). This study aims to evaluate protein and protein fragments with high antigenicity for protein-based vaccines, which is one of the most reliable and safe methods among vaccine platforms against SARS-CoV-2.

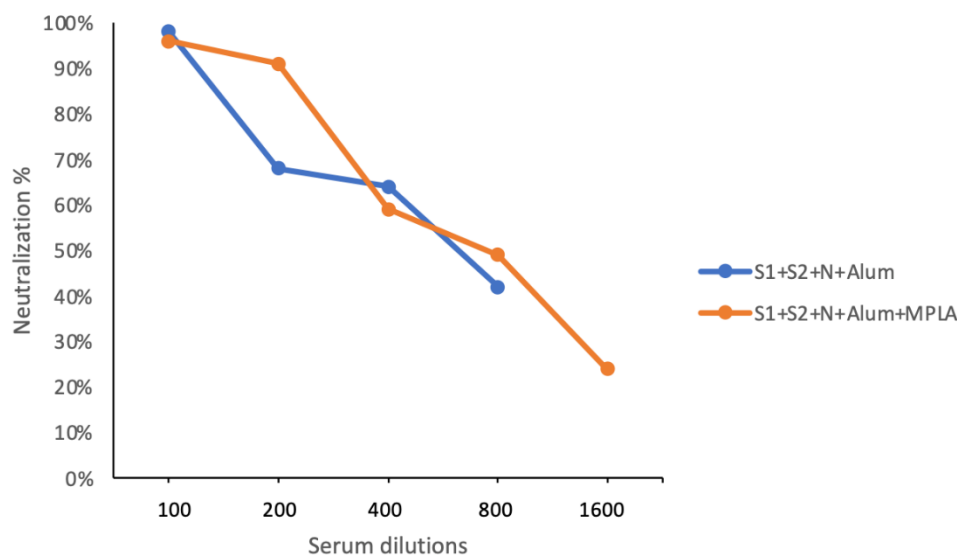


Figure 3. 24 Neutralization antibody levels of immunized mice sera against RBD.

As a result of epitope analysis, regions with the highest antigenic properties were selected as fragment proteins. The S1 fragment, one of the gene fragments chosen for this study, contains the RBD region which enables the binding sites of SARS-CoV-2 to the ACE-2 receptor. Therefore, it induces a neutralizing antibody response against the virus. To measure this neutralization capacity, Plaque Reduction Neutralization Test (PRNT) was performed at Ankara University, Faculty of Veterinary Medicine. According to the results of this test, the serum sample diluted 1:5 provided 100% neutralization. Also, a surrogate virus neutralization assay was performed using recombinant antigens to measure the strength of the immunization and the neutralizing antibody titer. According to this test, the cut-off value is universally determined as 20%, Alum only formulation > 1: 800 titers, and Alum +

MPLA formulation gave positive results even at 1:1600 titers(Figure 3.24). In conclusion, these proteins have been shown to be highly protective, and the neutralizing antibodies produced against the combined vaccine candidate are quite potent.

3.7 Determination of IFN- γ Response of Immunized Mice

The Th2 type cellular response is related to IgG1 and IL-4, -5 and -10, whereas the Th1 type cellular response is related to IFN- γ mediated activation of macrophages and IgG2a production. The Th1-type response is essential for the efficient removal of the virus since SARS-CoV-2 causes an intracellular infection. Th1-type cells activate neutrophils and macrophages via IFN- γ to generate an immune response against intracellular pathogens (Sugai *et al.*, 2005; Fedel *et al.*, 2015). The first line of defense of the human body against viral pathogens is the interferon response. IFNs prevent virus replication by stimulating the production of hundreds of IFN-stimulated genes, some of which have antiviral properties. In this regard, IFN- γ levels were observed to assess the strength of the Type-1 T helper cell response. IFNs are pro-inflammatory cytokines and are crucial for both innate and adaptive immunity. The primary IFN secreting cells are natural killer (NK) and activated T cells. IFN- γ is responsible for many different functions including the activation of macrophages, mediation of immunity against bacteria and viruses, improving antigen presentation, orchestrating innate immune system activation, controlling the Th1/Th2 ratio, and regulating cellular proliferation and apoptosis (Boehm *et al.*, 1996, Billiau *et al.*,1997). Additionally, by switching antibody classes to IgG2a, IFN- γ activates complement-fixation through antibodies which results in the opsonization and clearance of pathogens (Finkelman *et al.*, 1988; Schoenborn and Wilson, 2007).

Cell cultures were initiated from spleens taken from immunized mice 15 days after the second dose. These cells were induced with recombinant antigens to measure

IFN- γ levels to determine the Th1-type response. PBS was used as a negative control, and Concanavalin A (ConA) was used as a positive control.

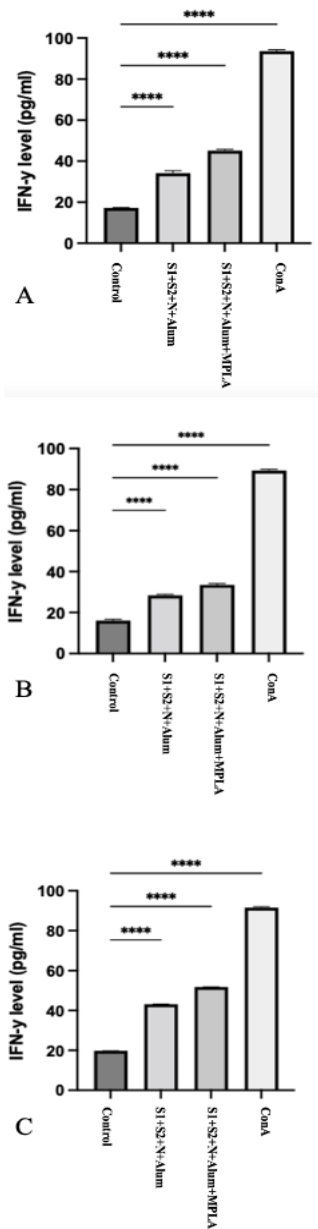


Figure 3.25 Production of IFN- γ by spleen cells of immunized mice. S1 fragment protein (A), S2 fragment protein (B), and Nucleocapsid protein (C). PBS as negative and ConA as positive controls. A statistically significant ($p < 0.001$) increase compared to control is shown with three asterisks.

The cytokine ELISA showed an increase in IFN- γ level compared to the negative control group (Figure 3.25), as expected from the results of previous IgG2a studies (Figure 3.23). Especially in cells induced by S2 fragment and N protein which contain many T cell epitopes (Grifoni, 2020), the IFN- γ level was significantly increased. In addition, since the TLR antagonist MPLA induced IFN- γ production through Th1 cell activation, it was observed that the IFN- γ increase in the groups injected with formulations containing MPLA was higher for all antigens. An elevated antibody titer is not enough for the clearance of the pathogen alone. However, an increase in IFN- γ levels indicates a cell-mediated immune response and contributes to the inactivation of the pathogen with a high antibody level. Overall, these results proved that both S1+S2+N+Alum and S1+S2+N+Alum+MPLA formulations could trigger Th1 type response.

This data proves that the immunity induced by the formulation prepared with these three antigens is composed of both antibody and cell-mediated origin and how potent the antigens are as vaccine candidates.

The COVID-19 pandemic continues, with new variants still emerging. Despite the existence of vaccines that are rapidly developed and approved for immediate use, the need for vaccines with more prolonged protective effects, fewer side effects, and more adaptability against new variants continues. However, our formulation model can be quickly adapted to include important variant proteins. We sought to create formulations that contained Omicron RBD fragments in our ongoing work in this approach. The immunization trial for Omicron RBD, which was obtained using the same technique, is currently in progress.

To eliminate the novel virus, a "multi-antigen" approach could be helpful. This approach is based on simultaneously targeting the B and T-cell epitopes of the virus, thereby eliciting a balanced B- and T-cell response, and effectively eliminating the virus without inducing tissue damage. In this study, a Spike fragment containing RBD was selected to generate neutralizing antibody response, and Nucleocapsid

protein was selected for a strong antibody response. In addition, the S2 fragment was chosen alongside Nucleocapsid to induce T cell-mediated cytotoxic response and provide long-term immunity by producing T memory cells.

Alum derivatives are generally preferred as adjuvants. Alum contributes to the Th2-type response, but the Th2 response shows weak antiviral properties. The Th1-type response is needed for the stimulation of neutrophils and macrophages for virus elimination. Therefore, MPLA, a potent antigen that triggers a TH1 response by stimulating IFN- γ is thus a suitable adjuvant for the vaccine to induce a cytotoxic response against coronavirus.

CHAPTER 4

CONCLUSION

- In this study, the immunogenicity of 2 recombinant Spike protein fragments and the whole nucleocapsid protein of SARS-CoV-2 as vaccine antigens were assessed by measuring the antigen-specific antibody levels and interferon levels.
- Immunoglobulin G titers against virus antigens were measured with sera from mice immunized with S1-S2-N-Alum and S1-S2-N-Alum+MPLA. Both groups showed a considerable rise in specific IgG titers ($p < 0.01$) against recombinant S1 and S2 fragment proteins and Nucleocapsid protein. An increased total antibody level indicated a robust humoral response was developed.
- The IgG2a response is an indicator of the cellular response that plays an essential role in the elimination of the pathogen. A significant increase in antigen-specific IgG2a titers was observed in immunized groups compared to the control group using ELISA. However, this increase in S1, S2, and N antigen-specific IgG2a levels was 6.7, 3.1, and 2.5-fold higher in the Alum+MPLA combination adjuvant immunized group than in the Alum-only group, respectively. Even though the S1 fragment protein contains the RBD and triggers the neutralizing antibody response, it is thought to be weak in inducing a robust cellular response and elicits an inadequate IgG2a response in the Alum-only formulation, fortunately there was 6.7-fold increase in antigen-specific IgG2a levels observed in the formulation supplemented with MPLA.

- Although vaccines trigger the production of many antibodies against the SARS-2 virus, very few of these antibodies can prevent the virus from binding to the cell surface. Therefore, these antibodies, called neutralizing antibodies, are critical in the defense of host cells against the virus. Neutralizing antibodies are directly connected to the protection granted by the vaccine and the length of this protection. This study examined the effect of S1 fragment protein containing the RBD region on neutralizing antibody production. Neutralization studies were carried out with two different methods. The first method used was the plaque reduction neutralization test (PRNT), which is the gold standard in terms of neutralization studies. It was observed that immunized mouse sera diluted 1:5 neutralized all viruses. The other method used was that ACE-2 receptor binding tests using the S1 fragment protein. This method was used to determine the titers of antibodies that specifically neutralize the RBD region. While 1:5 diluted sera neutralized all the viruses cultured in the plate in PRNT, ACE-2-RBD binding assay revealed that even a titer of 1:1600 had a neutralization rate higher than the cut-off value of 20%.
- As a result of cytokine ELISA tests performed to detect IFN- γ levels, used as an indicator of Th-1 induced immunity, an increase in interferon levels was observed in both formulations compared to the control group. The titers of IFN- γ were induced against three antigens, and it was observed that the titer of IFN- γ produced in N protein-induced spleen cells was higher than those induced by S1 or S2. These results demonstrated the potent T cell stimulating characteristics of the Nucleocapsid protein. The increase in IFN- γ proves the strong cellular response against recombinant antigens, and in addition to the antibody response, these results indicate that S1 and S2 fragment proteins and N protein are suitable vaccine antigen candidates as for combating the COVID-19 pandemic.

- In line with the results obtained in this study, it was observed that when S1, S2 fragments, and N protein are used together, they elicit powerful B and T cell responses.

REFERENCES

- Al-Jighefee, H. T., Najjar, H., Ahmed, M. N., Qush, A., Awwad, S., & Kamareddine, L. (2021). COVID-19 Vaccine Platforms: Challenges and Safety Contemplations. *Vaccines*, 9(10),1196.<https://doi.org/10.3390/vaccines9101196>
- Alanagreh, L., Alzoughool, F., & Atoum, M. (2020). The Human Coronavirus Disease COVID-19: Its Origin, Characteristics, and Insights into Potential Drugs and Its Mechanisms. *Pathogens*, 9(5), 331. <https://doi.org/10.3390/pathogens9050331>
- Albert, E., Aurigemma, G., Saucedo, J., & Gerson, D. S. (2021). Myocarditis following COVID-19 vaccination. *Radiology Case Reports*. <https://doi.org/10.1016/j.radcr.2021.05.033>
- Alving, C., Glass, M., & Detrick, B. (1992). Summary: Adjuvants/ Clinical Trials Working Group, AIDSRes. *Human Retroviruses*, 8 (8), 1427-1430.
- Azkur, A. K., Akdis, M., Azkur, D., Sokolowska, M., Veen, W., Brügger, M., O'Mahony, L., Gao, Y., Nadeau, K., & Akdis, C. A. (2020). Immune response to SARS-CoV-2 and mechanisms of immunopathological changes in COVID-19. *Allergy*, 75(7), 1564–1581. <https://doi.org/10.1111/all.14364>
- Bai, Z., Cao, Y., Liu, W., & Li, J. (2021). The SARS-CoV-2 Nucleocapsid Protein and Its Role in Viral Structure, Biological Functions, and a Potential Target for Drug or Vaccine Mitigation. *Viruses*, 13(6), 1115. <https://doi.org/10.3390/v13061115>
- Berger, A. (2000). Science commentary: Th1 and Th2 responses: what are they? *BMJ*, 321(7258), 424–424. <https://doi.org/10.1136/bmj.321.7258.424>

- Billiau, A. (1996). Interferon-gamma: biology and role in pathogenesis. *Adv Immunol*, 62:61.
- Blakney, A. K., & Bekker, L.-G. (2022). DNA vaccines join the fight against COVID-19. *The Lancet*, 399(10332), 1281–1282. [https://doi.org/10.1016/S0140-6736\(22\)00524-4](https://doi.org/10.1016/S0140-6736(22)00524-4)
- Boehm, U., Klamp, T., Groot, M., & Howard, J. (n.d.). Cellular responses to interferon-gamma. *Annu Rev Immunol*, 15:749–795.
- Bowen, J. E., Addetia, A., Dang, H. V., Stewart, C., Brown, J. T., Sharkey, W. K., Sprouse, K. R., Walls, A. C., Mazzitelli, I. G., Logue, J. K., Franko, N. M., Czudnochowski, N., Powell, A. E., Dellota, E., Ahmed, K., Ansari, A. S., Cameroni, E., Gori, A., Bandera, A., & Posavad, C. M. (2022). Omicron spike function and neutralizing activity elicited by a comprehensive panel of vaccines. *Science*. <https://doi.org/10.1126/science.abq0203>
- Callow, K. A., Parry, H. F., Sergeant, M., & Tyrrell, D. A. J. (1990). The time course of the immune response to experimental coronavirus infection of man. *Epidemiology and Infection*, 105(2), 435–446. <https://doi.org/10.1017/s0950268800048019>
- Chai, J., Cai, Y., Pang, C., Wang, L., McSweeney, S., Shanklin, J., & Liu, Q. (2021). Structural basis for SARS-CoV-2 envelope protein recognition of human cell junction protein PALS1. *Nature Communications*, 12(1). <https://doi.org/10.1038/s41467-021-23533-x>
- Chan, J. F.-W., Kok, K.-H., Zhu, Z., Chu, H., To, K. K.-W., Yuan, S., & Yuen, K.-Y. (2020). Genomic characterization of the 2019 novel human-pathogenic coronavirus isolated from a patient with atypical pneumonia after visiting Wuhan. *Emerging Microbes & Infections*, 9(1), 221–236. <https://doi.org/10.1080/22221751.2020.1719902>
- Chen, I.-Yin., Moriyama, M., Chang, M.-F., & Ichinohe, T. (2019). Severe Acute Respiratory Syndrome Coronavirus Viroporin 3a Activates the NLRP3

Inflammasome. *Frontiers in Microbiology*, 10.
<https://doi.org/10.3389/fmicb.2019.00050>

Chen, N., Zhou, M., Dong, X., Qu, J., Gong, F., Han, Y., Qiu, Y., Wang, J., Liu, Y., Wei, Y., Xia, J., Yu, T., Zhang, X., & Zhang, L. (2020). Epidemiological and clinical characteristics of 99 cases of 2019 novel coronavirus pneumonia in Wuhan, China: a descriptive study. *The Lancet*, 395(10223).
[https://doi.org/10.1016/s0140-6736\(20\)30211-7](https://doi.org/10.1016/s0140-6736(20)30211-7)

Cornillez-Ty, C., Lialo, L., Yates, J., Kuhn, P., & Buchmeier, M. (2009). Severe acute respiratory syndrome coronavirus nonstructural protein 2 interacts with a host protein complex involved in mitochondrial biogenesis and intracellular signaling. *J. Virol*, 83, 10314–10318.

Costa, F., Silva, R., & Boccaccini, A. R. (2018, January 1). *7 - Fibrous protein-based biomaterials (silk, keratin, elastin, and resilin proteins) for tissue regeneration and repair* (M. A. Barbosa & M. C. L. Martins, Eds.). ScienceDirect; Woodhead Publishing.
<https://www.sciencedirect.com/science/article/pii/B9780081008034000073>

Crooke, S. N., Ovsyannikova, I. G., Kennedy, R. B., & Poland, G. A. (2020). Immunoinformatic identification of B cell and T cell epitopes in the SARS-CoV-2 proteome. *Scientific Reports*, 10(1). <https://doi.org/10.1038/s41598-020-70864-8>

Cui, L., Wang, H., Ji, Y., Yang, J., Xu, S., Huang, X., Wang, Z., Qin, L., Tien, P., Zhou, X., Guo, D., & Chen, Y. (2015). The Nucleocapsid Protein of Coronaviruses Acts as a Viral Suppressor of RNA Silencing in Mammalian Cells. *Journal of Virology*, 89(17), 9029–9043.
<https://doi.org/10.1128/jvi.01331-15>

Dawood, F. S., Ricks, P., Njie, G. J., Daugherty, M., Davis, W., Fuller, J. A., Winstead, A., McCarron, M., Scott, L. C., Chen, D., Blain, A. E., Moolenaar, R., Li, C., Popoola, A., Jones, C., Anantharam, P., Olson, N., Marston, B. J., & Bennett, S. D. (2020). Observations of the global epidemiology of COVID-19 from the pre-pandemic period using web-based surveillance: a

- cross-sectional analysis. *The Lancet Infectious Diseases*, 0(0).
[https://doi.org/10.1016/S1473-3099\(20\)30581-8](https://doi.org/10.1016/S1473-3099(20)30581-8)
- de Haan, C. A. M., de Wit, M., Kuo, L., Montalto-Morrison, C., Haagmans, B. L., Weiss, S. R., Masters, P. S., & Rottier, P. J. M. (2003). The glycosylation status of the murine hepatitis coronavirus M protein affects the interferogenic capacity of the virus in vitro and its ability to replicate in the liver but not the brain. *Virology*, 312(2), 395–406. [https://doi.org/10.1016/s0042-6822\(03\)00235-6](https://doi.org/10.1016/s0042-6822(03)00235-6)
- DeDiego, M. L., Álvarez, E., Almazán, F., Rejas, M. T., Lamirande, E., Roberts, A., Shieh, W.-J., Zaki, S. R., Subbarao, K., & Enjuanes, L. (2007). A Severe Acute Respiratory Syndrome Coronavirus That Lacks the E Gene Is Attenuated In Vitro and In Vivo. *Journal of Virology*, 81(4), 1701–1713. <https://doi.org/10.1128/JVI.01467-06>
- Dejnirattisai, W., Huo, J., Zhou, D., Zahradník, J., Supasa, P., Liu, C., Duyvesteyn, H. M. E., Ginn, H. M., Mentzer, A. J., Tuekprakhon, A., Nutalai, R., Wang, B., Dijokaite, A., Khan, S., Avinoam, O., Bahar, M., Skelly, D., Adele, S., Johnson, S. A., & Amini, A. (2022). SARS-CoV-2 Omicron-B.1.1.529 leads to widespread escape from neutralizing antibody responses. *Cell*. <https://doi.org/10.1016/j.cell.2021.12.046>
- Diamond, M. S., & Kanneganti, T.-D. (2022). Innate immunity: the First Line of Defense against SARS-CoV-2. *Nature Immunology*, 23(2), 165–176. <https://doi.org/10.1038/s41590-021-01091-0>
- Dutta, S., Panthi, B., & Chandra, A. (2022). All-Atom Simulations of Human ACE2-Spike Protein RBD Complexes for SARS-CoV-2 and Some of its Variants: Nature of Interactions and Free Energy Diagrams for Dissociation of the Protein Complexes. *The Journal of Physical Chemistry*, 126(29), 5375–5389. <https://doi.org/10.1021/>
- Fedele, G., Cassone, A., & Ausiello, C. M. (2015). T-cell immune responses to bordetella pertussisinfection and vaccination: Graphical Abstract

Figure. Pathogens and Disease, 73(7), ftv051.
<https://doi.org/10.1093/femspd/ftv051>

Fehr, A. R., & Perlman, S. (2015). Coronaviruses: An Overview of Their Replication and Pathogenesis. *Coronaviruses*, 1282, 1–23. https://doi.org/10.1007/978-1-4939-2438-7_1

Felsenstein, S., Herbert, J. A., McNamara, P. S., & Hedrich, C. M. (2020). COVID-19: Immunology and treatment options. *Clinical Immunology*, 215, 108448. <https://doi.org/10.1016/j.clim.2020.108448>

Ferner, R. E., & Aronson, J. K. (2020). Remdesivir in covid-19. *BMJ*, m1610. <https://doi.org/10.1136/bmj.m1610>

Finkelman, F., Katona, I., Mosman, T., & Coffman, R. (n.d.). IFN-gamma regulates the isotype of Ig secreted during in vivo humoral immune responses. *J Immunol*, 140:1022-1027.

Gallais, F., Velay, A., Nazon, C., Wendling, M.-J., Partisani, M., Sibilia, J., Candon, S., & Fafi-Kremer, S. (2020). Intrafamilial Exposure to SARS-CoV-2 Associated with Cellular Immune Response without Seroconversion, France. *Emerging Infectious Diseases*, 27(1). <https://doi.org/10.3201/eid2701.203611>

Gorbalenya, A. E., Baker, S. C., Baric, R. S., de Groot, R. J., Drosten, C., Gulyaeva, A. A., Haagmans, B. L., Lauber, C., Leontovich, A. M., Neuman, B. W., Penzar, D., Perlman, S., Poon, L. L. M., Samborskiy, D. V., Sidorov, I. A., Sola, I., Ziebuhr, J., & Coronaviridae Study Group of the International Committee on Taxonomy of Viruses. (2020). The species Severe acute respiratory syndrome-related coronavirus : classifying 2019-nCoV and naming it SARS-CoV-2. *Nature Microbiology*, 5(4), 1–9. <https://doi.org/10.1038/s41564-020-0695-z>

Grifoni, A., Sidney, J., Zhang, Y., Scheuermann, R. H., Peters, B., & Sette, A. (2020). A Sequence Homology and Bioinformatic Approach Can Predict

- Candidate Targets for Immune Responses to SARS-CoV-2. *Cell Host & Microbe*, 27(4), 671-680.e2. <https://doi.org/10.1016/j.chom.2020.03.002>
- Grifoni, A., Sidney, J., Zhang, Y., Scheuermann, R. H., Peters, B., & Sette, A. (2020). A Sequence Homology and Bioinformatic Approach Can Predict Candidate Targets for Immune Responses to SARS-CoV-2. *Cell Host & Microbe*, 27(4), 671-680.e2. <https://doi.org/10.1016/j.chom.2020.03.002>
- Guo, Y.-R., Cao, Q.-D., Hong, Z.-S., Tan, Y.-Y., Chen, S.-D., Jin, H.-J., Tan, K.-S., Wang, D.-Y., & Yan, Y. (2020). The origin, transmission and clinical therapies on coronavirus disease 2019 (COVID-19) outbreak – an update on the status. *Military Medical Research*, 7(1). <https://doi.org/10.1186/s40779-020-00240-0>
- Guo, Y., Han, J., Zhang, Y., He, J., Yu, W., Zhang, X., Wu, J., Zhang, S., Kong, Y., Guo, Y., Lin, Y., & Zhang, J. (2022). SARS-CoV-2 Omicron Variant: Epidemiological Features, Biological Characteristics, and Clinical Significance. *Frontiers in Immunology*, 13. <https://doi.org/10.3389/fimmu.2022.877101>
- Gupta, R., Paswan, R. R., Saikia, R., & Borah, B. K. (2020). Insights into the Severe Acute Respiratory Syndrome Coronavirus-2: Transmission, Genome Composition, Replication, Diagnostics and Therapeutics. *Current Journal of Applied Science and Technology*, 71–91. <https://doi.org/10.9734/cjast/2020/v39i2130825>
- Han, Y., Du, J., Su, H., Zhang, J., Zhu, G., Zhang, S., Wu, Z., & Jin, Q. (2019). Identification of Diverse Bat Alphacoronaviruses and Betacoronaviruses in China Provides New Insights Into the Evolution and Origin of Coronavirus-Related Diseases. *Frontiers in Microbiology*, 10. <https://doi.org/10.3389/fmicb.2019.01900>
- Hani, V., Ganesh, G., Reddy M, V., & Ahmed, S. S. (2022). A review on risk assessment of formulation development and technology transfer of COVID-19 vaccines. *Vitae*, 29(2). <https://doi.org/10.17533/udea.vitae.v29n2a348750>

- Huang, Y., Yang, C., Xu, X., Xu, W., & Liu, S. (2020). Structural and functional properties of SARS-CoV-2 spike protein: potential antivirus drug development for COVID-19. *Acta Pharmacologica Sinica*, 41(9), 1141–1149. <https://doi.org/10.1038/s41401-020-0485-4>
- Jackson, C. B., Farzan, M., Chen, B., & Choe, H. (2021). Mechanisms of SARS-CoV-2 entry into cells. *Nature Reviews Molecular Cell Biology*, 23, 1–18. <https://doi.org/10.1038/s41580-021-00418-x>
- Jaimes, J. A., André, N. M., Chappie, J. S., Millet, J. K., & Whittaker, G. R. (2020). Phylogenetic Analysis and Structural Modeling of SARS-CoV-2 Spike Protein Reveals an Evolutionary Distinct and Proteolytically Sensitive Activation Loop. *Journal of Molecular Biology*, 432(10), 3309–3325. <https://doi.org/10.1016/j.jmb.2020.04.009>
- Jiang, H., Li, Y., Zhang, H., Wang, W., Men, D., Yang, X., Qi, H., Zhou, J., & Tao, S. (2020). Global profiling of SARS-CoV-2 specific IgG/ IgM responses of convalescents using a proteome microarray. <https://doi.org/10.1101/2020.03.20.20039495>
- Jiang, H., Li, Y., Zhang, H., Wang, W., Yang, X., Qi, H., Li, H., Men, D., Zhou, J., & Tao, S. (2020). SARS-CoV-2 proteome microarray for global profiling of COVID-19 specific IgG and IgM responses. *Nature Communications*, 11(1). <https://doi.org/10.1038/s41467-020-17488-8>
- Jimenez-Guardeño, J. M., Nieto-Torres, J. L., DeDiego, M. L., Regla-Nava, J. A., Fernandez-Delgado, R., Castaño-Rodríguez, C., & Enjuanes, L. (2014). The PDZ-Binding Motif of Severe Acute Respiratory Syndrome Coronavirus Envelope Protein Is a Determinant of Viral Pathogenesis. *PLoS Pathogens*, 10(8), e1004320. <https://doi.org/10.1371/journal.ppat.1004320>
- John, G., Sahajpal, N. S., Mondal, A. K., Ananth, S., Williams, C., Chaubey, A., Rojiani, A. M., & Kolhe, R. (2021). Next-Generation Sequencing (NGS) in COVID-19: A Tool for SARS-CoV-2 Diagnosis, Monitoring New Strains

- and Phylodynamic Modeling in Molecular Epidemiology. *Current Issues in Molecular Biology*, 43(2), 845–867. <https://doi.org/10.3390/cimb43020061>
- Khan, M. T., Irfan, M., Ahsan, H., Ahmed, A., Kaushik, A. C., Khan, A. S., Chinnasamy, S., Ali, A., & Wei, D.-Q. (2021). Structures of SARS-CoV-2 RNA-Binding Proteins and Therapeutic Targets. *Intervirology*, 64(2), 55–68. <https://doi.org/10.1159/000513686>
- Khan, M. T., Zeb, M. T., Ahsan, H., Ahmed, A., Ali, A., Akhtar, K., Malik, S. I., Cui, Z., Ali, S., Khan, A. S., Ahmad, M., Wei, D.-Q., & Irfan, M. (2020). SARS-CoV-2 nucleocapsid and Nsp3 binding: an in silico study. *Archives of Microbiology*. <https://doi.org/10.1007/s00203-020-01998-6>
- Kool, M., Soullié, T., van Nimwegen, M., Willart, M. A. M., Muskens, F., Jung, S., Hoogsteden, H. C., Hammad, H., & Lambrecht, B. N. (2008). Alum adjuvant boosts adaptive immunity by inducing uric acid and activating inflammatory dendritic cells. *Journal of Experimental Medicine*, 205(4), 869–882. <https://doi.org/10.1084/jem.20071087>
- Kudlay, D., & Svistunov, A. (2022). COVID-19 Vaccines: An Overview of Different Platforms. *Bioengineering*, 9(2), 72. <https://doi.org/https://doi.org/10.3390/bioengineering9020072>
- Kuo, L., & Masters, P. S. (2003). The Small Envelope Protein E Is Not Essential for Murine Coronavirus Replication. *Journal of Virology*, 77(8), 4597–4608. <https://doi.org/10.1128/jvi.77.8.4597-4608.2003>
- Kyriakidis, N. C., López-Cortés, A., González, E. V., Grimaldos, A. B., & Prado, E. O. (2021). SARS-CoV-2 vaccines strategies: a comprehensive review of phase 3 candidates. *Npj Vaccines*, 6(1). <https://doi.org/10.1038/s41541-021-00292-w>
- Lai, C.-C., Shih, T.-P., Ko, W.-C., Tang, H.-J., & Hsueh, P.-R. (2020). Severe acute respiratory syndrome coronavirus 2 (SARS-CoV-2) and coronavirus disease-2019 (COVID-19): The epidemic and the challenges. *International Journal*

- of Antimicrobial Agents, 55(3), 105924.
<https://doi.org/10.1016/j.ijantimicag.2020.105924>
- Lai, C.-C., Shih, T.-P., Ko, W.-C., Tang, H.-J., & Hsueh, P.-R. (2020). Severe acute respiratory syndrome coronavirus 2 (SARS-CoV-2) and coronavirus disease-2019 (COVID-19): The epidemic and the challenges. *International Journal of Antimicrobial Agents*, 55(3), 105924.
<https://doi.org/10.1016/j.ijantimicag.2020.105924>
- Le Bert, N., Tan, A. T., Kunasegaran, K., Tham, C. Y. L., Hafezi, M., Chia, A., Chng, M. H. Y., Lin, M., Tan, N., Linster, M., Chia, W. N., Chen, M. I.-C., Wang, L.-F., Ooi, E. E., Kalimuddin, S., Tambyah, P. A., Low, J. G.-H., Tan, Y.-J., & Bertoletti, A. (2020). SARS-CoV-2-specific T cell immunity in cases of COVID-19 and SARS, and uninfected controls. *Nature*, 584(7821), 457–462. <https://doi.org/10.1038/s41586-020-2550-z>
- Lee, Y.-S., Hong, S.-H., Park, H.-J., Lee, H.-Y., Hwang, J.-Y., Kim, S. Y., Park, J. W., Choi, K.-S., Seong, J. K., Park, S.-I., Lee, S.-M., Hwang, K.-A., Yun, J.-W., & Nam, J.-H. (2021). Peptides Derived From S and N Proteins of Severe Acute Respiratory Syndrome Coronavirus 2 Induce T Cell Responses: A Proof of Concept for T Cell Vaccines. *Frontiers in Microbiology*, 12. <https://doi.org/10.3389/fmicb.2021.732450>
- Li, F. (2016). Structure, Function, and Evolution of Coronavirus Spike Proteins. *Annual Review of Virology*, 3(1), 237–261. <https://doi.org/10.1146/annurev-virology-110615-042301>
- Li, Q., Wang, Y., Sun, Q., Knopf, J., Herrmann, M., Lin, L., Jiang, J., Shao, C., Li, P., He, X., Hua, F., Niu, Z., Ma, C., Zhu, Y., Ippolito, G., Piacentini, M., Estaquier, J., Melino, S., Weiss, F. D., & Andreano, E. (2022). Immune response in COVID-19: what is next? *Cell Death & Differentiation*, 29(6), 1107–1122. <https://doi.org/10.1038/s41418-022-01015-x>
- Lin, S.-Y., Liu, C.-L., Chang, Y.-M., Zhao, J., Perlman, S., & Hou, M.-H. (2014). Structural Basis for the Identification of the N-Terminal Domain of

- Coronavirus Nucleocapsid Protein as an Antiviral Target. *Journal of Medicinal Chemistry*, 57(6), 2247–2257. <https://doi.org/10.1021/jm500089r>
- Liu, W., Liu, L., Kou, G., Zheng, Y., Ding, Y., Ni, W., Wang, Q., Tan, L., Wu, W., Tang, S., Xiong, Z., & Zheng, S. (2020). Evaluation of Nucleocapsid and Spike Protein-Based Enzyme-Linked Immunosorbent Assays for Detecting Antibodies against SARS-CoV-2. *Journal of Clinical Microbiology*, 58(6). <https://doi.org/10.1128/JCM.00461-20>
- Lodish, H., Berk, A., Kaiser, C. A., Krieger, M., Scott, M. P., Bretscher, A., & Matsudaira, P. (2008). *Molecular cell biology*. Macmillan.
- Malik, Y. S., Sircar, S., Bhat, S., Sharun, K., Dhama, K., Dadar, M., Tiwari, R., & Chaicumpa, W. (2020). Emerging novel Coronavirus (2019-nCoV) - Current scenario, evolutionary perspective based on genome analysis and recent developments. *Veterinary Quarterly*, 1–12. <https://doi.org/10.1080/01652176.2020.1727993>
- Mascart, F., Verscheure, V., Malfroot, A., Hainaut, M., Piérard, D., Temerman, S., Peltier, A., Debrie, A.-S., Levy, J., Del Giudice, G., & Loch, C. (2003). Bordetella pertussis Infection in 2-Month-Old Infants Promotes Type 1 T Cell Responses. *The Journal of Immunology*, 170(3), 1504–1509. <https://doi.org/10.4049/jimmunol.170.3.1504>
- McBride, R., van Zyl, M., & Fielding, B. (2014). The Coronavirus Nucleocapsid Is a Multifunctional Protein. *Viruses*, 6(8), 2991–3018. <https://doi.org/10.3390/v6082991>
- Min, L., & Sun, Q. (2021). Antibodies and Vaccines Target RBD of SARS-CoV-2. *Frontiers in Molecular Biosciences*, 8. <https://doi.org/10.3389/fmolb.2021.671633>
- Motozono, C., Toyoda, M., Zahradnik, J., Saito, A., Nasser, H., Tan, T. S., Ngare, I., Kimura, I., Uriu, K., Kosugi, Y., Yue, Y., Shimizu, R., Ito, J., Torii, S., Yonekawa, A., Shimono, N., Nagasaki, Y., Minami, R., Toya, T., & Sekiya,

- N. (2021). SARS-CoV-2 spike L452R variant evades cellular immunity and increases infectivity. *Cell Host & Microbe*, 29(7), 1124-1136.e11. <https://doi.org/10.1016/j.chom.2021.06.006>
- Mu, J., Fang, Y., Yang, Q., Shu, T., Wang, A., Huang, M., Jin, L., Deng, F., Qiu, Y., & Zhou, X. (2020). SARS-CoV-2 N protein antagonizes type I interferon signaling by suppressing phosphorylation and nuclear translocation of STAT1 and STAT2. *Cell Discovery*, 6(1). <https://doi.org/10.1038/s41421-020-00208-3>
- Nelson, G., Buzko, O., Spilman, P., Niazi, K., Rabizadeh, S., & Soon-Shiong, P. (2021). *Molecular dynamic simulation reveals E484K mutation enhances spike RBD-ACE2 affinity and the combination of E484K, K417N and N501Y mutations (501Y.V2 variant) induces conformational change greater than N501Y mutant alone, potentially resulting in an escape mutant.* <https://doi.org/10.1101/2021.01.13.426558>
- Nieto-Torres, J. L., Verdiá-Báguena, C., Jimenez-Guardeño, J. M., Regla-Nava, J. A., Castaño-Rodríguez, C., Fernandez-Delgado, R., Torres, J., Aguilera, V. M., & Enjuanes, L. (2015). Severe acute respiratory syndrome coronavirus E protein transports calcium ions and activates the NLRP3 inflammasome. *Virology*, 485, 330–339. <https://doi.org/10.1016/j.virol.2015.08.010>
- Organization, W. H. (2020). Laboratory testing for coronavirus disease 2019 (COVID-19) in suspected human cases: interim guidance, 2 March 2020. [Apps.who.int. https://apps.who.int/iris/handle/10665/331329](https://apps.who.int/iris/handle/10665/331329)
- Park, E. J., Myint, P. K., Appiah, M. G., Darkwah, S., Caidengbate, S., Ito, A., Matsuo, E., Kawamoto, E., Gaowa, A., & Shimaoka, M. (2021). The Spike Glycoprotein of SARS-CoV-2 Binds to β 1 Integrins Expressed on the Surface of Lung Epithelial Cells. *Viruses*, 13(4), 645. <https://doi.org/10.3390/v13040645>
- Perdew, G. H., Heuvel, J. P. V., & Peters, J. M. (2008). Regulation of gene expression. Springer Science & Business Media.

- Perlman, S. (2020). Another Decade, Another Coronavirus. *New England Journal of Medicine*, 382(8). <https://doi.org/10.1056/nejme2001126>
- Perraut, R., Hundt, E., Garraud, O., Enders, B., & Gysin. (1993). Comparison of the Effects of Adjuvants and Adjuvant Doses on the Quantitative and Qualitative Antibody Response to Selected Antigens in New World Squirrel Monkeys *Saimiri sciureus*. *Vaccine*, 11 (7), 730-736.
- Plotkin, S. A., & Plotkin, S. L. (2011). The development of vaccines: how the past led to the future. *Nature Reviews Microbiology*, 9(12), 889–893. <https://doi.org/10.1038/nrmicro2668>
- Polack, F. P., Thomas, S. J., Kitchin, N., Absalon, J., Gurtman, A., Lockhart, S., Perez, J. L., Pérez Marc, G., Moreira, E. D., Zerbini, C., Bailey, R., Swanson, K. A., Roychoudhury, S., Koury, K., Li, P., Kalina, W. V., Cooper, D., Frenck, R. W., Hammitt, L. L., & Türeci, Ö. (2020). Safety and Efficacy of the BNT162b2 mRNA Covid-19 Vaccine. *New England Journal of Medicine*, 383(27). <https://doi.org/10.1056/nejmoa2034577>
- Pulendran, B., S. Arunachalam, P., & O’Hagan, D. T. (2021). Emerging concepts in the science of vaccine adjuvants. *Nature Reviews Drug Discovery*, 20(6), 454–475. <https://doi.org/10.1038/s41573-021-00163-y>
- Rabinovich, Klein, Hali BF., N. R., Klein, D. L., & Hali, B. (1994). *Science*, 265, 1401- 1404. *Science*, 265, 1401- 1404,
- Rahimi, A., Mirzazadeh, A., & Tavakolpour, S. (2020). Genetics and genomics of SARS-CoV-2: A review of the literature with the special focus on genetic diversity and SARS-CoV-2 genome detection. *Genomics*. <https://doi.org/10.1016/j.ygeno.2020.09.059>
- Redondo, N., Zaldívar-López, S., Garrido, J. J., & Montoya, M. (2021). SARS-CoV-2 Accessory Proteins in Viral Pathogenesis: Knowns and

Unknowns. *Frontiers in Immunology*, 12.
<https://doi.org/10.3389/fimmu.2021.708264>

Ross, P. J., Sutton, C. E., Higgins, S., Allen, A. C., Walsh, K., Misiak, A., Lavelle, E. C., McLoughlin, R. M., & Mills, K. H. G. (2013). Relative Contribution of Th1 and Th17 Cells in Adaptive Immunity to *Bordetella pertussis*: Towards the Rational Design of an Improved Acellular Pertussis Vaccine. *PLoS Pathogens*, 9(4), e1003264.
<https://doi.org/10.1371/journal.ppat.1003264>

Ruch, T. R., & Machamer, C. E. (2012). The Coronavirus E Protein: Assembly and Beyond. *Viruses*, 4(3), 363–382. <https://doi.org/10.3390/v4030363>

Schoeman, D., & Fielding, B. C. (2019). Coronavirus envelope protein: current knowledge. *Virology Journal*, 16(1). <https://doi.org/10.1186/s12985-019-1182-0>

Schoenborn, J., & Wilson, C. (2007). Regulation of interferon- γ during innate and adaptive immune responses. *Adv Immunol.* *Adv Immunol*, 96:41-101.
Science, 265, 1401- 1404, 1994.

Sekine, T. (2020). Robust T cell immunity in convalescent individuals with asymptomatic or mild COVID-19. *Cell* 183, 158–168.

Shin, D., Mukherjee, R., Grewe, D., Bojkova, D., Baek, K., Bhattacharya, A., Schulz, L., Widera, M., Mehdipour, A. R., Tascher, G., Geurink, P. P., Wilhelm, A., van der Heden van Noort, G. J., Ovaa, H., Müller, S., Knobloch, K.-P., Rajalingam, K., Schulman, B. A., Cinatl, J., & Hummer, G. (2020). Papain-like protease regulates SARS-CoV-2 viral spread and innate immunity. *Nature*, 1–6. <https://doi.org/10.1038/s41586-020-2601-5>

Singh, J., Rahman, S. A., Ehtesham, N. Z., Hira, S., & Hasnain, S. E. (2021). SARS-CoV-2 variants of concern are emerging in India. *Nature Medicine*.
<https://doi.org/10.1038/s41591-021-01397-4>

- Strange, W. (2020, April 8). COVID-19 Vaccine and Antiviral Drug Development. FPM. <https://www.fpm.org.uk/blog/covid-19-vaccine-and-antiviral-drug-development/>
- Sugai, T., Mori, M., Nakazawa, M., Ichino, M., Naruto, T., Kobayashi, N., Kobayashi, Y., Minami, M., & Yokota, S. (2005). A CpG-containing oligodeoxynucleotide as an efficient adjuvant counterbalancing the Th1/Th2 immune response in diphtheria–tetanus–pertussis vaccine. *Vaccine*, 23(46-47), 5450–5456. <https://doi.org/10.1016/j.vaccine.2004.09.041>
- Ura, T., Okuda, K., & Shimada, M. (2014). Developments in Viral Vector-Based Vaccines. *Vaccines*, 2(3), 624–641. <https://doi.org/10.3390/vaccines2030624>
- Vabret, N., Britton, G. J., Gruber, C., Hegde, S., Kim, J., Kuksin, M., Levantovsky, R., Malle, L., Moreira, A., Park, M. D., Pia, L., Risson, E., Saffern, M., Salomé, B., Selvan, M. E., Spindler, M. P., Tan, J., van der Heide, V., Gregory, J. K., & Alexandropoulos, K. (2020). Immunology of COVID-19: current state of the science. *Immunity*, 52(6). <https://doi.org/10.1016/j.immuni.2020.05.002>
- Vabret, N., Britton, G. J., Gruber, C., Hegde, S., Kim, J., Kuksin, M., Levantovsky, R., Malle, L., Moreira, A., Park, M. D., Pia, L., Risson, E., Saffern, M., Salomé, B., Selvan, M. E., Spindler, M. P., Tan, J., van der Heide, V., Gregory, J. K., & Alexandropoulos, K. (2020). Immunology of COVID-19: current state of the science. *Immunity*, 52(6). <https://doi.org/10.1016/j.immuni.2020.05.002>
- Vafaeinezhad, A., Atashzar, M. R., & Baharlou, R. (2021). The Immune Responses against Coronavirus Infections: Friend or Foe? *International Archives of Allergy and Immunology*, 1–14. <https://doi.org/10.1159/000516038>
- Wang, B., Zhong, C., & Tieleman, D. P. (2021). Supramolecular Organization of SARS-CoV and SARS-CoV-2 Virions Revealed by Coarse-Grained Models

- of Intact Virus Envelopes. *Journal of Chemical Information and Modeling*, 62(1), 176–186. <https://doi.org/10.1021/acs.jcim.1c01240>
- Wang, N., Shang, J., Jiang, S., & Du, L. (2020). Subunit Vaccines Against Emerging Pathogenic Human Coronaviruses. *Frontiers in Microbiology*, 11. <https://doi.org/10.3389/fmicb.2020.00298>
- Wang, P., Nair, M. S., Liu, L., Iketani, S., Luo, Y., Guo, Y., Wang, M., Yu, J., Zhang, B., Kwong, P. D., Graham, B. S., Mascola, J. R., Chang, J. Y., Yin, M. T., Sobieszczyk, M., Kyratsous, C. A., Shapiro, L., Sheng, Z., Huang, Y., & Ho, D. D. (2021). Antibody Resistance of SARS-CoV-2 Variants B.1.351 and B.1.1.7. *Nature*. <https://doi.org/10.1038/s41586-021-03398-2>
- Wang, Y., Grunewald, M., & Perlman, S. (2020). Coronaviruses: An Updated Overview of Their Replication and Pathogenesis. *Methods in Molecular Biology* (Clifton, N.J.), 2203, 1–29. https://doi.org/10.1007/978-1-0716-0900-2_1acs.jp cb.2c00833
- What is the Novavax vaccine, and why does the world need another type of COVID-19 vaccine? (n.d.). www.gavi.org. Retrieved August 11, 2022, from <https://www.gavi.org/vaccineswork/what-novavax-vaccine-and-why-does-world-need-another-type-covid-19-vaccine>
- World Health Organization. (2021, January 12). The different types of COVID-19 vaccines. www.who.int. <https://www.who.int/news-room/feature-stories/detail/the-race-for-a-covid-19-vaccine-explained>
- Wu, A., Peng, Y., Huang, B., Ding, X., Wang, X., Niu, P., Meng, J., Zhu, Z., Zhang, Z., Wang, J., Sheng, J., Quan, L., Xia, Z., Tan, W., Cheng, G., & Jiang, T. (2020). Genome Composition and Divergence of the Novel Coronavirus (2019-nCoV) Originating in China. *Cell Host & Microbe*, 27(3), 325–328. <https://doi.org/10.1016/j.chom.2020.02.001>
- Yadav, P. D., Sapkal, G. N., Abraham, P., Ella, R., Deshpande, G., Patil, D. Y., Nyayanit, D. A., Gupta, N., Sahay, R. R., Shete, A. M., Panda, S., Bhargava,

- B., & Mohan, V. K. (2021). Neutralization of variant under investigation B.1.617 with sera of BBV152 vaccinees. *Clinical Infectious Diseases*. <https://doi.org/10.1093/cid/ciab411>
- Yadav, R., Chaudhary, J. K., Jain, N., Chaudhary, P. K., Khanra, S., Dhamija, P., Sharma, A., Kumar, A., & Handu, S. (2021). Role of Structural and Non-Structural Proteins and Therapeutic Targets of SARS-CoV-2 for COVID-19. *Cells*, 10(4), 821. <https://doi.org/10.3390/cells10040821>
- Yi, C., Ling, Z., Lu, X., Fu, Y., Yang, Z., Wangmo, S., Chen, S., Zhang, Y., Ma, L., Gu, W., Lu, H., Sun, X., & Sun, B. (2022). A SARS-CoV-2 antibody retains potent neutralization against Omicron by targeting conserved RBM residues. *Cellular & Molecular Immunology*. <https://doi.org/10.1038/s41423-022-00853-6>
- Yilmaz, Ç. (2011). *Immune Responses Against The Recombinant Fimx And Putative Peptidyl-Prolyl Cis-Trans Isomerase From Bordetella Pertussis* [M.S. - Master of Science]. Middle East Technical University.
- Yilmaz, Ç., Apak, A., Özcengiz, E., & Özcengiz, G. (2016). Immunogenicity and protective efficacy of recombinant iron superoxide dismutase protein from *Bordetella pertussis* in mice models. *Microbiology and Immunology*, 60(11), 717–724. <https://doi.org/10.1111/1348-0421.12445>
- Yuan, S., Balaji, S., Lomakin, I. B., & Xiong, Y. (2021). Coronavirus Nsp1: Immune Response Suppression and Protein Expression Inhibition. *Frontiers in Microbiology*, 12. <https://doi.org/10.3389/fmicb.2021.752214>
- Zhang, C., Maruggi, G., Shan, H., & Li, J. (2019). Advances in mRNA vaccines for infectious diseases. *Frontiers in Immunology*, 10(594). <https://doi.org/10.3389/fimmu.2019.00594>
- Zhou, P., Yang, X.-L., Wang, X.-G., Hu, B., Zhang, L., Zhang, W., Si, H.-R., Zhu, Y., Li, B., Huang, C.-L., Chen, H.-D., Chen, J., Luo, Y., Guo, H., Jiang, R.-D., Liu, M.-Q., Chen, Y., Shen, X.-R., Wang, X., & Zheng, X.-S. (2020). A

pneumonia outbreak associated with a new coronavirus of probable bat origin. *Nature*, 579(7798). <https://doi.org/10.1038/s41586-020-2012-7>

Zhu, N., Zhang, D., Wang, W., Li, X., Yang, B., Song, J., Zhao, X., Huang, B., Shi, W., Lu, R., Niu, P., Zhan, F., Ma, X., Wang, D., Xu, W., Wu, G., Gao, G. F., & Tan, W. (2020). A Novel Coronavirus from Patients with Pneumonia in China, 2019. *New England Journal of Medicine*, 382(8). <https://doi.org/10.1056/nejmoa2001017>

APPENDICES

A. STRUCTURES OF PLASMID VECTORS AND SIZE MARKERS

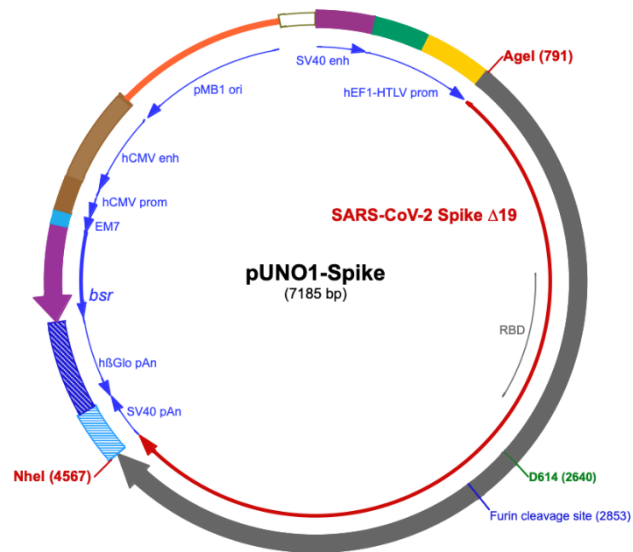


Figure A.1 pUNO1-Spike Expression Vector (Invivogen)

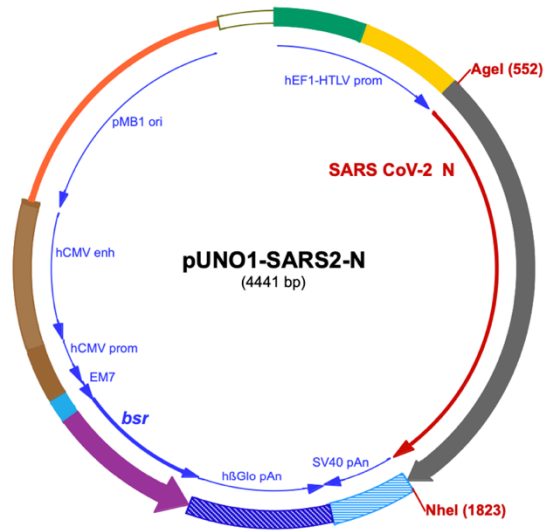


Figure A.2 pUNO1-Nucleocapsid Expression Vector (Invivogen)

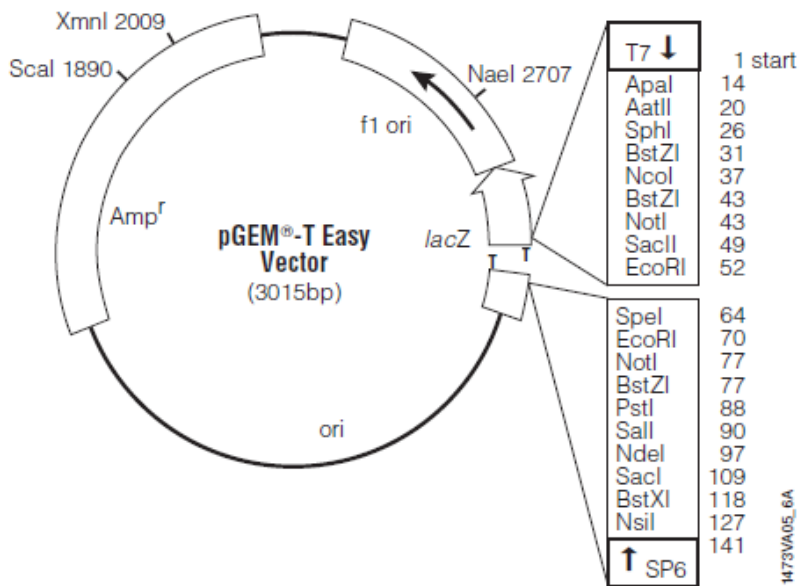


Figure A.3 pGEM®-T Easy Cloning Vector (Promega #A1360)

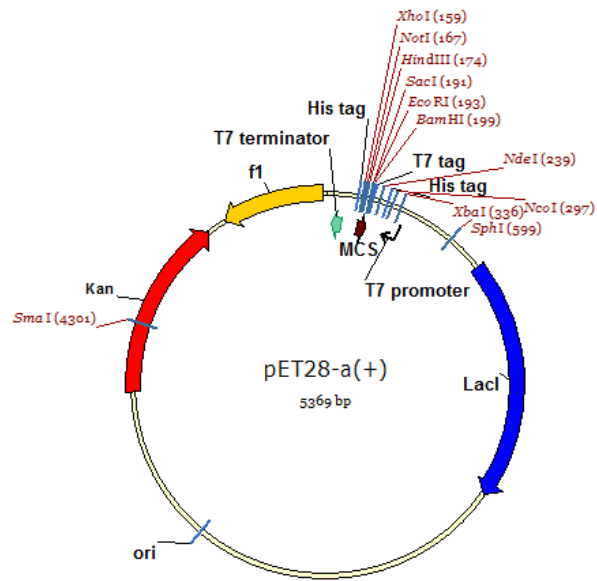


Figure A.4 pET-28a(+) Expression Vector (Novagen #69864-3)

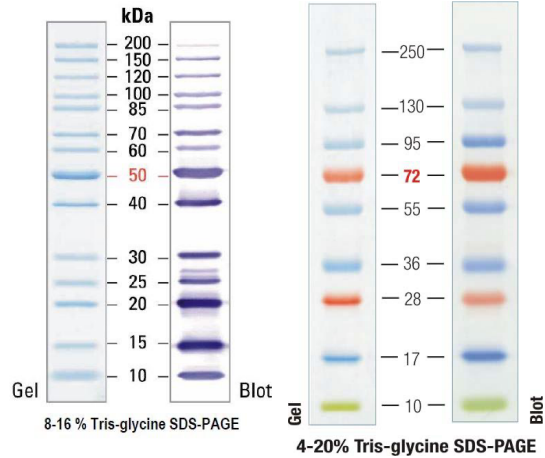


Figure A.5 PageRuler™ Plus Prestained Protein Ladder (Thermo Scientific #26619) (A) and PageRuler™ Unstained Protein Ladder (Thermo Scientific #26614) (B).

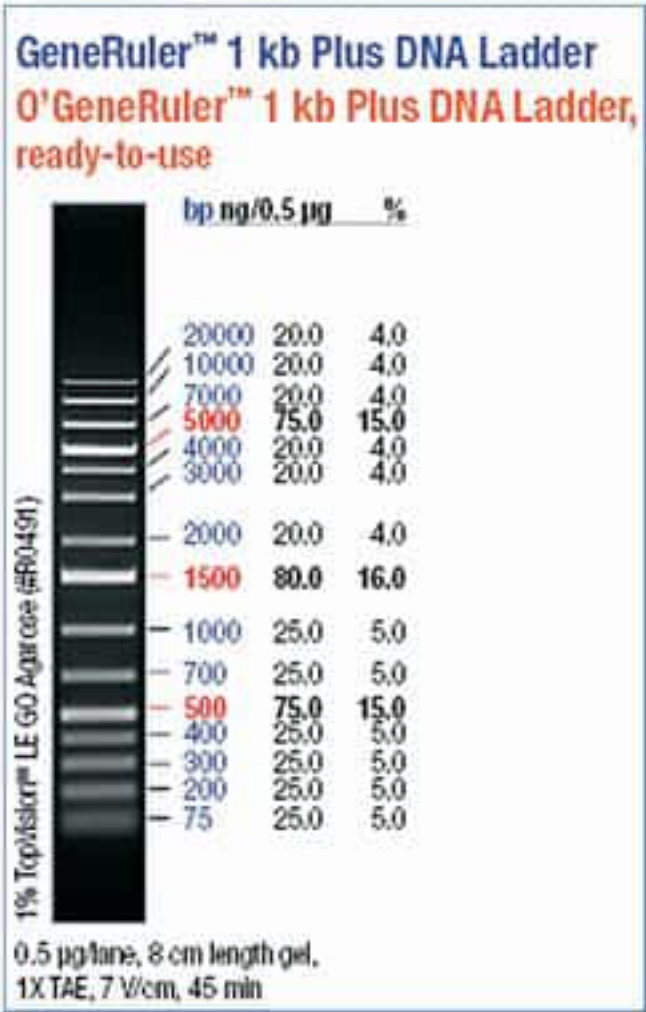


Figure A.6 1 kb plus DNA Ladder (GeneRuler # SM1333)

B. COMPOSITION AND PREPARATION OF CULTURE MEDIA

B1. Luria Broth:

- Tryptone 10g
- Yeast Extract 5g
- NaCl 10g
- Distilled water up to 1000 mL

Final pH is 7.0; sterilized at 121oC for 15 minutes.

B2. Luria Agar:

- Tryptone 10g
- Yeast Extract 5g
- NaCl 10g
- Agar 15g
- Distilled water up to 1000 mL

Final pH is 7.0; sterilized at 121oC for 15 minutes.

C. SOLUTIONS AND BUFFERS

C1. Agarose Gel Electrophoresis

C1.1. TAE Buffer (50X)

- Tris-base 242 g
- Glacial acetic acid 57.1 mL
- EDTA (0.5 M, pH 8.0) 100mL
- Distilled water up to 1000 mL

C1.2. Loading Buffer (10X)

- Bromophenol blue (w/v) 0.25%
- Xylene cyanol FF (w/v) 0.25%
- Sucrose (w/v) 40%

C2. SDS-Polyacrylamide Gel Electrophoresis (PAGE)

C2.1. Acrylamide/Bis

- Acrylamide 146 g
- N,N'-Methylene-bis acrylamide 4 g
- Distilled water up to 500 mL

C2.2. Tris HCl (1.5 M)

- Tris-base 54.45 g
- Distilled water 150 mL

pH is adjusted to 8.8 with HCl, distilled water to 300 mL, and stored at 4°C.

C2.3. Tris HCl (0.5 M)

- Tris-base 6 g
- Distilled water 50 mL

pH is adjusted to 6.8 with HCl, distilled water to 100 ml, and stored at 4°C.

C2.4. Running Buffer (10X)

- Tris-base 30 g
- Glycine 144 g
- SDS 10 g
- Distilled water up to 1000 mL

C2.5. Sample Loading Buffer (6X)

- Tris-HCl (1 M, pH 6.8) 3.5 mL
- Glycerol 3.6 mL
- SDS 1.03 g
- β -mercaptoethanol 0.5 mL
- Bromophenol blue 0.0013 g
- Distilled water up to 10 mL

C2.6. Fixation Solution

- Ethanol 40%
- Glacial acetic acid 10%
- Distilled water 50%

C2.7. Coomassie Blue R-250 Stain

- Coomassie Blue R-250 0.25 g
- Methanol 125 mL
- Glacial acetic acid 25 mL
- Distilled water 100 mL

C2.8. Destaining Solution

- Methanol 100 mL
- Glacial acetic acid 100 mL
- Distilled water 800 mL

C3. Western Blot

C3.1. Transfer Buffer (1X)

- Methanol 200 mL
- Tris-base 3.63 g
- Glycine 14.4 g
- SDS 0.37 g
- Distilled water up to 1000 mL

C3.2. Tris-buffered Saline, TBS (1X)

- Tris-base 2.42 g
- NaCl 29.2 g
- Distilled water up to 1000 mL

C4. Protein Purification

C4.1. LEW (Lysis- Wash) Buffer (pH 8.0)

- Urea 8 M
- NaCl 300 mM
- NaH₂PO₄ 50 mM

C4.2. LEW (Elution) Buffer (pH 8.0)

- Urea 8 M
- NaCl 300 mM
- NaH₂PO₄ 50 mM
- Imidazole 250 mM

C5. *E. coli* Competent Cell Preparation

C5.1. Buffer I

- RuCl 100 mM
- Kac 30 mM
- CaCl₂ 10 mM
- Glycerol 15%

pH is adjusted to 5.8 with dilute acetic acid, and the filter is sterilized.

C5.2. Buffer II

- CaCl₂ 75 mM
- RuCl 10 mM
- MOPS 10 mM
- Glycerol 15%

pH is adjusted to 6.5 with 0.2 M KOH, and the filter is sterilized.

C6. IPTG (Isopropyl-β-D-thiogalactoside) for Colony Selection

- IPTG 100 mg
- Distilled water 1 ml

The solution was filter sterilized and stored at -20°C.

C7. X-Gal (5-bromo-4-chloro-3-indolyl-B-D-galactoside)

- X-Gal 20 mg
- Dimethylformamide 1 mL

The solution was stored at -20°C, protected from light.

C8. Plasmid Isolation

C8.1. STE Buffer

- Sucrose (w/v) 10.3%
- Tris-HCl (pH 8.0) 25 mM
- EDTA (pH 8.0) 25 mM

C8.2. Lysis Buffer

- NaOH 0.3 M
- SDS (w/v) 2%

C9. ELISA for Detection of Antibody Titers

C9.1. Carbonate/Bicarbonate Buffer (0.05 M)

- Na₂CO₃ 1.59 g
- NaHCO₃ 3.88 g
- Distilled water up to 1000 mL

pH is adjusted to 9.6 and stored at 4°C.

C9.2. Washing Solution (1X PBS - 0.1% Tween-20)

- NaCl 8 g
- KCl 0.2 g
- Na₂HPO₄ 1.44 g
- KH₂PO₄ 0.24 g
- Tween-20 1 ml
- Distilled water up to 1000 mL

pH is adjusted to 7.2 and stored at 4°C.

C9.3. Blocking Solution

- 2% (w/v) BSA in 1X PBS - 0.1% Tween-20.

D. SUPPLIERS OF CHEMICALS, ENZYMES, AND KITS

D1. Chemicals	Suppliers
Acrylamide	Sigma
Agar-agar	Sigma
Agarose	Sigma
Ammonium persulfate	BioRad
Ampicillin	Sigma
Anti-mouse IgG	Sigma
Bovine serum albumin	Sigma
Bromophenol blue	Merck
CaCl ₂ .2H ₂ O	Merck
Coomassie Blue G-250	Sigma
Coomassie Blue R-250	Sigma
Dimethylformamide	Merck
dNTPs	ThermoScientific
DTT	Sigma
EDTA	Sigma
Ethanol	Merck
Ethidium Bromide	Sigma
Fetal bovine serum	Biochrom
Formaldehyde	Merck
Glacial acetic acid	Merck
Glycerol	Merck
Glycine	Merck
H ₂ SO ₄	Merck
HCl	Merck
IPTG	Cayman
Isopropanol	Merck

Kanamycin	Sigma
KCl	Merck
KH ₂ PO ₄	Merck
Luria Broth	Merck
Methanol	Merck
MnCl ₂	Merck
N,N-Methylene-bis acrylamide	Merck
Na ₂ CO ₃	Merck
Na ₂ HPO ₄	Merck
NaCl	Merck
NaHCO ₃	Merck
NaOH	Merck
Non-essential aminoacids	Biochrom
Penicillin/streptomycin	Biochrom
Phenol/chloroform/isoamylalcohol	Merck
Phosphoric acid	Merck
Potassium acetate	Merck
SDS	Merck
Skim milk	Merck
Streptavin-HRP	BPS
TEMED	BioRad
TMB	ThermoScientific
Tris-base	Merck
Tris-HCl	Merck
Tween-20	Merck
Urea	Merck
X-gal	Merck
2-mecaptoethanol	Merck

D2. Enzymes

<i>Bam</i> HI	NEB
<i>Sac</i> I	NEB
<i>Nhe</i> I	NEB
T4 DNA ligase	ThermoScientific
<i>Taq</i> DNA polymerase	ThermoScientific

D3. Kits

AP Conjugate Substrate Kit	Biorad
Gel Extraction Kit	ThermoScientific
pGEM-T Easy Vector System	Promega
Plasmid Midi Kit	ThermoScientific
Ni60 columns	Takara

